CZECH TECHNICAL UNIVERSITY IN PRAGUE

Faculty of Civil Engineering
Experimental Centre

Development of Lightweight Refractory Composites Based on Aluminous Cement

DOCTORAL THESIS

Ing. Marcel Jogl

Doctoral study programme: Civil Engineering
Branch of study: Physical and Material Engineering

Doctoral thesis tutor: Pavel Reiterman, Ph.D.

Prague, 2021

CZECH TECHNICAL UNIVERSITY IN PRAGUE
Faculty of Civil Engineering
Thákurova 7, 166 29 Praha 6

DECLARATION

Ph.D. student's name: Marcel Jogl

Title of the doctoral thesis: Development of Lightweight Refractory Composites Based on Aluminous Cement

I hereby declare that this doctoral thesis is my own work and effort written under the guidance of the tutor Pavel Reiterman, Ph.D.
All sources and other materials used have been quoted in the list of references.

The doctoral thesis was written in connection with research on the project: P104/12/0791: Fibre-Reinforced Cement Composites for High-Temperature Applications.

In Prague on 20.7.2021

signature

CZECH TECHNICAL UNIVERSITY IN PRAGUE
Faculty of Civil Engineering
Thákurova 7, 166 29 Praha 6

ACKNOWLEDGEMENT

Foremost, I would like to express my sincere gratitude to my supervisor, Pavel Reiterman, Ph.D., for his patience, motivation, knowledge, and support during my studies and research. His guidance has helped me countless times in the research and writing of this work.

Besides my supervisor, I would like to thank Prof. Petr Konvalinka, Assoc. Prof. Eva Vejmelková, and my colleagues for their encouragement, advice, and insightful comments.

I gratefully acknowledge the support provided by the Czech Science Foundation under project P104/12/0791: Fibre-Reinforced Cement Composites for High-Temperature Applications.

My sincerest thanks also go to Prof. Toshihiko Kuwabara for his guidance during my year-long internship at the Tokyo University of Agriculture and Technology; as well as a special thanks to the foundation "Nadání Josefa, Marie a Zdeňky Hlávkových" for providing me financial support.

Abstrakt

Vývoj nových kompozitních materiálů je celosvětově mimořádně progresivní odvětví inženýrské činnosti. Principem kompozitů je kombinace rozdílných materiálů, kterou vzniká zcela nový materiál se specifickými vlastnostmi. Tato disertační práce přispívá do kategorie experimentálního výzkumu a vývoje speciálních kompozitů. Snahou této studie je příprava lehčených žárovzdorných kompozitů s dobrými mechanickými vlastnostmi, které by vedly k technicky ekonomickým řešením.

Oheň patří k jednomu z nejnebezpečnějších aspektů betonových konstrukcí. Pokud je beton vystaven vysokým teplotám, jeho mechanické chování se dramaticky mění s nárůstem teploty. Důležitá není pouze maximální teplota, ale také doba, po kterou je konstrukce vystavena extrémní teplotě, a rychlost, s jakou teplota stoupá. To vše může vést k explozivnímu odprýskávání betonu s vážnými důsledky pro konstrukci a osoby v její blízkosti. Účelem navrhovaných kompozitů je působit jako tepelná bariéra ve volitelném tvaru a snížit tak přenos tepla z vysokoteplotního zdroje.

Křemičité kamenivo a cementové kompozity na bázi portlandského cementu nejsou schopny odolat účinkům vysokých teplot, proto směsi v tomto experimentu jsou navrženy na bázi hlinitanového cementu a obsahují pouze složky, které odolávají vysokým teplotám. Pro účel výzkumu byly připraveny malé hranolové vzorky vystavené teplotám 105, 400, 600 a 1000 °C. Výstupem této práce je analýza vlivu žáruvzdorných komponentů a jejich reakce na postupné teplotní zatížení. Fyzikálními a mechanickými zkouškami byly zkoumány a vyhodnoceny různé kombinace lehčeného kameniva, provzdušňovací přísady a vláken v navržených směsích.

Experimentální výsledky prokázaly pozitivní účinek použitých materiálů v žáruvzdorné kompozici. Mechanické vlastnosti navržených kompozitů dosáhly hodnot vysoké kvality, též i další užitné vlastnosti. Ani při zvýšené teplotě 1 000 °C nedošlo k nepříznivým účinkům, jako je zmíněné explozivní odprýskávání.

Klíčová slova:

Lehčený kompozit, žáruvzdorné materiály, teplotní zatížení, zbytkové mechanické vlastnosti, hlinitanový cement, čedičová vlákna.

Abstract

The development of new composite materials is a worldwide extremely progressive branch of engineering activity. The principle of composite materials is a combination of different materials providing an entirely new material with specific properties. The effort of the present thesis is the preparation of lightweight refractory composites with good mechanical properties, which would reach technically economical solutions.

Fire belongs to one of the most dangerous aspects of concrete structures. If concrete is subject to high temperatures, its mechanical behavior changes dramatically with the increase in temperature. It is not only the maximum temperature that is important, but also the time at which the structure is exposed to the extreme temperature and the rate at which the temperature rises. All that can lead to explosive spalling with serious consequences to the structure and people. The purpose of the proposed composite is to act as a thermal barrier in an optional form and reduce the heat transfer from a high-temperature source.

Silica composites based on Portland cement and silica aggregates are not able to resist the effects of high temperatures, therefore, the mixtures in this experiment include only components that can resist high temperatures. For the experimental program, small prismatic specimens based on aluminous cement were prepared and exposed to temperatures of 105, 400, 600, and 1000 °C. One output of this study is the analysis of the influence of refractory compositions and their response to gradual temperature loading. Various compositions of lightweight aggregates, air-entraining additives, and fibers were investigated and evaluated by physical and mechanical testing.

Experimental results have shown a positive effect of the used materials in a refractory composition. The mechanical properties of the designed composites have achieved values of high quality, as well as other utility properties. No adverse effects, such as explosive spalling, occurred even when the temperature had been increased to 1000 °C.

Keywords:

Lightweight composite, refractories, temperature loading, residual mechanical properties, aluminous cement, basalt fibers.

Table of contents

List of chemical equations……...VI

List of tables……...VII

List of figures……..IX

Used symbols…….XII

Chemical formulas……XIII

Notations and abbreviations……..…..XIV

Objectives of the study……..1

1 Introduction…….. 2

1.1 Role of research and development……2

1.2 Background……...3

1.3 Scope of the work…….... 5

2 State of the art……...6

2.1 Fire resistance……... 6

2.2 Concrete and high temperatures……... 7

2.2.1 Effect of elevated temperatures on concrete and concrete structures…….. 9

2.2.1.1 Effect of elevated temperatures on cement paste……..10

2.2.1.2 Effect of elevated temperatures on aggregate……...12

2.2.2 Effect of fire on concrete and concrete structures……. 15

2.3 Explosive spalling……. 17

2.3.1 Mechanisms of explosive spalling…….19

2.3.2 Prevention of explosive spalling……21

2.4 Refractory concrete…… 22
2.4.1 Calcium aluminate cement (CAC)……23
2.4.1.1 Mineralogical composition of CAC……..25
2.4.1.2 Hydration of CAC……27
2.4.1.3 Conversion of CAC hydrates……..... 30
2.4.1.4 Carbonation of CAC hydrates……...32
2.4.1.5 CAC hydrates at elevated temperatures…… 34
2.4.2 Aggregates for high-temperature applications……...34
2.4.3 Fiber reinforcement……... 37
2.5 Lightweight refractory concrete…… 39
3 Experimental investigations……... 42
3.1 Designed mixtures and their components…….. 43
3.1.1 First part – Application of an air-entraining agent…… 44
3.1.2 Second part – Addition of basalt fibers……. 46
3.1.3 Third part – Utilization of LWA……49
3.2 Specimen preparation…….....51
3.2.1 Mixture formation……..52
3.2.2 Flow table test……53
3.2.3 Specimen casting process……..... 53
3.2.4 Specimen curing procedure……... 55
3.2.5 Specimen drying procedure……... 55
3.3 High-temperature treatment……....56
3.4 Measurement methods……....59
4 Results and discussion……62
4.1 Evaluation of previous experiments……... 62

4.2 Physical changes caused by high temperatures……..66
4.2.1 Color change……..66
4.2.2 Shrinkage……...67
4.2.3 Density……...68
4.3 Residual mechanical properties…….....71
4.3.1 Flexural strength…… 71
4.3.2 Fracture energy…….. 74
4.3.3 Compressive strength…….80
5 Conclusion……..83
5.1 Summary results of the experiments…….. 83
5.2 Achieved goals……... 86
5.3 Proposals for future research…….....90
References……...92

List of chemical equations

(2.1) $Ca(AlO_2)_2 + 4H_2O \leftrightarrow Ca^{2+} + 2Al(OH)_4^-$ 27

(2.2) $2CAH_{10} \rightarrow C_2AH_8 + AH_3$ amorph. + 9H 31

(2.3) $3C_2AH_8 \rightarrow 2C_3AH_6 + AH_3$ cryst. + 9H 31

(2.4) $3CAH_{10} \rightarrow C_3AH_6 + 2AH_3$ cryst. + 18H 31

(2.5) $CAH_{10} + CO_2 \rightarrow CaCO_3 + AH_3 + 7H$ 33

(2.6) $C_2AH_8 + 2CO2 \rightarrow CaCO_3 + AH_3 + 5H$ 33

(2.7) $C_3AH_6 + 3CO2 \rightarrow 3CaCO_3 + AH_3 + 3H$ 33

(2.8) $CAH_{10} \rightarrow C_2AH_8 + AH_3$ amorph. 34

(2.9) $C_2AH_8 + AH_3$ amorph. $\rightarrow C_3AH_6 + 2AH_3$ cryst. 34

(2.10) $C_3AH_6 + 2AH_3$ cryst. $\rightarrow C_{12}A_7 + CA + H$ 34

(2.11) $C_3AH_6 + 2AH_3$ cryst. + $A \rightarrow CA + H$ 34

List of tables

Table 2.1 Influence of environmental factors on heated concrete [43]. 8

Table 2.2 List of changes taking place in concrete during heating [46, 54]. 16

Table 2.3 Classification of CAC [77, 78]. 23

Table 2.4 Comparison of hydration heat values of different types of cement [80]. 25

Table 2.5 Hydration products depending on the surrounding temperature [77, 82, 85, 85]. 29

Table 2.6 Characteristics of crystalline state CAC hydrates [77]. 30

Table 2.7 The conversion rate of CAH_{10} and C_2AH_8 to C_3AH_6 depending on temperature [80]. 32

Table 2.8 Physical and mechanical properties of aggregates used in dense refractory concretes. 35

Table 2.9 Physical and mechanical properties of lightweight aggregates used in refractory concretes [43, 88, 89]. 36

Table 2.10 Physical and mechanical properties of fibers used in fiber-reinforced concretes. 38

Table 3.1 Simplified scheme of the experimental work. 43

Table 3.2 Chemical composition and physical properties of used CAC. 44

Table 3.3 Chemical composition of used basalt fibers. 48

Table 3.4 Chemical composition of Liaver. 50

Table 3.5 Physical properties of Liaver. 51

Table 3.6 Composition of studied lightweight specimens. 51

Table 5.1 Identification of test specimens. 83

Table 5.2 Mass loss of specimens subjected to elevated temperature. 89

List of figures

Figure 2.1 Microstructure of concrete heated to 600 °C (SEM, 50×) [54]. 13

Figure 2.2 DTA of four types of aggregates, measured during heating at 10 °C/min [54]. 14

Figure 2.3 Combined thermal stress and pore pressure in triggering spalling [61]. 20

Figure 2.4 Summary of the CAC hydration mechanism [80]. 28

Figure 2.5 Schematic representation of temperature profile as a function of time for a CAC paste [81]. 28

Figure 2.6 SEM image of the interfacial transition zone in lightweight concrete between an expanded clay aggregate and the paste. Hydration products are visible inside the outer LWA pores [121]. 40

Figure 2.7 Segregation of LWC - upper and lower slice in a concrete specimen [125]. 41

Figure 3.1 Górkal 40 calcium aluminate cement. 45

Figure 3.2 Microporan 2 air-entraining agent. 46

Figure 3.3 Basalt fibers, with a diameter of 13 μm and a length of 6.35 mm. 49

Figure 3.4 Expanded glass Liaver; (A) fraction of 0.25–0.50 mm, (B) fraction of 0.5–1.0 mm. 50

Figure 3.5 Horizontal laboratory mixer model SP-200D. 52

Figure 3.6 Flow table for cement mortar. 53

Figure 3.7 Steel molds for creating test specimens. 54

Figure 3.8 Vibrating table RM1. 55

Figure 3.9 Drying oven SalvisLab Thermocenter TC240. 56

Figure 3.10 Electric furnace 10013V. 58

Figure 3.11 Temperature-loading process in time. 58

Figure 3.12 Electromechanical compression system MTS 100 with test detail. 60

Figure 3.13 Hydraulic pressure machine EU 40 with test detail. 61

Figure 4.1 Relative values of flexural strength, specimens dried at 105 °C. 63

Figure 4.2 Relative values of compressive strength, specimens dried at 105 °C. 63

Figure 4.3 Relative values of density, specimens dried at 105 °C. 64

Figure 4.4 Density development of the cement-based paste with a 10% dose of an air-entraining additive, in correlation with different water-cement ratios. 64

Figure 4.5 Residual values of flexural strength. 65

Figure 4.6 Residual values of density. 65

Figure 4.7 Color change of an aluminous cement-based composite. 66

Figure 4.8 Visible cracks on the specimen surface after heating to 400°C. 68

Figure 4.9 Density values after exposure to elevated temperatures. 68

Figure 4.10 Mass loss of specimens subjected to elevated temperatures. 69

Figure 4.11 Residual density values after exposure to 1000 °C. 70

Figure 4.12 Flexural strength after exposure to elevated temperatures. 72

Figure 4.13 Loss of flexural strength as a function of elevated temperature. 73

Figure 4.14 Residual flexural strength values after exposure to 1000 °C. 74

Figure 4.15 Fracture energy values after exposure to elevated temperatures. 75

Figure 4.16 Load-deflection curve for the evaluation of fracture energy after 105 °C. 76

Figure 4.17 Load-deflection curve for the evaluation of fracture energy after 400 °C. 76

Figure 4.18 Load-deflection curve for the evaluation of fracture energy after 600 °C. 77

Figure 4.19 Load-deflection curve for the evaluation of fracture energy after 1000 °C. 77

Figure 4.20 Residual fracture energy values after exposure to 1000 °C. 78

Figure 4.21 Load-deflection curve of specimens subjected to 105 °C. 79

Figure 4.22 Load-deflection curve of specimens subjected to 1000 °C. 79

Figure 4.23 Compressive strength after exposure to elevated temperatures. 81

Figure 4.24 Loss of compressive strength as a function of elevated temperature. 81

Figure 4.25 Residual compressive strength values after exposure to 1000 °C. 82

Figure 5.1 Relation between flexural strength and density of specimens. 84

Figure 5.2 Relation between compressive strength and density of specimens. 85

Figure 5.3 Residual flexural strength values after exposure to 1000 °C. 87

Figure 5.4 Residual density values after exposure to 1000 °C. 88

Used symbols

Latin uppercase

F	Force [N]
F_f	Maximum fracture load [N]
F_c	Maximum failure load [N]
R_f	Flexural strength [MPa]
R_c	Compressive strength [MPa]
G_f	Fracture energy [J/m^2]
M	Bending moment [N.mm]
W	Section modulus [mm^3]
A	Load area [mm^2]

Latin lowercase

$r_ø$	Pore diameter [nm]
l	Length of the support span [mm]
b	Specimen width [mm]
h	Specimen height [mm]

Greek letters and symbols

σ_f	Flexural stress [MPa]
σ_c	Compressive stress [MPa]
ρ	Density/Bulk density [kg/m^3]
δ	Deflection [mm]

Chemical formulas

Al_2O_3	Aluminum oxide/Alumina/Corundum
$Al(OH)_3/Al(OH)_3/AH_3$	Aluminum hydroxide/Gibbsite/Bayerite/Norstrandite
$CaO·Al_2O_3·10H_2O/CAH_{10}$	Calcium aluminate decahydrate
$CaCO_3$	Calcium carbonate/Calcite/Vaterite/Aragonite
$Ca(OH)_2$	Calcium hydroxide/Portlandite/Slaked lime
$CaMg(CO_3)_2$	Calcium magnesium carbonate/Dolomite
CaO	Calcium oxide/Quicklime
$3CaO·2SiO_2·3H_2O/C\text{-}S\text{-}H$	Calcium silicate hydrate
$CaSO_4·2H_2O/CSH_2$	Calcium sulfate dihydrate/Gypsum
CO_2	Carbon dioxide
$Ca_2Al_2SiO_7/C_2AS$	Dicalcium aluminosilicate/Gehlenite
$2CaO·Al_2O_3·8H_2O/C_2AH_8$	Dicalcium aluminate octahydrate
Ca_2SiO_4/C_2S	Dicalcium silicate/Belite
H_2O	Dihydrogen monoxide/Water
$Ca_{12}Al_{14}O_{33}/C_{12}A_7$	Dodecacalcium hepta-aluminate/Mayenite
$3CaO·Al_2O_3·3CaSO_4·32H_2O$	Hexacalcium aluminate trisulfate hydrate/Ettringite
FeO	Iron (II) oxide/Ferrous oxide/Wüstite
Fe_2O_3	Iron (III) oxide/ Ferric oxide/Hematite
Li_2CO_3	Lithium carbonate
$MgCO_3$	Magnesium carbonate/Magnezite
$CaAl_2O_4/Ca(AlO_2)_2/CA$	Monocalcium aluminate/Krotite
$CaAl_4O_7/CA_2$	Monocalcium dealuminate/Grossite
SiO_2	Silicon dioxide/Silica
$Ca_4Al_2Fe_2O_{10}/C_4AF$	Tetracalcium aluminoferrite/Ferrite
TiO_2	Titanium dioxide/Titania
Ca_3SiO_5/C_3S	Tricalcium silicate/Alite
$3CaO·Al_2O_3·6H_2O/C_3AH_6$	Tricalcium aluminate hexahydrate/Katoite

Notations and abbreviations

CAC	Calcium aluminate cement
DTA	Differential thermal analysis
HAC	High-aluminate cement
HPC	High-performance concrete
LWA	Lightweight aggregate
LWAC	Lightweight aggregate concrete
LWC	Lightweight concrete
LWCC	Lightweight cement-based composite
LWRC	Lightweight refractory concrete
LWRCC	Lightweight refractory cement-based composite
PE	Polyethylene
PP	Polypropylene
PVA	Polyvinyl alcohol
PC	Portland cement
SEM	Scanning electron microscope
TGA	Thermogravimetric analysis

Objectives of the study

Operation at high temperatures is of fundamental importance to many major sectors of industry, including material production and processing, chemical engineering, power generation, and more. Refractory materials ensure the stability of load-bearing construction members. They limit the generation and spread of heat, fire, and smoke.

The objective is to achieve a convenient lightweight refractory cement-based composite (LWRCC) with a maximum efficiency, optional shape, and acceptable manufacturing and operating costs.

Key factors in meeting this objective:

- Utilization of environmentally friendly components,
- Application of fibers,
- Easy workability in arbitrary shapes,
- Achieving values of density less than 1800 kg/m^3,
- Sufficient dimensional stability,
- Prevention of explosive spalling under temperature loads,
- Satisfactory residual strength after exposure to temperatures up to 1000 °C.

Chapter 1

Introduction

1.1 Role of research and development

Building materials have evolved not only with trends, but also with demands for durability, size, and control over surrounding environments. With the developing knowledge of structures and material behavior, it is possible to create materials of higher properties, e.g., by improving the properties of existing raw materials or by managing the production of entirely new materials.

In the context of technological possibilities, the processing and production of composite materials are becoming increasingly used. Composites allow the development of new properties with significantly more efficient utilization. Due to the demand for new building materials, it is necessary to actively participate in the development of composite materials. Composites are very advantageous materials because they are essentially made for the final application, not only with their structure and properties but also with the manufacturing technology. It is necessary to consider not only the correct selection of raw materials but also their mixing ratio [1].

1.2 Background

The development of new refractory materials for thermal insulation is crucial for the improvement of the technical and economic performance of furnaces and thermal units for different purposes [2]. Such materials are commonly used for furnaces and all kinds of thermal equipment to resist various physical and chemical changes and mechanical actions. Refractory materials can be divided into several classes based on the manufacture procedure, chemical composition, porosity content, and the method of application [3].

One of the most well-known techniques for the production of refractories and ceramics is the mixing of several components in the form of powder, formation of the mixture to the final shape, and firing to the suitable temperature, where the desired properties are attained [4]. Different bonding systems, such as a ceramic bond, hydraulic bond, and organic bond, can be used for the formation of refractories. The ceramic bond is a bond that is activated through ceramization reactions at high temperatures, while the hydraulic bond is ensured by the hydration of cement added to the product [5].

The production of refractories with the ceramic bond is carried out by a complex, energy-extensive technology. It is associated with high energy consumption for drying and high-temperature burning. On the basis of refractories with the hydraulic bond, it is possible to produce large-sized products with an intricate shape, as well as a monolithic lining that does not require burning [2]. The properties of such refractory materials depend mainly on the type of cement/binder and the fine refractory additives used for its manufacturing. The structural concrete made with Portland cement (PC), the most common type of cement in general use, reaches a critical stage at a temperature of over 500 ˚C, which causes the material disintegration of traditional concrete. It is worth mentioning that even very resistant concrete is not able to withstand the effects of high temperatures. Therefore, aluminous cement is used as a binder component of the experimental composites designed in this research. The quality of aluminous cement is mainly specified by the amount of aluminum oxide (Al_2O_3). The maximum working temperature of aluminous based concrete is over 1400 ˚C. The basic physical and mechanical properties of composites based on aluminous cement were investigated in previous experiments [6].

Lightweight Concrete (LWC), or a Lightweight Cement-Based Composite (LWCC), is an effective and easy way to reduce the dead load of the structure. LWC is mainly formed by porous materials and high contents of air bubbles. That is the reason why its coefficients of heat conduction and linear expansion are smaller than those of ordinary concrete. Therefore, LWC provides better thermal conservation, high-temperature resistance, and fire endurance.

A number of studies have investigated the strength and shear behavior of LWC for its application in construction [7–9]. The problem of LWC occurs at the quarry. Lightweight concrete has a significantly lower fracture toughness and tensile strength than normal concrete. The lack of fracture toughness is commonly solved by the application of fibers. Various short fibers are often used to increase the tensile strength and reduce the brittleness of concrete. They ensure the increase of the material's load capacity [10–14]. Current experience suggests that in the case of fiber-reinforced concrete, crack formation and crack widths are reduced, especially at an early age. It allows better operational resistance than fiber-free concrete due to the limited volume changes and increased tensile strength [15–17]. Fibers can be made of natural materials such as asbestos, sisal, basalt, and cellulose or artificial ones such as glass, steel, carbon, and polymers. However, not all these fibers can be successfully used in refractory composites due to their flammability. Refractory fibers significantly contribute to the reduction of crack formation, which is associated with structural transformation due to high temperatures [18–20]. This has a positive impact on the residual properties of refractories [21, 22].

1.3 Scope of the work

The thesis starts with an introduction. The second chapter continues with the analysis of the effect of high temperatures on common concrete. It describes the cause of explosive spalling and how to prevent it. Furthermore, the chapter presents an overview of the available knowledge about refractory concretes. In the third chapter, the preparation of experimental specimens and acquaintance with selected components for their creation are described. Considerable effort has been placed on reducing the density of the refractory specimens by adding an air-entraining additive and environmentally friendly products. Subsequently, the specimens were subjected to a high-temperature treatment. In the fourth part of the work, the results of the designed LWRCC compositions were provided by physical and mechanical testing after exposure to different levels of high-temperature loading. The results are graphically analyzed, then compared and discussed. In the fifth and the last chapter, the most important findings are summarized according to the set objectives, and the requirements for subsequent experiments are stated.

Chapter 2

State of the art

2.1 Fire resistance

According to the EN 13501-1 European Standard, building materials can be classified in terms of their reaction and resistance to fire, which will determine whether a material can be used and when additional fire protection needs to be applied to it. Another important European Standard is the fire resistance of building structures, which is defined in EN 13501-2. Fire resistance means the ability of a building structure to withstand the effect of a fully developed fire.

Fire resistance is an essential issue for any structural element, rather than a generic building material. Structural elements must have an adequate resistance to fulfill their designed function for a certain period of time in the event of a fire. That time is classified in stages from 15 to 180 minutes. The designed function depends on the element's position and role within the structure, and the time component related to the time elapsed before one of the fire limit states below is breached:

- The structure should retain its load-bearing capacity.
- The structure should protect people from flames and harmful gases.
- The structure should shield people from heat.

During a fire, no temperature growth higher than 140 ºC should occur on the side of the structure which is not exposed to the fire. The heat flux generated by a fire in concrete structures produces differential temperatures, moisture levels, and pore pressures. These changes can critically affect the concrete's function at the mentioned limit states.

2.2 Concrete and high temperatures

Concrete is a heterogeneous multiphase composite material with relatively inert aggregates held together by a hydrated cement paste. The cement paste is generally composed of 70–80 % of a layered calcium-silicate-hydrate (C-S-H) gel, 20 % of calcium hydroxide/Portlandite ($Ca(OH)_2$), and other chemical compounds [23]. C-S-H is produced by the reaction of tricalcium silicate (C_3S) or dicalcium silicate (C_2S) with water. It is frequently described as a gel rather than a crystalline material because no consistent structure is discernible using the X-ray diffraction. Its composition is also variable, but stoichiometrically it usually contains approximately twice as much calcium oxide (CaO) as silicon dioxide (SiO_2) plus a quantity of water. Because it has no fixed composition, it is usually written as C-S-H, implying no particular stoichiometry[24]. Bonding water within the layers (gel water) determines the strength, stiffness, and creep properties of the cement paste via hydrogen bonds [25].

The bond region is affected by the surface roughness of the aggregate and its chemical/physical interactions [26]. The chemical interaction relates to the chemical reactions between the aggregate and the cement paste that can be either beneficial or detrimental. The physical interaction relates to the dimensional compatibility between the aggregate materials and the cement paste. Although concrete is non-combustible and has the highest fire resistance classification (class A1) under EN 13501-1:2007- A1:2009, a fire impact on concrete causes a decrease in its quality. EN 13501-1:2007-A1:2009 specifies the fire classification method for construction products and building members.

The behavior of concrete at high temperatures depends on the exposure conditions. Concrete is sensitive to the temperature level, heating rate, thermal cycling, and temperature duration (as long as chemical and physical transformations occur). Concrete undergoes sequences of structural changes at elevated temperatures and the whole structure of the cement paste degrades and the bearing capacity decreases rapidly [27]. Table 2.1 presents the summary of the environmental factors that affect heated concrete and indicates their relative influence [25].

Table 2.1 Influence of environmental factors on heated concrete [25].

Factor	Influence	Comment
Temperature Level	*	Chemical-physical structure and most properties.
	**	The properties of some concrete (e.g., compressive strength and modulus of elasticity) heated up to about 500 °C and under 20–30 % load can vary less than if heated without load.
Heating Rate	*	>5 °C/min: Becomes significant → explosive spalling.
	**	<2 °C/min: Second order influence.
Cooling Rate	*	<2 °C/min: Negligible influence.
	**	>2 °C/min: Cracking could occur.
	*	Quenching with very significant influence.
Thermal Cycling	**	Sealed concrete: Influence in so far as it allows a longer duration of temperature for hydrothermal transformations to develop.
	**	Unsealed concrete: Significant influence mainly during the first cycle at a given temperature.
Duration at temperature	*	Sealed concrete: Duration at a temperature above 100 °C → Continuing hydrothermal transformation.
	**	Unsealed concrete: Only significant at early stages while transformation decay.
Load-Temp. Sequence	*	Essential, not usually appreciated.
Load Level	*	<30 %: Linear influence on Transient Creep at least in the range up to 30 % cold strength.
	*	>50 %: Failure could occur during heating at high load levels.
Moisture Level	*	Sealed: A very significant influence on the structure of cement paste and properties of concrete above 100 °C.
	**	Unsealed: Small influence on thermal strain and transient creep, particularly above 100 °C.

* First order influence; ** Second order influence

An unsealed cement paste (i.e., allowed to dry) behaves very differently from a moist sealed cement paste above 100 °C, the former is dominated by dehydration processes, while the latter is dominated by hydrothermal chemical transformations and reactions [28].

Under normal conditions, most concrete structures are subjected to a temperature of ambient environmental conditions. However, there are important cases where these structures may be exposed to much higher temperatures (e.g., building fires, chemical and metallurgical industrial applications in which the concrete is in close proximity to furnaces, etc.) [25]. The problematic behavior of concrete, silicate-based composites, and concrete structures at elevated temperatures is still the object of interest, due to the wide range of different types of concrete and reinforced concrete structures exposed to short- and long-term temperature loads in the range from 100 to 1200 °C. The effect of temperature depends mainly on the composition of concrete, its density, and homogeneity [28].

2.2.1 Effect of elevated temperatures on concrete and concrete structures

The analysis of changes in the cement matrix and the study of transport phenomena are rather complicated. Concrete's thermal properties are more complex than for most materials because not only is concrete a composite material whose constituents have different properties, but its properties also depend on moisture and porosity. Thermally-induced dimensional changes, a loss of structural integrity, and release of moisture and gases resulting from the migration of free water can adversely affect the physical, thermal, and mechanical properties of concrete and the safety of concrete structures [25].

The behavior of concrete under the effect of high temperatures is well described in research studies [29–32]. When a concrete member is exposed to a high temperature, changes are seen in its physical and mechanical properties. These changes occur in the form of crack formation, disintegration and dispersion in concrete, and a decrease in the compressive strength and elasticity modulus [33].

2.2.1.1 Effect of elevated temperatures on cement paste

Apart from the crystalline transformations occurring mainly in the aggregate materials during heating, several degradation reactions occur primarily in the cement paste resulting in a progressive breakdown in the structure of concrete. An increase in temperature produces significant changes in the chemical composition and microstructure of the hardened PC paste [25].

The heating of the cement paste results in drying. Water gets gradually loose from the material. The order in which water is removed from heated concrete depends on the energy that binds the water and the solid. First, free water from the cement paste evaporates through the capillaries, then physically and chemically bound water leaves the material. The process of removing water that is chemically bound to the cement hydrate is the last phase [27]. The dehydration process of the cement paste only considers the structural water in the paste that cannot evaporate. The water in the hydrated cement paste is classified according to the degree of difficulty to be removed. Besides the water vapor in the pores, there are four types of water [34]:

- *Capillary water* is the water that exists in the pores larger than about 5 nm. Capillary water is not affected by the attractive force exerted by the solid surface. Two subcategories of capillary water according to the pore diameter $r_{ø}$ are defined. The water in larger pores ($r_{ø}$ >50nm) is called free water because its removal will not significantly change the volume of the paste; the water in smaller pores (50nm >$r_{ø}$ >5nm) is held by capillary tension, and its removal will cause the shrinkage of the paste.

- *Adsorbed water* is the water that is adsorbed on the solid surface, which is influenced by attractive forces. A major portion of adsorbed water can be lost when the relative humidity is less than 30 %.

- *Interlayer water* is the water existing in the C-S-H structure. That interlayer water will be lost when the relative humidity is less than 11 %.

- *Chemically bound water* is an integral part of the microstructure of hydrates. This kind of water cannot be removed by decreasing the relative humidity of the environment alone. It can be removed when the hydrates are heated, and dehydration processes are triggered.

The capillary water, adsorbed water, and interlayer water are also called evaporable water, which cannot be retained after drying. Non-evaporable water includes the chemically bound water in hydrates [34].

The drying of cement pastes is required before the microstructure investigation using the gas adsorption technique. An ideal drying method, which would give reproducible results that could not only perfectly remove the "non-bound" water but, at the same time, preserve the microstructure, unfortunately, does not exist. The D-drying method is favored by many cement laboratories as the best standard drying method and is believed to be efficient in removing completely the non-bound water and to be the best microstructure preserving drying method compared to other methods [35].

Changes in the chemical composition and microstructure of a hardened PC paste occur gradually over a temperature range from room temperature to 1000 °C. At room temperature, between 30 and 60 % of the saturated cement paste is occupied by evaporable water, which is driven off at a temperature of about 105 °C. At temperatures above 105 °C, the strongly absorbed and chemically combined water (i.e., hydration water) is gradually lost from the cement paste hydrates, with the dehydration essentially completed approximately at 900 °C (at 1 atm pressure) [25].

The mechanical properties of the cement paste are strongly affected by the chemical bonds and cohesion forces between the sheets of the C-S-H gel. It is assumed that about 50 % of the cement paste strength is provided by the bond strength (large C-S-H gel sheet area); therefore, when the temperature increases beyond 400 °C, the evaporation of water between the C-S-H gel sheets strongly affects the mechanical properties of the cement paste [36]. Thanks to the chemical and mineralogical composition, portlandite is among the dominant products of cement hydration. The effect of temperature leads to the decomposition of portlandite at intervals approximately from 460 to 540 °C. This reaction

can be described by the equation $Ca(OH)_2 \rightarrow CaO + H_2O$[27]. At a temperature of 800 °C, C-S-H breaks down completely. Therefore, the critical temperature for concrete ranges from approximately from 400 to 900 °C. In this range, concrete loses most of its strength [37].

The dehydration process of the C-S-H gel causes a decrease in the volume of hydrates, which increases the porosity of the cement paste. The total volume of pores grows; consequently, the average size of the pores grows, too. This has a naturally inapt effect on the mechanical properties of the whole concrete. The shrinkage of the hydrated phase and the expansion of the non-hydrated phase results in the strain in the cement paste. The cement paste expands around 200 °C, while it shrinks intensively after exceeding this temperature [27].

The heating of concrete makes its aggregate volume grow, and at the same time, it causes the counteraction of the cement paste which surrounds it. As a result, the cement paste-aggregate bond is the weakest point in the heated concrete [37].

2.2.1.2 Effect of elevated temperatures on aggregate

The aggregate, like nearly all solid substances, expands with increasing temperatures. Therefore, the thermal expansion of the aggregate is an important property as regards the influence of higher temperatures. Thermal expansion of an aggregate depends on its mineralogical composition since all minerals differ in their thermal expansion properties. The type of minerals governs the chemical and physical changes that occur during heating [37]. Polymineralic stones may be prone to the disintegration that results from the thermal incompatibility of their components. For those stones, differences in thermal strain can cause intercrystalline stresses and failure [36].

To a large extent, damage to concrete is caused by cracking, which arises due to mismatched thermal strains between the coarse aggregates and the matrix. Figure 2.1 shows an example of thermally damaged concrete which is made with silico-calcareous aggregates and heated to 600 °C [36].

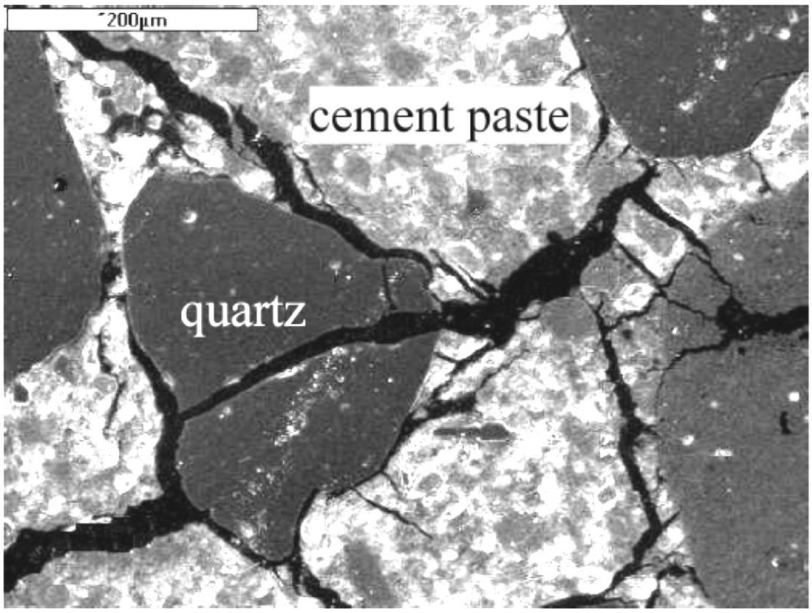

Fig. 2.1 Microstructure of concrete heated to 600 °C (HPC, 50×) [36].

A suitable aggregate for high-temperature-resistant concrete has to prove a low coefficient of thermal expansion and negligible residual strain [27]. For example, the concrete containing basalt aggregates has a lower thermal expansion coefficient than the concrete containing calcareous aggregates. Aggregates normally occupy 70–80 % of the volume in concrete, therefore, the behavior at elevated temperatures is strongly influenced by the type and properties of the aggregate [37, 38]. The commonly used aggregate materials are thermally stable up to 300–350 °C. The thermal stability of aggregates is a property that determines the effect of aggregates on the performance of concrete at high temperatures [39]. Thermally stable aggregates are characterized by chemical and physical stability at high temperatures, which is determined by dilatometry, as well as thermogravimetric analysis (TGA), and differential thermal analysis (DTA) [36].

A natural aggregate must not change its mechanical properties; primarily it must not lose its compressive strength and must not show changes in volume at higher temperatures. The aggregates that are thermally stable up to a given temperature show no weight loss, no thermal reactions, and negligible residual strain. Basalt, diabase, and andesite are the most suitable natural rocks. On the other hand, siliceous aggregates and granite are the least suitable rocks. Quartz containing aggregates and sands change normally at 573 °C due to the transformation of α-quartz (trigonal) to β-quartz

(hexagonal) with an accompanying increase in volume by approx. 5.7 %. This volumetric increase is clearly visible on the DTA curves in Figure 2.2 [36].

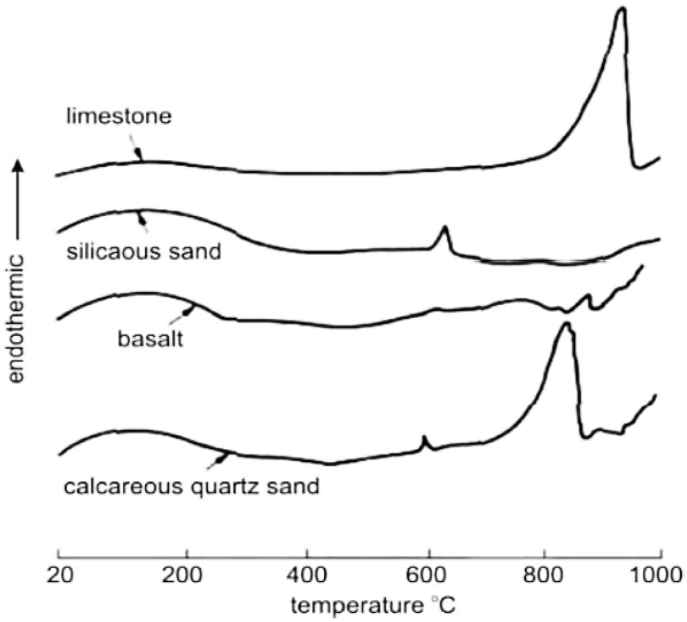

Fig. 2.2 DTA of four types of aggregates, measured during heating at 10 °C/min [36].

Most non-siliceous aggregates such as magnesite ($MgCO_3$), dolomite ($CaMg(CO_3)_2$), and limestone (different crystal forms of $CaCO_3$) are stable up to about 600 °C [25]. Calcium carbonate ($CaCO_3$) decomposes completely into quicklime (CaO) and carbonate dioxide (CO_2) between 900–950 °C, with partial dissociation occurring at temperatures as low as 700 °C [25]. Additionally, the CaO formed during decarbonation may hydrate when cooling, with a consequent 44 % expansion.

Further heating of an aggregate leads to its melting. The melting temperature varies along with the mineralogical composition, for most igneous rocks it is above 1000 °C. The melting temperature of granite is 1210–1250 °C, while basalts melt at 1280 °C, which is accompanied by gas release and expansion [36]. For example, the thermal stability of different types of siliceous and calcareous aggregates subjected to high temperatures is presented in the research of Niry [40] and Savva [41].

2.2.2 Effect of fire on concrete and concrete structures

The interest in the behavior of concrete at high temperatures mainly results from the many cases of fires taking place in buildings, high-rise buildings, tunnels, and drilling platforms [36]. Fire represents one of the most severe risks to buildings and structures. Being a primary construction material, the properties of concrete after exposure to fire have gained a great deal of attention since the 1940s [42].

Once a fire starts and the contents and/or materials in a building are burning, then the fire spreads via radiation, convection, or conduction with flames reaching temperatures of between 600 and 1200 °C, even up to 1350 °C in tunnels [37]. Harm is caused by the combination of the effects of smoke and gases which are emitted from burning materials, and the effects of flames and high air temperatures. Concrete itself is considered a construction material that provides satisfactory fire resistance properties, in the majority of applications, concrete can be described as potentially ‘fireproof‘. It does not produce any toxic fumes, smoke, or drip molten particles when exposed to fire, unlike some plastics and metals, so it does not add to the fire load.

However, it needs to be emphasized, when a concrete structural member is exposed to a fire, a number of physical and chemical changes can occur. These changes have a final impact on the mechanical and deformation properties of the concrete structure. Table 2.2 show related temperature levels within concrete (not the flame temperature) with some indicative changes in its properties. The exception is explosive spalling, where the temperature range is on the concrete surface and depends on the heating rate and the type of concrete [28].

Table 2.2 List of changes taking place in concrete during heating [28, 36].

Temperature range	Changes
20–80 °C	Slow capillary water loss. Reduction in cohesive force as the water expands.
80–150 °C	Noticeable increase in "hot" water permeability. Loss of chemically bound water starts. Ettringite dehydration ($3CaO \cdot Al_2O_3 \cdot 3CaSO_4 \cdot 32H_2O$).
150–170 °C	Gypsum decomposition ($CaSO_4.2H_2O$).
170–200 °C	C-S-H gel dehydration. Loss of physically bound water increase in internal pore pressure.
200 °C	Beginning of explosive spalling.
300–400 °C	350 °C, break up of some siliceous aggregates. 374 °C, the critical temperature of water, then free water is no longer present.
400 °C	Formation of cracks.
400–600 °C	460–540 °C, Portlandite decomposition $Ca(OH)_2 \rightarrow CaO + H_2O$. 573 °C, $\alpha \rightarrow \beta$ quartz expansive inversion. Marked increase in "basic" creep.
600 °C	Concrete is not functioning at its full structural capacity.
600–800 °C	Second phase of the C-S-H decomposition, formation of β-C_2S.
800–1000 °C	Total loss of water of hydration. Ceramic binding initiation which replaces hydraulic bonds. 900–950 °C, Calcite decomposition $CaCO_3 \rightarrow CaO + CO_2$ (release of CO_2).
1000–1300 °C	Melting of some concrete components.
1300 °C	Total decomposition of concrete.

One of the main problems is the above-mentioned explosive spalling of concrete at high temperatures, which is caused by tension inside the cement matrix. In some special cases, even a much lower temperature may cause explosive spalling of concrete, which results in a loss of material endangering the bearing capacity of the concrete member. Consequently, both the separating/insulating and load-bearing functions of the concrete member could be compromised [28, 36]. Any concrete exposed to temperatures above 300 °C is removed and replaced. In reality, the behavior of concrete in a fire can be rather complex and will very much depend on a number of factors including mix the design, imposed loads, and structural design.

2.3 Explosive spalling

The spalling of concrete exposed to a fire is understood to be an explosive detachment of large or small pieces of concrete from the concrete surface subjected to heating. The action of explosive spalling is caused by the accumulation of steam when releasing physically bound water. The factors influencing this phenomenon are:

- *Heating rate* (especially above 3 °C/min) has a significant influence on the occurrence of explosive spalling. The probability and severity of explosive spalling increase with the increase in the heating rate. However, when spalling does occur, it does so within a consistent temperature range, regardless of the heating rate [43].

- *Permeability* of the material is an important factor influencing the critical pressure level because it affects the rate of vapor release. Concrete of higher quality generally possesses higher density and, therefore, offers lower permeability.

- *Pore saturation level* (especially above 2–3 % moisture content by the weight of concrete), however, it has been found that even a small amount of moisture can cause the spalling of concrete [44]. It indicates that a fixed limit on the moisture content does not prevent concrete from spalling.

- *Type of aggregate*: the importance of the aggregate is often seriously underestimated. The probability of explosive spalling is substantially lower for concrete containing low thermal expansion aggregates.

- *Reinforcement:* the presence or absence of reinforcement was found to be a more important factor in spalling than the amount of reinforcement. However, the congestion of steel bars or tendons, with only small spaces between them, is considered to induce the formation of cracks and may, therefore, promote spalling [43].

- *Thickness of concrete members*: explosive spalling is unlikely to occur in very thin members, because moisture tends to escape more readily, thus preventing the build-up of pore pressure. Experimental evidence also suggests that explosions are less likely in thick members greater than about 200–300mm. Explosive spalling is, therefore, most likely to occur in 'medium' size members [43].

- *State of stress*: applied loads and restraint increase the susceptibility of concrete members to spalling. An increase in compressive stresses, either by a reduction in the section size or an increase in loading, encourages explosive spalling [43].

- *Heating profile*: heating from two faces encourages spalling more than heating from one face only. Because of their exposure to fire on one side, slabs behave more favorably than beams regarding explosive spalling. Corners, especially acute-angled ones, have a marked spalling tendency. It is, therefore, preferable to employ structural members with simple external shapes without pronounced projecting features [43].

Spalling results in a reduction of the load-bearing capacity of a concrete member. Spalling can be divided into four categories: (1) aggregate spalling; (2) local dislodging of relatively minor portions of the surface or edges; (3) explosive dislodging of small pieces of concrete from the surface; (4) explosive dislodging of a few large pieces of concrete, resulting in a gradual reduction of the cross-section. The first three types occur during the first 20–30 min of a fire and are influenced by the heating rate, while the fourth occurs after 30–60 min of a fire and is influenced by the maximum temperature [28]. The spalling of concrete is described in the literature worldwide [30, 36, 45, 46].

2.3.1 Mechanisms of explosive spalling

There are two mechanisms of explosive spalling:

- thermal stress spalling,
- pore pressure spalling.

They act singly or in combination depending upon the section size, material, and moisture content. At a sufficiently high heating rate, dry concrete can experience explosive spalling. This is attributed to the excessive thermal stress generated by rapid heating and results in temperature gradients that induce compressive stresses close to the heated surface (due to restrained thermal expansion) and tensile stresses in the cooler interior areas. Surface compression may be augmented by loads or prestress, which are superimposed upon the thermal stresses [43]. In experiments, it is possible to separate the two forms of spalling. For example, thermal stress spalling would not develop in concrete that has zero thermal expansion as experienced with some lightweight aggregate concretes [47]. This allows the determination of the influence of pore pressure spalling. However, it should be noted that a lightweight aggregate is highly porous and the additional moisture in the pores would promote pore pressure spalling [47].

As the temperature rises, the water vapor pressure increases. If the microstructure of the concrete is open, usually due to a high water-cement ratio, the vapor can escape rapidly, thereby significantly reducing its pressure. On the other hand, if the concrete has high density and low porosity, the water vapor pressure can reach high values. Heating causes water to transport into a cooler area creating a fully saturated layer of concrete. This area is characterized by low permeability and acts as an impermeable barrier for gases. In parallel, the temperature rise changes the water into steam, which cannot escape. This results in the internal pressure build-up (up to 3 MPa) [36]. That exceeds the concrete's tensile strength, and the concrete surface layer breaks due to high internal pressure. This state is particularly observed in HPC (high-performance concrete) [46, 48], which is often used for tunnels and bridges. HPC is characterized by low permeability and so the pore pressure can build up easily.

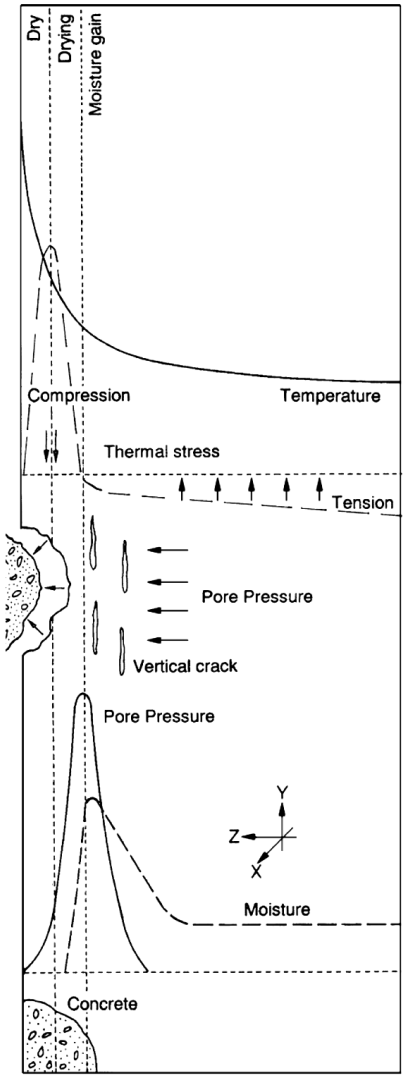

Fig. 2.3 Combined thermal stress and pore pressure in triggering spalling [43].

Explosive spalling generally occurs in the early stages of a fire during a rapid heating of the surface, under a combined action of pore pressure, compression in the exposed surface region, and internal cracking (see Figure 2.3). Cracks develop parallel to the surface when the sum of the stresses exceeds the tensile strength of the material. This is accompanied by a sudden release of energy and a violent failure of the heated surface region [43].

According to other explanations [36], spalling results from brittle fracture and delamination buckling caused by compressive biaxial thermal stresses parallel to the heated surface. It was also pointed out that the internal pressure build-up cannot be the only reason for the spalling occurrence. When a crack produced by the pore pressure starts to open, the internal pore pressure immediately drops. Thus, it has been concluded that

the pore pressure can only act as a trigger for the spalling phenomenon. Once the pore pressure has triggered the cracking, its growth and the resulting explosive spalling depend on the thermal stresses. Therefore, this complex phenomenon still remains difficult to understand.

2.3.2 Prevention of explosive spalling

In terms of prevention, the most effective method to reduce the risk of explosive spalling would be to address the mechanisms in the design of a concrete mixture by adding (1) fibers, (2) an air-entraining agent, and (3) the use of low-thermal expansion aggregates. The risk of spalling is also reduced if the moisture content is low and the permeability of concrete is high. However, for the case of an existing structure, (4) a thermal barrier provides protection against spalling. The criteria for the thickness of thermal barriers are based on the maximum temperature.

An appropriate use of fiber reinforcement could limit the extent of spalling, although not prevent the phenomenon itself. Recently, it was found that the addition of 0.05–0.1 % by the weight of polypropylene fibers in a concrete mixture completely eliminated explosive spalling even in high strength concrete (60–110 N/mm^2) but not necessarily in ultra-high strength concrete (>150 N/mm2) [43]. The application of polypropylene fibers and their melting between 160–200 °C provide channels for moisture movement within the concrete, thus increasing its permeability and reducing the pore pressure [49–51]. It was proved that fibers with a higher slenderness ratio are more suitable. The porous structure of concrete is then more interconnected and the expanded water vapor has an easier way to escape without damaging the concrete [27].

The addition of the air-entraining agent has the effect of reducing the moisture content and increasing the absorption value. This reduces the pore saturation, thus alleviating pore pressure [26, 52].

It has been generally concluded that the concrete containing a low thermal expansion aggregate, especially lightweight aggregates (LWA), has a lower risk of explosive spalling. However, this only applies to concrete with relatively dry aggregates, since it has been shown that lightweight aggregate concrete (LWAC) has a high susceptibility to spalling if the aggregate is saturated [43, 48]. The water in LWAs either

comes from prewetting of the aggregates, absorption from fresh concrete, or penetration from the environment. The increased moisture content will lead to both an increased pore pressure and an increased temperature gradient during a fire. Thus, the moisture content is the direct factor for the explosive spalling of LWACs [53].

2.4 Refractory concrete

Refractory concrete is a special material that combines the properties of concrete and refractory building materials. Concrete with higher resistance to high temperatures implies higher demands for individual components. The most essential part of designing refractory concrete is the choice of a binder. Depending on the type of binder, refractory concrete is distinguished into:

- refractory concrete with a hydraulic binder (cement),
- refractory concrete with a chemical binder (water glass, etc.).

For the production of refractory concrete, used in the construction of thermal units, foundations of industrial furnaces, and other structures subjected to prolonged heating, calcium aluminate cement (CAC) is the most suitable binder [54–57]. CAC, also known as aluminous cement, is available from most cement producers today. The history of the CAC production started in the twenties of the 20th century. The rapid evolution of its initial mechanical parameters was convenient for the post-war requirements of the building industry at the time, which was focused on the restoration of the infrastructure [58].

CAC and its hydration products significantly control the final properties, behavior, and thermal resistance of concrete; in particular, the contact zone between the hydration products and the surface of aggregates and fibers is of importance [58]. Cement is the most important part. However, other components are also important: the aggregate, types of admixtures and additives, method of reinforcement, and addition of polypropylene fibers [27]. Water provides the necessary plasticity and hydration of the concrete mixture.

Care should be taken to ensure the accurate dosing of the components and good concrete compaction. The mixture is cold mixed in a mixer and compacted into molds. The mixture hardens at ordinary temperatures before drying. Refractory concrete is fired only during the high-temperature operation. All refractory concretes should be expected to decrease in strength after exposure to high temperatures.

2.4.1 Calcium aluminate cement (CAC)

CAC is a finely ground inorganic substance, fundamentally different from PC. It contains calcium aluminates compared to calcium silicates contained in PC, and silicate components are undesirable. According to the chemical composition (amount of Al_2O_3), CAC is divided into four classes, see Table 2.3.

Table 2.3 Classification of CAC [59, 60].

Major classes of CAC and typical chemical composition (%)						
Class	**Color**	**Al_2O_3**	**CaO**	**$FeO+Fe_2O_3$**	**SiO_2**	**TiO_2**
CAC 40	Light brown	37.5–45.5	36.5–39.5	12.0–18.0	1.6–5.0	<4.0
CAC 50	Light grey	50.8–54.5	36.0–39.0	1.0–10.0	2.0–5.5	<4.0
CAC 70	White	68.5–71.0	28.0–31.0	<0.5	0.2–0.6	<0.5
CAC 80	White	79.5–82.0	16.2–17.8	0.2	0.35	<0.3

CAC is made by grinding a solid compound formed by the fusion or sintering of high-iron bauxite and limestone (low purity), low-iron bauxite with limestone (intermediate purity), or aluminum hydroxide and hydrated/slaked lime (high purity). Bauxite is a sedimentary rock, a heterogeneous material composed primarily of one or more aluminum hydroxide ($Al(OH)_3$) minerals plus various mixtures of silica (SiO_2), iron oxides (FeO, Fe_2O_3), titania (TiO_2), and other impurities in trace amounts [61].

The main properties of CAC can be summarized as follows [62]:

- Working time is shorter than with ordinary PC (it can be retarded or accelerated using some chemical and/or mineral admixtures, e.g., lime, PC, Li_2CO_3, etc.). Generally, it is longer than 2 hours but shorter than 4 hours.

- High early strength (according to European Standards, at 6 and 24 hours must be higher than 18 and 40 MPa). Almost within 6 hours, it reaches such strength that it is higher than the 28 days strength value of ordinary PC.

- High abrasion resistance due to its high alumina content.

- High corrosion resistance and high durability under severe environmental effects such as sulfate attack, acid attack, etc. (In the hydration reaction of CAC, unlike in ordinary PC, no $Ca(OH)_2$ is formed. In addition, gypsum used in the PC production is not utilized in the CAC production. That is why the durability problem of PC, mainly due to the presence of $Ca(OH)_2$, does not occur in CAC).

- Refractoriness up to 1400°C (the significant amount of Al_2O_3 that possesses the refractoriness property by itself causes high heat resistance in CAC).

Despite all its properties, such type of cement has only limited applications nowadays; it is used mainly for special purposes. CAC is primarily used for (1) high heat refractory applications. Other uses include (2) applications where resistance to chemical, biological, and acidic attacks (pH >4) is required; (3) high-early-strength, (4) high-abrasion resistance, and (5) quick-setting mixtures; and (6) as part of the expansive component in some shrinkage-compensating cement.

CAC gains strength much faster than ordinary PC and predominantly consists of calcium aluminates that can produce large amounts of hydration heat, i.e., the heat evolved in the hydration reaction of calcium aluminate-based phases, during the first 24 hours. The main phase, which is responsible for this property, is monocalcium aluminate

(CA). This allows (7) the use of CAC in winter where conventional concreting is not possible. The hydration heat of CAC and ordinary PC is compared in Table 2.4.

Table 2.4 Comparison of hydration heat values of different types of cement [62].

Cements	Heat of hydration (cal/g) at				
	1 day	3 days	7 days	28 days	90 days
CAC	77–93	78–94	78–95		
Rapid hardening cement	35–71	45–89	51–91	70–100	
Ordinary PC	23–46	42–65	47–75	66–94	80–105

CAC is used to make concrete in much the same manner as PC. The most frequently used CAC has approximately 40 % of alumina (marked as CAC 40). CACs with higher alumina contents are used particularly for refractory applications, whereas those with alumina contents of especially 40 % are used for both refractory and partial structural applications [62].

Hydrated high-alumina cement (HAC), containing ≥70 % of Al_2O_3 (marked as CAC 70 or CAC 80), exhibits rapid strength gains (up to 96.5 MPa in 24 hours and 124.1 MPa in 28 days for a water-cement ratio of 0.5), and also has sufficient resistance to chemical corrosion and thus may be used as a refractory material at temperatures ranging from 1500 °C to 1800 °C [25, 59]. However, HAC costs several times more than common PC and must be protected against a water loss during curing. HAC develops a heat of curing ≈2.5 times higher than PC (which may develop cracking and strength reduction in thick sections) and can contribute to accelerated steel corrosion [25].

2.4.1.1 Mineralogical composition of CAC

As stated previously, the main phase of the most frequently used CAC 40 is monocalcium aluminate (CA), whereas the minor phases are dodecacalcium hepta-aluminate ($C_{12}A_7$), tetracalcium aluminoferrite (C_4AF), dicalcium silicate (C_2S), and dicalcium aluminosilicate (C_2AS). In the case of CACs with an Al_2O_3 content over 70 %, phases such as CA, monocalcium dialuminate (CA_2), and corundum (a crystalline form of Al_2O_3)

are present. The brief information about the mineralogical compounds of CAC is as follows [62]:

- *Monocalcium aluminate*: CA is the main constituent of all types of CAC. It is primarily responsible for the specific cementitious behavior of this type of cement. Its setting is slow, whereas it hardens very rapidly. It is formed by heating an equimolar blend of CaO and Al_2O_3 above 800 °C.

- *Monocalcium dialuminate*: CA_2 is the most refractory phase, however, requiring a long time to be completely hydrated.

- *Dodecalcium hepta-aluminate*: $C_{12}A_7$ has low refractoriness and is contained in CAC in small percentages. The formation of a hydrate from this mineral and CA represents the first stage of strength development. Nevertheless, $C_{12}A_7$ does not contribute to the strength. Because of its higher reactivity, leading to excessively rapid hydration, it is not regarded as a very desirable constituent of CAC except in minor amounts.

- *Tetracalcium aluminoferrite*: C_4AF is the second most abundant component of CAC 40. Despite this, it makes no or very little contribution to the setting and strength development.

- *Dicalcium silicate*: C_2S behaves as in PC, i.e., its hydration is slow and its contribution to strength is at later ages rather than at early ages.

- *Dicalcium aluminosilicate*: C_2AS is also known as Gehlenite. CAC generally contains a limited amount of SiO_2, mostly less than 5 %. That is why; both C2S and C_2AS are present in CAC in limited amounts. Like C_2S, C_2AS sets slowly and contributes to the strength after a considerable period.

2.4.1.2 Hydration of CAC

The hydration of CAC is an exothermic reaction that begins with the dissolution when water comes into contact with a cement particle surface [63]:

$$Ca(AlO_2)_2 + 4H_2O \leftrightarrow Ca^{2+} + 2Al(OH)_4^- \quad (2.1)$$

The dissolution of the cement anhydrous phase increases the concentrations of the Ca^{2+} and $Al(OH)_4^-$ ions in the solution. After some time, the concentration of these ions in water reaches the solubility limit, which is followed by the precipitation of the hydrated calcium aluminate phase, favoring further dissolution of the anhydrous phase. As a result, a cyclic process of ion dissolution-precipitation proceeds until most (or all) of the anhydrous cement particles exposed to water have been consumed [63].

Meanwhile, the pH value of the liquid phase increases up to 12. It is followed by the nucleation and precipitation of the calcium aluminate hydrate crystals and gibbsite (crystalline form of AH_3). These hydrate crystals start to precipitate close to the unreacted clinker surface by forming a gel layer which is permeable to water. Therefore, further hydration of the underlying clinker grains occurs easily as a continuous process as long as enough water for dissolution and hydration is available [62].

As seen in Figure 2.4, at the initial stage, the hydration crystals form a gel layer coating the unreacted grains. The mixture is still plastic. Depending on the progress in the crystal formation as a result of continuous dissolution-precipitation, the hydrated phases tend to form strong bonds among the neighboring clinker grains, resulting in the so-called setting phenomenon. As the hydration proceeds further, the bonds between the cement grains gain strength, also referred to as the hardening of a cement paste. Finally, the final stable structure is formed when the water is used up and no further hydration crystal grows [62, 63].

Minerals (CA, $C_{12}A_7$) dissolving in water ← Continuous dissolving and precipitation

$Ca^{2+} + Al(OH)_4^-$

↓

Oversaturation, pH rises up to 12

↓

Precipitation of CAH_{10}, C_2AH_8, C_3AH_6, and AH_3 crystals →

↓

Growth of crystals around cement grains (cement setting)

↓

Bonding between cement grains (strength development)

Fig. 2.4 Summary of the CAC hydration mechanism [62].

As mentioned before, the hydration of CAC is an exothermic reaction in which a certain amount of heat is released causing an increase in the cement paste temperature. A small temperature increase is observed when the hydration of calcium aluminate begins (region I, Figure 2.5), which is followed by a dormant period (region II). The hydrate precipitation is followed by an increase in the heat released (region III) [63].

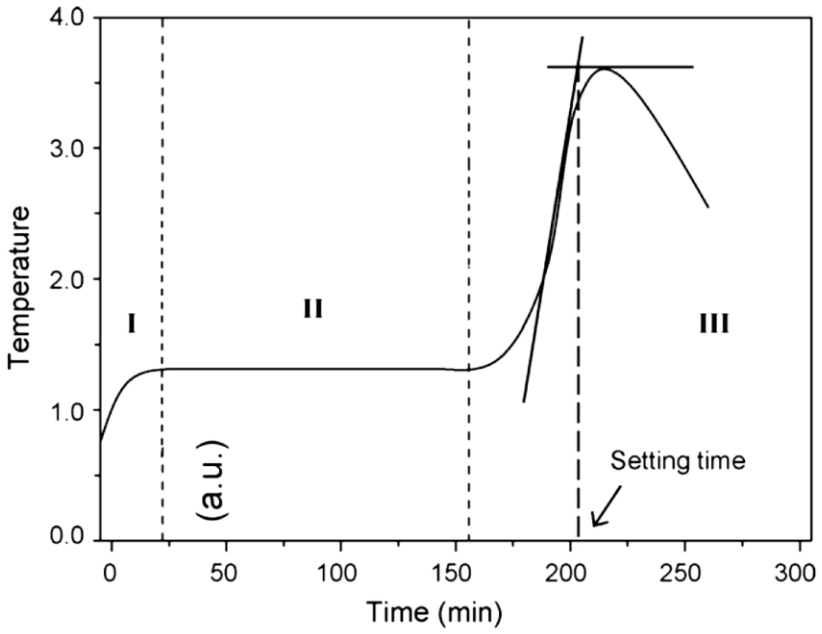

Fig. 2.5 Schematic representation of the temperature profile as a function of time for a CAC paste [63].

The hydration process is faster in comparison with PC, therefore, the setting time (time between the initial and final set) is shorter. That is also connected with a higher hydration heat [64]. The hydration of CAC is essentially different from the hydration of PC since the resulting calcium aluminate hydrates depend on the temperature at which the hydration occurs:

Table 2.5 Hydration products depending on the surrounding temperature [59, 65–67].

	Estimated temperature ranges		Calcium aluminate hydrates
CA + 10H	10–27 °C	→	CAH_{10}
2CA + 11H	15–36 °C	→	C_2AH_8 + AH_3 amorph.
3CA + 12H	above 35 °C	→	C_3AH_6 + AH_3 cryst. + H

(C = CaO; A = Al_2O_3; H = H_2O)

The characteristics of refractory concretes largely depend on the initial CAC matrix characteristics, including its phase composition and structure, as well as on their changes under high temperatures.

Which hydration products are formed within solidified concrete depends to a certain extent on the holding temperature [65]. It is emphasized that the estimated temperature ranges are not strictly determined, because the composition of the hydration products is highly dependent on the self-heating of the binder mass due to the heat released in the CAC hydration [59]. Depending on the hydration product composition, the properties of freshly prepared concrete may differ. It is noted that the mechanical strength of the CAC matrix held at low temperatures is higher than that held at elevated temperatures [65]. However, it should be mentioned that the kinetics of cement hydration decreases at lower temperatures, resulting in a longer time for the cement paste to set [63].

Table 2.6 Characteristics of crystalline state CAC hydrates [59].

Hydrates	The chemical composition (%)			The structure	Density (g/cm^3)
	CaO	Al_2O_3	H_2O		
CAH_{10}	16.6	30.1	53.3	Hexagonal	1.743
C_2AH_8	31.3	28.4	40.3	Hexagonal	1.950
C_3AH_6	44.4	27.0	28.6	Cubic	2.527
AH_3	-	65.4	34.8	Hexagonal	2.420

In Table 2.6, the characteristics of the crystalline state hydrates are presented. The complete hydration of CA to the CAH_{10} phase needs higher amounts of water compared with those of CA to C_2AH_8 and C_3AH_6. For the formation of the CAH_{10} phase, the required water-solid ratio is 1.13, whereas for that of $C_2AH_8 + AH_3$ it is 0.63, and for that of $C_3AH_6 + AH_3$ it is 0.46 [62].

The CAH_{10} and C_2AH_8 hydrates are metastable and, after a certain period of time, they are transformed into C_3AH_6 and gibbsite. For example, at room temperature (≈20 °C), CAH_{10} can be transformed into C_3AH_6 (irregular cubic crystals), gibbsite, and water over several years [59, 68]. This process is called conversion.

2.4.1.3 Conversion of CAC hydrates

CAC is mostly not recommended for structural and load-bearing purposes. The reason for the forbiddance is the chemical phenomenon known as conversion, which causes a significant decrease in strength of the hardened CAC matrix [47]. Several collapses of load-bearing structures made from CAC in the seventies and eighties intensified the scientific research into CAC hydration products and their long-term properties [58].

The conversion kinetics depends on the temperature and humidity and is linked to the symmetry in the crystal structure of stable hydrates. The nucleation and growth of a symmetric crystal of C_3AH_6 require a simultaneous organization of the atoms in all three dimensions. By contrast, metastable hydrates are non-symmetric crystals with a strong orientation (plates), which nucleate and grow more easily [59].

The conversion of hydrates, according to the works [57, 68, 69], can be described by the reactions:

$$2CAH_{10} \rightarrow C_2AH_8 + AH_3 \text{ amorph.} + 9H \quad (2.2)$$

$$3C_2AH_8 \rightarrow 2C_3AH_6 + AH_3 \text{ cryst.} + 9H \quad (2.3)$$

$$3CAH_{10} \rightarrow C_3AH_6 + 2AH_3 \text{ cryst.} + 18H \quad (2.4)$$

The cubic form of C_3AH_6 is a thermodynamically stable product of CAC hydration with a higher specific density. According to the conversion reactions of CAH_{10} to C_3AH_6 given above, 60 % of chemically bound water is released causing a reduction in the hydrate volume by 53 %. On the other hand, throughout the conversion of C_2AH_8 to C_3AH_6, 37.5 % of chemically bound water is liberated, resulting in a decrease in the hydrate volume by 34 % [62]. Consequently, the conversion leads to increased binder porosity, cracking, a loss of integrity of CAC based concrete, and a gradual decrease of mechanical parameters, usually accompanied by visual changes when the binding part of such concrete turns red [58].

As noted above, conversion is affected by the temperature and humidity. The main factor affecting the conversion is temperature. Either the hydration temperature or the ambient temperature throughout the service life of CAC primarily determines the rate and the amount of conversion reactions of CAH_{10} and C_2AH_8 phases to C_3AH_6. As seen in Table 2.7, the conversion rate increases significantly as the temperature increases. At 5 °C, the completion of conversion takes more than 20 years and that is why it is not a wrong interpretation that there is no conversion. However, above 50 °C, the conversion process is almost immediate [62]. An increased temperature during the initial hydration may also accelerate the subsequent rate of conversion.

Table 2.7 The conversion rate of CAH_{10} and C_2AH_8 to C_3AH_6 depending on temperature [62].

Temperature (°C)	CAH_{10}	C_2AH_8
5	>20 years	>20 years
10	19 years	17 years
20	2 years	21 months
30	75 days	55 days
50	32 hours	21 hours
90	2 minutes	35 seconds

Although conversion is primarily temperature-dependent, the w/c ratio and humidity of the CAC matrix system throughout its service life play an important role. At higher temperatures, humidity is more crucial and, therefore, the time required for the completion of conversion increases greatly as the moisture content of the CAC matrix is reduced. In other words, conversion occurs more rapidly when the process occurs under humid conditions and the rate of conversion decreases significantly if the relative humidity drops below the saturation level of the CAC matrix [62].

2.4.1.4 Carbonation of CAC hydrates

As a result of the conversion phenomenon, there is a significant reduction in the diffusion resistance factor and an increase in the penetration of carbonate dioxide (CO_2) into the cement matrix by pores, capillaries, and other readily permeable sites. The presence of airborne CO_2 causes the carbonation of CAC hydrates to calcium carbonate ($CaCO_3$), aluminum hydroxide (AH_3), and water [55, 57]. In fact, primarily vaterite or aragonite are created, while calcite occurs later due to the recrystallization at higher moisture contents. The structure of aluminum hydroxide is in most cases amorphous, rarely bayerite or norstrandite can occur [64].

Carbonation occurs according to the following formulas:

$$CAH_{10} + CO_2 \rightarrow CaCO_3 + AH_3 + 7H \quad (2.5)$$

$$C_2AH_8 + 2CO_2 \rightarrow CaCO_3 + AH_3 + 5H \quad (2.6)$$

$$C_3AH_6 + 3CO_2 \rightarrow 3CaCO_3 + AH_3 + 3H \quad (2.7)$$

Practically, controlled carbonation can serve as a prevention for the conversion process because the metastable hydrates are transformed during the hydration, and thus no changes and porosity increase further occur. However, the formation of calcium $CaCO_3$ is not beneficial in terms of high-temperature resistance of CAC. The most affecting factors of the carbonation rate are the amount of CO_2, diffusion, permeability, high moisture content or humidity, and temperature [64].

Alkalinity can also play important roles. In the presence of alkalis, the decomposition of calcium aluminate hydrates, as well as aluminum hydroxide, is much faster. This process is the so-called alkaline hydrolysis and leads to a dramatic decrease in mechanical strength. However, this was observed when the pH factor was 14, while lower values show no significant impact on the mechanical properties or weight loss [64].

In comparison with conversion, or carbonation respectively, alkaline hydrolysis is a much faster process. The effect can be observed even after one week. Moreover, both conversion and alkaline hydrolysis have synergic effects. Due to conversion, the porosity increases which leads to the permeability growth, and thus alkaline hydrolysis goes up. In the case of alkaline hydrolysis, the amount of C_3AH_6 is significantly lowered, thus the equilibrium of the system is changed and, consequently, the conversion process is accelerated [64].

The effect of conversion and carbonation can be significantly reduced by high compaction, a small water coefficient (not exceeding 0.40), and a cement content of at least 400 kg/m^3. These steps significantly increase the diffusion resistance of the concrete and make the cement matrix so dense that it compensates for increased porosity [55, 57].

2.4.1.5 CAC hydrates at elevated temperatures

When CAC is heated, free, and physically and chemically bound water is removed from it. According to Antonovič [59], it is indicated that dehydration by heating follows the scheme:

$$CAH_{10} \rightarrow C_2AH_8 + AH_3 \text{ amorph.} \quad (2.8)$$

$$C_2AH_8 + AH_3 \text{ amorph.} \rightarrow C_3AH_6 + 2AH_3 \text{ cryst.} \quad (2.9)$$

$$C_3AH_6 + 2AH_3 \text{ cryst.} \rightarrow C_{12}A_7 + CA + H \quad (2.10)$$

$$C_3AH_6 + 2AH_3 \text{ cryst.} + A \rightarrow CA + H \quad (2.11)$$

First, at a temperature of 100 ºC, the weakly bound water in the amorphous AH_3 is removed, while CAH_{10} dehydrates at a temperature of 120 ºC. C_2AH_8 dehydrates in the range from 170 to 195 ºC, crystalline gibbsite in the range from 210 to 300 ºC, while the crystalline hydrate C_3AH_6 starts decomposing in the range from 240 to 370 ºC. After dehydration at a temperature of 500–800 ºC, $C_{12}A_7$ is formed, which, under heating at 1000 ºC, is converted to CA, CA_2 [59].

When focused on the strength development, during the temperature loading at about 300 °C, the mechanical strength starts to decrease due to phase dehydration. This decrease continues up to 1000 ºC, then the sintering process begins, which leads to a progressive growth in mechanical strength.

2.4.2 Aggregates for high-temperature applications

Many common coarse aggregates are unsuitable for high-temperature service because they contain quartz, which exhibits a large volume change at ≈573 °C. For the reasons of the reaction of aggregates to high temperatures, a suitable aggregate for concrete would be that with a low coefficient of thermal expansion and negligible residual strain. Accordingly, natural aggregates based on crushed stone and gravel suitable for use above 900 °C are limited to pumice, tuff, scoria, basalt, andesite, diabase, pyrophyllite, olivine, corundum, chromite, etc. [25, 27]. Table 2.8 presents some examples of typical aggregates for dense refractory concretes.

Table 2.8 Physical and mechanical properties of aggregates used in dense refractory concretes.

Type of aggregate	Density (kg/m^3)	Porosity (%)	Compressive strength (MPa)	Max. service temperature (°C)	Thermal conductivity (W/m.K)
Andesite	2200–2650	10.0–15.0	86–203	900–1100	0.60–1.26
Basalt	2700–3000	0.1–1.5	110–338	1050	0.80–2.90
Corundum	3900–4100	0.0–1.0	2500–3000	1650–1750	25.0–46.0
Diabase	2810–3030	0.3–2.7	124–303	1100–1200	0.70–0.76
Gabbro	2810–3030	0.3–2.7	124–303	1100–1200	1.70–2.50
Syenite	2600–2970	0.9–1.9	186–434	1050	1.84
Trachyte	2200–2700	0.0–10.0	35–88	930	1.72–2.51

In practice, most aggregates for refractory concretes contain mainly alumina (Al_2O_3) and silica (SiO_2) in various forms. Artificial aggregates are the most suitable aggregates for refractory concretes, which are likely to be exposed to extreme temperatures. After high-temperature treatment, crushed fireclay, bauxite, mullite, and calcined flint are stable up to temperatures of 1300 °C; aggregates such as fused alumina or carborundum can be used up to 1600 °C; for temperatures up to 1800 °C, special high-alumina cement (HAC), and a fused-alumina aggregate are required [25].

Artificial aggregates are also usually produced for some special purposes, for example, to produce lightweight refractory concrete. Such aggregates are generally characterized by a low bulk density. Some of such artificial aggregates are byproducts of an unrelated industrial process such as blast furnace slag, cinder, etc. Examples of lightweight aggregates for high-temperature purposes are shown in Table 2.9.

Table 2.9 Physical and mechanical properties of lightweight aggregates used in refractory concretes [25, 70, 71].

Compressive strength	Type of aggregate	Particle shape and surface texture	Density (kg/m^3)	Bulk density (kg/m^3)
Max.	Expanded clay	Rounded and slightly rough particles	Coarse 600–1600 Fine 1300–1800	300–900
↓	Sintered fly ash	Similar to expanded clay	1000–1900	600–1100
	Expanded shale and slate	Often angular, slightly rounded and smooth surface	Coarse 500–1400 Fine 1600–1800	400–1200
	Foamed blast	Irregular, angular	1000–2100	400–1100
	Furnace slag	Particles with rough and opened pore surface	1400–2200	800–1250
	Pumice	Rounded particles with open texture, but smooth surface	550–1650	350–650
	Sintered industrial waste	Angular with opened pored surface	1000–1600	500–800
	Expanded perlite	Rounded, angular shape and rough surface	200–950	100–300
↓	Expanded glass	Rounded with closed surface	300–1100	150–600
Min	Vermiculite	Cubical	100–600	60–200

Compressive strength	Type of aggregate	24hours water absorption capacity (%)	Max. service temperature (°C)	Thermal conductivity (W/m.K)	Compressive strength (MPa)
Max.	Expanded clay	5–30	1100	0.24–0.91	2.0–62.0
↓	Sintered fly ash	20	1100	0.32–0.91	2.8–55.0
	Expanded shale and slate	5–15	1100	0.19–0.91	1.4–27.5
	Foamed blast	10–15	1000	0.24–0.93	2.0–24.0
	Furnace slag	5–10	1000	0.24–0.93	2.0–24.0
	Pumice	50	950	0.21–0.60	2.0–14.0
	Sintered industrial waste	15	1000	0.35–0.67	2.0–7.0
↓	Expanded perlite	—	1000	0.16–0.39	0.7–6.5
Min.	Expanded glass	5–25	750	0.07	1.2–3.5
	Vermiculite	—	1100	0.16–0.26	0.7–3.5

2.4.3 Fiber reinforcement

There are two main reasons for fiber application in refractory concretes:

The first is to provide a free space for evaporating water during the exposure to high temperatures. As previously mentioned in section 2.3.2 "Prevention of explosive spalling", polymer fibers, such as polypropylene (PP), polyethylene (PE), and polyvinyl alcohol (PVA) fibers, are mostly used for this purpose. Several studies have addressed the application of these fibers and their ability to moderate the destructive effect of expanded water vapor [51, 72, 73]. Due to the low melting point, the fibers, at temperatures above 150 °C, evaporate from the concrete and form small cavities inside the hardened concrete.

The structure of concrete becomes more porous and expanded water vapor can escape without substantial damage to the concrete microstructure. This effect limits the development of cracks in the concrete structure and the spalling of surface layers. However, this may also lead to a small reduction in the compressive strength [50, 75, 76]. It was proved that fibers with a higher slenderness ratio are more suitable. The porous structure of concrete is then more interconnected and the expanded water vapor has an easier way to escape without damaging the concrete [27].

Another reason for the use of fibers in refractory cement-based composites is to achieve a better load-carrying capacity and significantly contribute to the reduction of crack initiation, which accompanies the volume changes caused by the structural transformation due to high-temperature impacts [15, 17, 77]. The final properties of fiber-reinforced concrete are influenced by the fiber type used. It is necessary to use a reinforcing material with satisfactory properties and the required resistance to fire/heat. The primary characteristics that are desirable for reinforcement are high modulus, high strength, and high thermo-mechanical stability [78].

Providing excellent properties, asbestos fibers were among the most widespread solutions in the fire protection of structures thru fiber reinforcement. However, several later studies have proved the negative effect of asbestos on human health [79, 80]. The inhalation of asbestos fibers causes both serious non-cancerous diseases, including

asbestosis, pleural hyalinosis, and acute pleurisy, and cancerous diseases themselves. Therefore, asbestos is completely banned nowadays in Europe and some other countries [79, 81, 82]. Asbestos is now being replaced by modern materials, such as basalt, synthetics, carbon, glass, or ceramics. The seriousness of the harmful effects of asbestos is being studied by scientists around the world even today [83–86].

The suitable resistance of concrete with fiber addition to elevated temperatures is involved in the quality of the interfacial bond between the matrix and the fibers, especially in relation to elevated temperatures, to achieve the transfer of stresses [74, 87]. Among the various types of fibers shown in Table 2.10, steel fibers are the most used for most structural and non-structural purposes. They are also utilized for the strengthening of thermal resistance of structural concrete [88, 89]. However, steel fibers are not suitable for refractory composites, due to their apparent decrease in mechanical properties at approximately 600 °C and a subsequent recrystallization [90–92]. In fact, the increase in tensile strength caused by steel fibers can produce more violent explosive spalling of dense concrete because of the sudden release of a greater amount of energy at higher temperatures [43].

Table 2.10 Physical and mechanical properties of fibers used in fiber-reinforced concretes.

Type of fiber	Density (kg/m^3)	Tensile strength (MPa)	Modulus of elasticity (GPa)	Elongation at break (%)	Specific heat capacity (J/kg.K)	Max. service temperature (°C)
AR glass fiber	2700	3241	73.0	3.6	840	726
E glass fiber	2600	3790	72.0	4.8	846	840
S glass fiber	2490	4890	87.0	5.4	740	1056
PP fiber	910	750	3.8	25.0	1290	170
PE fiber	930	103	132.0	45.0	625	150
PVA fiber	1380	1250	26.0	22.0	900	225
Aramid fiber	1440	3150	130.0	3.7	1420	560
HS Carbon fiber	1780	6000	235.0	2.0	921	2100
HM Carbon fiber	1790	2350	358.0	1.4	945	2050
Ceramic fiber	3880	3100	370.0	1.2	1130	1750
Basalt fiber	2700	4840	110.0	3.1	822	1050
Steel fiber	7850	2850	210.0	23.0	463	600

2.5 Lightweight refractory concrete

Lightweight concrete (LWC) is advantageous in terms of reducing the dead load of the structure and providing better thermal insulation, high-temperature resistance, and fire endurance than ordinary concrete [93–95]. A possible direction of the weight reduction of refractory concrete is adding lightweight aggregates (LWA). For example, aggregates such as pumice, expanded perlite, and expanded clay (also known as ceramsite), which are made by burning, naturally have excellent resistance to high temperatures [53]. The presence of an air-entraining agent is also beneficial [96]. An air-entraining admixture incorporates air into the concrete mixture and creating a satisfactory air-void system. Another tool to reduce the density of refractory concrete is by randomly oriented short fibers, which can also provide better properties relative to tensile strength, thermal shock resistance, and thermal stress resistance [25].

The interfacial transition zone characteristics of LWACs are different from those of ordinary concretes. The improvement of the paste–aggregate bonding by the penetration of the cement paste into the surface pores of aggregates shown in Figure 2.6 is an important characteristic [93, 97, 98]. LWA absorbs water during mixing. Together with mixing water, parts of the binder components infiltrate into the porous LWA. The hydration products, therefore, grow not only towards the outer LWA surface, but also to a limited extent towards the inside of LWA. The LWA surface is rough and porous and permits very good mechanical interlocking [98]. The elastic modulus of lightweight aggregates is compatible with that of the cement paste, which reduces the tendency of microcracking in the transition zone between the concrete phases [93]. Some expanded clays exhibit reactive clinker phases, such as Gehlenite (C_2AS), on the outer shell of the coarse aggregate. These LWAs can, therefore, react with the binder components to a limited extent [98].

Compared to ordinary concrete, when the strength of the mortar matrix determines the strength of concrete, LWA is often less solid and less stiff than the matrix, depending on the specific gravity values of LWA. LWA is, therefore, decisive for the strength of a lightweight concrete structure. As a result, the concrete strength may lag behind the compressive strength of the matrix [98]. However, a number of works claim that the

residual mechanical properties of LWACs after exposure to high temperatures above 800 °C reach substantially higher values than ordinary concretes [99–101].

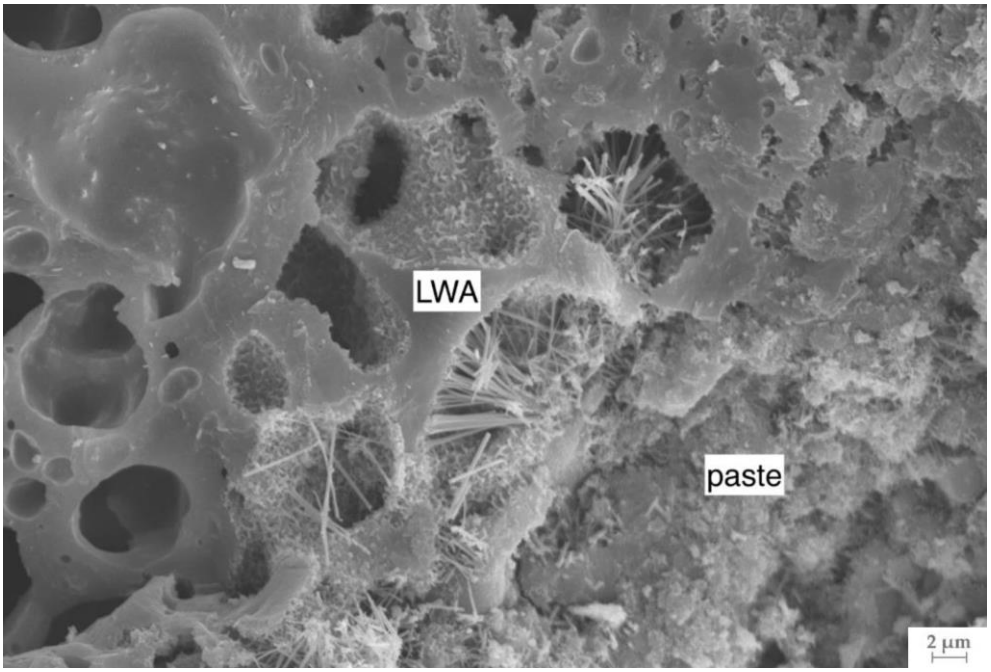

Fig. 2.6 SEM image of the interfacial transition zone in lightweight concrete between an expanded clay aggregate and the paste. Hydration products are visible inside the outer LWA pores [98].

Lightweight refractory concretes (LWRCs) are classified by density (880 to 1680 kg/m^3) and service temperature (927 to 1760 °C). Heat capacity is proportional to density; thus, it is low for these materials. The properties of LWRCs are time and temperature-dependent. When designed for heat retention purposes, the insulating concrete should not be subjected to impacts, heavy loads, abrasion, erosion, or other physical abuse. Normally, both the strength and the resistance to destructive forces decline as the density decreases [25, 102].

LWRC requires greater care in the selection of aggregates, aggregate gradation, and mixture design than any other concrete mixture. The differences in gradation and fines material contents between specific aggregate types can produce variations in cement-aggregate volumes, water requirements, and workability or plasticity characteristics. These variations can subsequently affect the porosity, strength, unit weight, and thermal expansion of concrete. As shown in Figure 2.7, due to the low bulk density of the

aggregates used in the production of LWRC, segregation problems may arise [70, 93]. The ability of fresh concrete to remain homogeneous during consolidation is a critical issue in the mixture design.

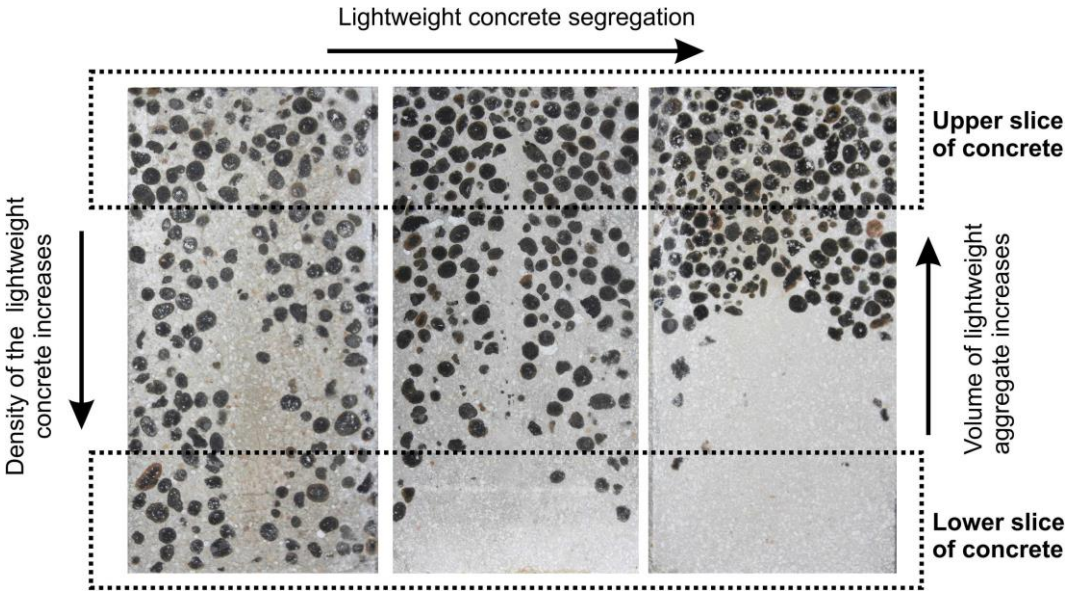

Fig. 2.7 Segregation of LWC - upper and lower slices in a concrete specimen [103].

Segregation refers to the movement of coarse aggregates relative to the cement mortar. There are two types of segregation, dynamic and static. Dynamic segregation occurs when the concrete is flowing and the coarse aggregate lags behind the cement mortar [104]. This kind of segregation can be caused by the input of any form of vibration energy into the fresh mixture during concrete transport or the filling of molds [105]. Static segregation occurs when the concrete mixture is at rest and the coarse aggregate sinks in the mortar [104]. Beyond the inhomogeneity of the aggregate distribution, segregation can weaken the interface between the aggregate and the cement paste [105]. Segregation may also cause lower flowability, aggregate blocking, higher drying shrinkage, and non-uniform compressive strength. Segregation resistance is normally achieved by reducing the w/c ratio and adding a finely powdered material such as silica fume, fly ash, or limestone powder [104].

Chapter 3

Experimental investigations

The experimental part of this work was carried out in the laboratories of CTU in Prague, Faculty of Civil Engineering, specifically in the Testing Hall of the D075 Experimental Center and the D018 Thermophysical Laboratory.

Decades of research have produced a considerable amount of material data, despite that there still remain areas that need further study. This experimental work aimed to investigate the effect of elevated temperatures on the physical and mechanical properties of newly designed LWRCCs, produced by mixing a hydraulic binder based on aluminous cement, lightweight aggregates, fibers, and an air-entraining additive in different combinations. In the tests, temperatures of 105, 400, 600, and 1000°C were chosen for ease of observation of the test results, see Table 3.1.

Table 3.1 Simplified scheme of the experimental work.

Component/material selection						
↓						
Preparation of test specimens						
REF	MP	MP-B	L1	L1-B	L2	L2-B
↓						
Curing procedure for 28 days						
↓						
Drying of specimens at 105 °C						
↓						
High-temperature treatment						
400 °C	400 °C	400 °C	1000 °C	1000 °C	1000 °C	1000 °C
600 °C	600 °C	600 °C				
1000 °C	1000 °C	1000 °C				
↓						
Three-point bending test						
↓						
Uniaxial compression test						
↓						
Evaluation of results						

3.1 Designed mixtures and their components

Designing a mixture of lightweight cement-based composites requires a specific method that is quite different from conventional concrete. The conventional design process can result in material segregation, as well as reduced strength and durability [106]. The major problem of lightweight concrete is to ensure sufficient homogeneity, especially in the case of fiber-reinforced concrete.

The input materials were selected based on the study of accessible knowledge and former work [107–111]. This thesis is based upon the presumption that all used materials formed at high temperatures can improve the fire resistance of the cement-based composite. CAC is adaptable and allows the technology to grow from simple traditional

refractory concrete to the design and installation of a system that can significantly increase the performance and durability of refractory concrete in one piece.

One of the possible directions of the weight reduction of a cement-based composite is adding lightweight aggregates. The problem with LWAC is its undesirable mechanical behavior. The fracture of lightweight concrete is characterized by cracks going through artificial aggregates, which makes it more brittle than normal concrete. Lightweight concrete in particular has significantly lower fracture toughness and tensile strength than normal concrete.

The lack of fracture toughness is commonly solved by the application of fibers, which also has a positive impact on the residual properties of refractories. Fiber reinforcement helps to resist predominantly the tensile stresses emerging from volume changes. Increasing the tensile strength of the final composite reduces crack initiation during temperature loading.

Another method to reduce the density of the experimental composite is the application of an air-entraining additive. The air-entrainer is a surface-active substance creating micro-sized air bubbles in the mixture. Compared to a composite containing artificial lightweight aggregates, this method provides a more economically advantageous option when creating a lightweight cement-based composite.

3.1.1 First part – Application of an air-entraining agent

As mentioned above, CAC is used for fabricating all test specimens in this research to ensure sufficient resistance to high temperatures. The resistance of CAC is directly affected by the content of Al_2O_3. In this research, Górkal 40 (brand name of CAC) shown in Figure 3.1 with an alumina content of 40 % was applied, which may be usable at a temperature up to 1300 ºC. Table 3.2 presents the chemical compositions and some physical properties of the used cement.

Table 3.2 Chemical composition and physical properties of used CAC.

The content of basic oxides, %				Physical properties	
Al_2O_3	CaO	SiO_2	Fe_2O_3	Specific gravity (g/cm^3)	Blaine fineness (m^2/kg)
40.80	32.50	2.88	12.12	3.00	310–380

Fig. 3.1 Górkal 40 calcium aluminate cement.

One part of the research is to present the usage of a liquid air-entraining additive as a method to economically reduce the density of refractory cement-based composites. In the previous experiment [112], cement pastes were combined with an air-entraining additive dosage, up to 10 % by the weight of the cement dose. According to the results shown in the next chapter, a dose of 10 % was chosen for the mixtures in the following research. The air-entraining agent is represented by the Microporan 2 product shown in Figure 3.2, with a density of 1005 ± 2 kg/m^3 and a pH value of 9–11 [113]. Microporan 2, commercially provided by the STACHEMA CZ Company, creates small air pores in the concrete or mortar mixture with a diameter of 10–300 μm (so-called effective air).

Entrained air dramatically improves the durability of concrete exposed to moisture during freeze-thaw cycles and significantly improves the concrete's resistance to volume changes and aggressive environments. Air-entraining agents can also reduce the surface tension of a fresh cement composition at low concentrations, increase the workability of fresh concrete, and reduce segregation and bleeding.

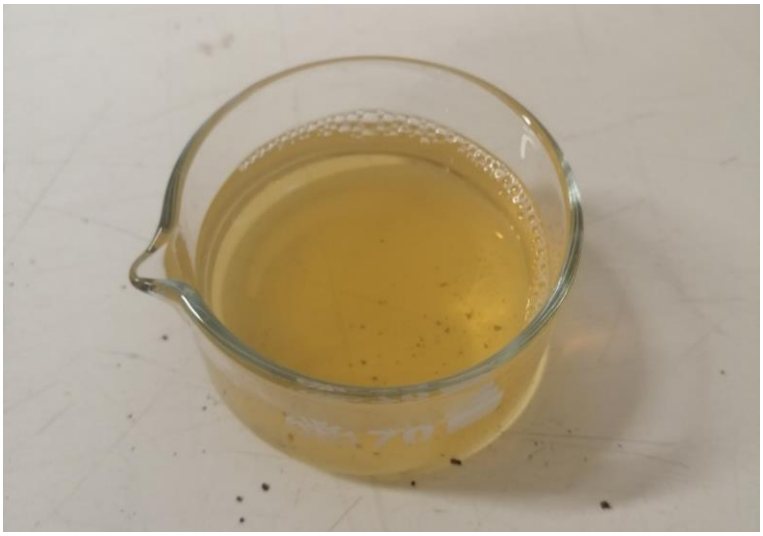

Fig. 3.2 Microporan 2 air-entraining agent.

The water-cement ratio does not affect the percentage reduction in strength after exposure to heat, but it has been confirmed that concrete with a lower water-cement ratio retains higher strength even after exposure to high temperatures [33]. In all mixtures, the water-cement ratio was kept at 0.25. It also positively affects the effect of the air-entrainer, which creates a satisfactory consistency of the mixture in combination with the fibers.

3.1.2 Second part – Addition of basalt fibers

This part is focused on the combination of chopped fibers and an air-entraining agent to analyze their degree of influence on the workability of a fresh mixture, the density, and residual properties of high-temperature loaded composites. The extent of the influence of fibers on the final mechanical properties of the refractory composite plays an important role in the experiment. The residual properties of refractories are often ensured by applying fiber reinforcement, which helps to resist predominantly the tensile stresses emerging from volume changes and reduces crack initiation [64, 114–116].

The choice of the reinforcing material is a major issue, especially for composites intended for special applications. The main fiber component of this analysis is made from basalt, a mineral of volcanic origin, see Figure 3.3. Basalt is the most abundant rock type in the Earth's crust and can present a porphyry, microcrystalline or glassy structure. From 1995, the fiber production technology was declassified, and civilian research began.

The production of fibers has, therefore, been developed only recently, in the last decades. The manufacturing process of a basalt fiber is similar to that of a glass fiber; however, basalt consumes less energy and does not need any additives for melting at a temperature around 1400 ºC. There are two possible ways of processing the molten material – the blowing technology and the technology of continuous spinning. The blowing technology is used to produce short and cheap fibers. Unfortunately, these fibers have poor mechanical properties. The second one is the spinneret method, which produces continuous fibers of better quality. These can then be cut in order to obtain a specific length of fibers. The diameter of basalt fibers ranges from 10 μm to 20 μm according to the production process and the quality of raw material [64, 117].

As a new type of environmentally friendly material with excellent physical and chemical properties, basalt fibers are widely used in several industry branches. The basalt fiber has good interfacial bonding properties with the cement paste, alkali-resistance, and extremely low absorbability. Mixed in the cement matrix as short (staple) or cut (chopped) fibers, they can improve the structural strength and lower the weight [117, 118]. The best basalt fiber property is fire resistance, which allows advanced applications in composites exposed to severe conditions, such as heat shields, thermal insulating barriers, and fire protection. Concerning the acquisition cost and their thermal properties, basalt fibers offer an excellent economic alternative to other high-temperature-resistant fibers, like glass and carbon fibers. The comparison of the physical properties of basalt fibers with other fibers is shown in chapter 2 in Table 2.9. To gain a better understanding, the next chapter also includes the comparison of the influence of basalt, carbon, and aramid fibers on the refractory cement paste after exposure to high temperatures. Basalt is also used to replace asbestos in almost all its possible applications: as an insulating material (since basalt has three times asbestos heat-insulating properties) or as a friction material [117]. Moreover, when using basalt fibers, there are no health risks, such as in the case of asbestos fibers.

The optimal amount of fibers, suitable for the cement composite production, depends on the type of composite, the used aggregate, cement, admixtures, and especially the material of the used fibers and their surface treatment. A dosage of 1.0 % by volume of basalt fibers usually suffices to eliminate the crack formation on the surface even after exposure to cyclic loading at 1000 °C. Moreover, the drying process could cause cracks; therefore, the fibers limit the crack propagation.

The chemical composition of the basalt fibers used in this work, with a diameter of 13 μm and a length of 6.35 mm, is presented in Table 3.3. The chemical composition, especially the content of SiO_2, affects the possibility of processing the fibers [58]. Basalt consists of a number of oxides with an essential impact on its final properties. The dominant SiO_2 is represented by 51.6–59.3 % by weight, the content of Al_2O_3 is 14.6–18.3 %, Fe_2O_3 + FeO about 9.0–14.0 %, CaO is contained by 5.9–9.4 %, and other oxides form just up to 5.3 % of weight [119].

Table 3.3 Chemical composition of used basalt fibers.

Basic oxides	Al_2O_3	CaO	SiO_2	MgO	Fe_2O_3 + FeO	Na_2O + K_2O
% weight	17.20	8.60	52.70	4.20	11.40	4.10

The mixtures were adjusted and tested with reference to previous experiments [90, 109, 110, 112, 120]. Three mix designs were created. The reference mixture REF represents a simple aluminous cement paste. The second mixture MP is an aluminous cement paste enriched with a dose of an air-entraining additive. The third mixture MP-B is a combination of an aluminous cement paste, an air-entraining additive, and basalt fibers. As mentioned, the basalt fibers are added in a dose of 1.0 % by volume. After the previous investigation [112], the amount of the air-entraining additive in the MP and MP-B mixture was set at 10 % by the weight of the cement dose.

Fig. 3.3 Basalt fibers, with a diameter of 13 μm and a length of 6.35 mm.

3.1.3 Third part – Utilization of LWA

Since the thermal properties of concrete and composites are mainly interrelated with the type of aggregates used [121], another important part of the research is focused on the application of expanded glass, Liaver, with a closed surface to reduce the final density and thermal conductivity of experimental composites. LWA Liaver shown in Figure 3.4 is produced by recycling waste glass sintered at a temperature of 750 to 900 ˚C in a rotary kiln by a patented technology. Liaver is dry, light, non-toxic, and free of dangerous substances, non-flammable (A1 classification of fire resistance), and highly resistant to pressure. The chemical composition and properties of Liaver are shown in Table 3.4 and Table 3.5.

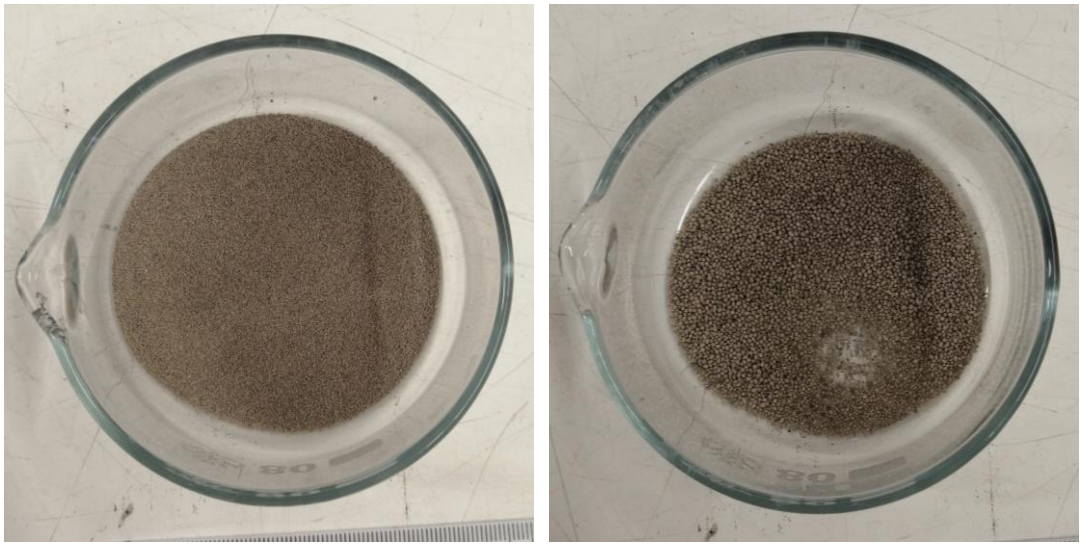

(A) (B)

Fig. 3.4 Expanded glass Liaver; (A) fraction of 0.25–0.50 mm, (B) fraction of 0.5–1.0 mm.

The raw materials for expanded aggregates can be of different origins, such as:

- waste materials (e.g., sewage sludge, waste glass, fly ash, etc.),
- natural raw materials (clay or slate) [122].

Expanded glass aggregates are a very lightweight material and have excellent thermal insulating properties, which can be used to produce lightweight thermal-insulating cement-based composites. Each year, due to humans' needs, a million tons of waste glass is generated worldwide. Glass is a non-biodegradable and chemically inert material that remains unchanged in the environment for a longer time, so the reuse of waste glass can reduce environmental hazards. Recycled products of waste glass are used in the concrete industry for various purposes nowadays [71].

Table 3.4 Chemical composition of Liaver.

The content of basic oxides, %						
Al_2O_3	CaO	SiO_2	Fe_2O_3	Na_2O	MgO	K_2O
2.0 ± 0.3	8.0 ± 2.0	71.0 ± 2.0	0.50 ± 0.2	13.0 ± 1.0	2.0 ± 1.0	1.0 ± 0.2

Table 3.5 Physical properties of Liaver.

Faction	Bulk density, kg/m^3	Density, kg/m^3	Grain strength, MPa
0.25 – 0.50 mm	300 ± 15 %	540 ± 15 %	3.4 ± 10 %
0.5 – 1.0 mm	250 ± 15 %	450 ± 15 %	3.3 ± 10 %

In this following stage of the research, four mixtures were designed containing LWA Liaver in two fractions. The presumed lower fracture toughness and tensile strength of cement-based composites with LWA were, according to the previously mentioned studies, solved by the application of fibers. Thus, two of these four mixtures were combined with basalt fibers. For an overview, the detailed composition of all studied composites produced for the following testing is shown in Table 3.6.

Table 3.6 Composition of studied lightweight specimens.

		REF	MP	MP-B	L1	L1-B	L2	L2-B
CAC [kg/m^3]		1735	1500	1270	1150	995	950	870
Water	w/c ratio	0.25	0.25	0.25	0.25	0.25	0.25	0.25
Air-entrainer	by weight of CAC	-	10 %	10 %	10 %	10 %	10 %	10 %
Liaver [kg/m^3]	0.25 – 0.5 mm	-	-	-	115	100	190	175
	0.5 – 1.0 mm	-	-	-	25	21	40	36
Basalt fiber	by volume	-	-	1 %	-	1 %	-	1 %

3.2 Specimen preparation

This section describes the production of test specimens, which were subsequently subjected to a three-point bending test and a uniaxial compression test. All procedures to prepare the specimens were carried out very carefully and according to the EN 196-1 European Standard [123]. Mistakes in the mixture design could negatively influence the rheological properties of a fresh cement-based composite and thus reduce the final properties of a hardened composite. The principal problem of a lightweight cement-based mixture is to ensure its sufficient homogeneity, especially in the case of fiber-reinforced concretes.

3.2.1 Mixture formation

For each series of the proposed REF, MP, and MP-B mixtures 24 test specimens were prepared. In the case of mixtures containing LWA Liaver, each designed series consisted of 12 test specimens. All components were first weighed carefully according to the proposed recipes, then mixed in a sufficiently large container to allow good mixing. Mixing was performed using a 20-liter horizontal laboratory mixer, model SP-200D, see Figure 3.5.

The following procedure was chosen to sufficiently disperse the fibers in the specimen composition. First, the lightweight aggregate was thoroughly mixed with the cement binder. The fibers were then gradually added to the mixer vessel. If the mixture was without the lightweight aggregate, the fibers and the cement binder were mixed as the first step. After the fiber bundles were dispersed in the dry mixture, water started to be poured into the vessel with constant stirring. The air-entraining agent is the last added component, whose effect is activated when used in a wet composite mixture. Immediately after preparing the fresh concrete, a flow table test was performed to determine the consistency of fresh concrete.

Fig. 3.5 Horizontal laboratory mixer model SP-200D.

3.2.2 Flow table test

The consistency of a fresh mixture is commonly determined by the employment of a flow table test. In this case, the EN 1015-3 standard method [124] for mortars was used since it is also applicable for mixtures with fine aggregates. The fresh mixture was placed in a special truncated cone-shaped mold with a base diameter of 100 mm and then compacted. Subsequently, the mold was removed, and the flow table shown in Figure 3.6 is lifted and dropped 15 times (approximately 1 fall per second). Two orthogonal diameters (of flowed mixtures) characterize the mixture flow. This test was performed to monitor the plasticity of fresh mixtures and to ensure a sufficient level of workability.

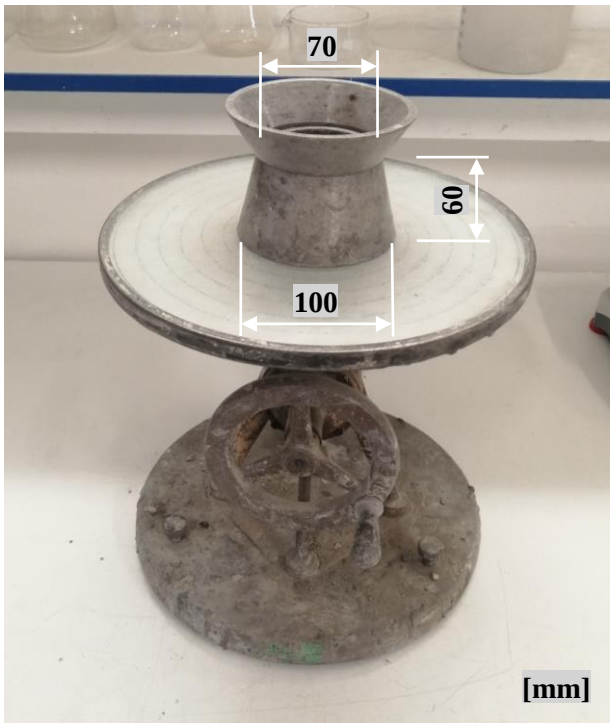

Fig. 3.6 Flow table for cement mortar.

3.2.3 Specimen casting process

The EN 196-1 European Standard [123] establishes compressive and flexural strength on prismatic specimens with dimensions of 40 mm × 40 mm × 160 mm. Steel molds with the same internal geometry were used to create the test specimens for the experimental program, see Figure 3.7. After mixing, all resulting composite mixtures were poured into

the steel molds and left to solidify at room temperature for 24 hours. The steel molds were wiped with an oil-based release agent to prevent the composite from attaching to the mold walls. The release agent forms a thin film that lubricates the mold walls, so the composite will be easier to take out from the steel mold once it has hardened.

Fig. 3.7 Steel mold for creating test specimens.

If necessary, the compaction of the mixtures could be performed on a vibrating table shown in Figure 3.8 at a frequency of 30 Hz. The specimen's upper surface was then eventually smoothed with a steel trowel. The compaction of mixtures depends on their workability, which is the ability of a fresh mixture to properly fill the mold with the desired effort and without reducing the composite's quality.

Fig. 3.8 Vibrating table RM1.

3.2.4 Specimen curing procedure

During the curing period, cement-based composites should be ideally maintained at controlled temperature and humidity to achieve the optimal strength and durability. Improper curing can cause scaling, reduced strength, poor abrasion resistance, and cracking [125].

In the case of CAC, care must be taken to avoid overheating due to the exothermic solidification of cement. To reduce the negative impact of a higher hydration heat, the fresh composite specimens were stored in an environment with a relative humidity of more than 90 % and at a temperature of 20 ± 2 °C, where the specimens were left till the 28th day of the hydration process.

3.2.5 Specimen drying procedure

After the curing procedure, the density of the specimens was determined. The weight of the specimens was recorded by an electronic analytical scale, with an accuracy of 0.01 g.

According to the manufacturing technology for monolithic refractories, after concrete maturity, it is necessary to carry out a drying procedure before the first elevated-temperature testing. A high heating rate may cause mechanical breakage of refractory concrete, most probably if the concrete is held at a low (<21 °C) temperature [126]. Therefore, the specimens were placed in the SalvisLab Thermocenter TC240 laboratory drying oven shown in Figure 3.9, where they were dried at 105 °C for 24 hours, to avoid mechanical damage, caused by sudden water evaporation from the inner pore structure under temperature loading [28, 65]. After drying, before the actual elevated-temperature testing, the density of the specimens was determined again and served as a reference value to the values identified after temperature loading.

Fig. 3.9 Drying oven SalvisLab Thermocenter TC240.

3.3 High-temperature treatment

A review of the methods used by various investigators for elevated-temperature testing of concrete indicates that, generally, the tests can be categorized according to cold or hot testing [25].

In hot testing, the specimens are gradually heated to a specified temperature, permitted to thermally stabilize at the temperature for a prescribed period of time, and

then tested at that temperature to determine the mechanical properties. During testing, the specimens are maintained in either an open environment where the water vapor can escape (unsealed) or a closed environment where the moisture is contained (sealed). The closed environment represents conditions for mass concrete where moisture does not have ready access to the atmosphere, and the open environment represents conditions where the element is either vented or has free atmospheric communication [25].

In cold testing, the specimens are gradually heated to a specified temperature, permitted to thermally stabilize at that temperature for a prescribed period of time, then permitted to slowly cool to the ambient temperature, and finally tested to determine the mechanical properties [25]. The material properties are greatly affected by factors such as the heating rate, maximum temperature, and exposure time to the temperature [36].

In this research, depending on the type of mixture, the manufactured composite specimens were exposed to an elevated temperature of 400 °C, 600 °C, and 1000 °C in the electric annealing lid furnace, type 10013V, as shown in Figure 3.10, which automatically increased the temperature by 10 °C/min from room temperature to the required value. The preset temperature was then automatically maintained for 3 hours, and the furnace subsequently cooled down naturally. The average cooling rate was about 1 °C/min. Figure 3.11 clearly describes the whole temperature-loading process in time. The specimens were left to cool down inside the furnace to prevent thermal shock. After cooling, the residual density, compressive and flexural strength, and fracture energy were determined, as described in the following section. In the case of specimens without LWA, the effects of different temperature degrees (400, 600, and 1000 °C) on their residual properties were monitored, while the composites containing LWA were only loaded at a temperature of 1000 °C. These composites were compared with the specimens without LWA in order to determine the most suitable composition under extreme conditions.

Fig. 3.10 Electric furnace 10013V.

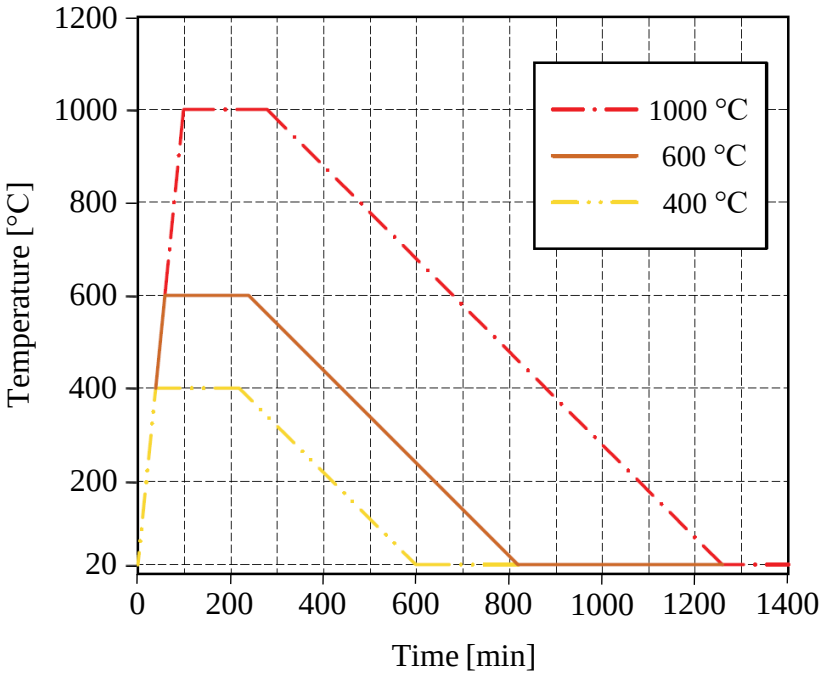

Fig. 3.11 Temperature-loading process in time.

3.4 Measurement methods

The performance of concrete can be measured by the change in its stiffness, strength, or some other property that would affect its main function in service. Consequently, much of the research conducted on concrete at elevated temperatures has concentrated on compressive strength as the fundamental property in examining its deterioration. However, it has been noted that compressive strength may not be such a good indicator of deterioration at elevated temperatures as tensile or flexural strength under short-term loading [25]. Most materials generally fail under tensile stress before they fail under compressive stress, so flexural strength represents the highest tensile stress experienced within the material before it fails. Flexural strength, also known as the modulus of rupture, is determined from prismatic specimens loaded in three-point or four-point bending until failure occurs. As the flexural strength is calculated based on linear-elastic conditions, it is a fictitious value, but convenient for comparison purposes [25].

The testing method itself has an important effect on the evaluation of the properties of heated materials. The most common way to study the influence of high temperatures on the properties of cement-based composites is the aforementioned cold testing and carrying out measurements, such as compression, bending, or tensile tests [36, 47]. The mechanical properties due to which the specimens were permitted to return from a high temperature to room temperature before testing are referred to as residual properties and represent the necessary information to investigate the effect of high temperatures on a material [42]. Therefore, in this experimental program, the basic physical-mechanical properties were determined (density, compressive and flexural strength, and fracture energy) and compared with the test results of the specimens unexposed to temperature loading. All properties were verified on 6 specimens of each mixture, before and after the temperature loading. A total of 120 test specimens were made for this experimental research.

As mentioned, all tests were carried out according to the methodology described in the European Standard Methods of Testing Cement – Part 1: Determination of Strength [123]. The flexural strength R_f values were calculated with the help of the maximum reached force F obtained through a three-point bending test. From this test, the fracture energy values were also determined based on force-deflection diagrams. Prismatic specimens were placed on cylindrical supports, with a lengthwise distance of 100 mm and loaded in a direction perpendicular to the direction of compaction, see Figure 3.12. The specimens were loaded in the middle of the span, at a set deflection speed of 0.18 mm/min, until the maximum load capacity. The MTS 100 electromechanical compression system was used for the three-point bending test. The flexural strength is then correlated with the measured compressive strength R_c, but the correlation is only an approximation.

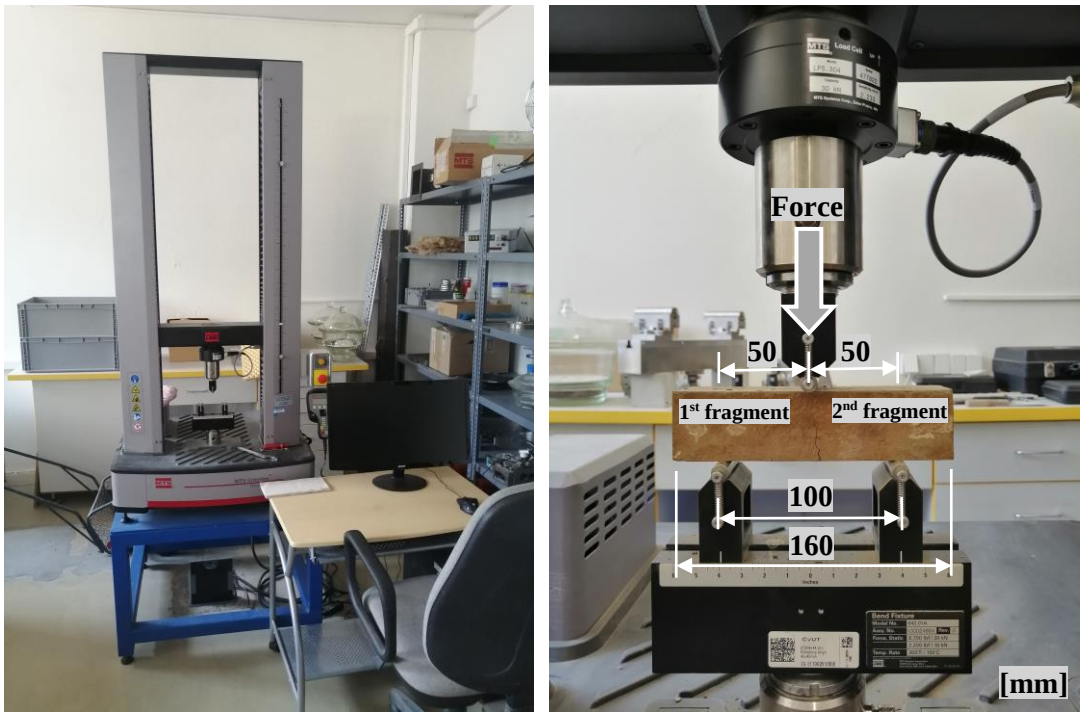

Fig. 3.12 Electromechanical compression system MTS 100 with test details.

The compressive strength values were obtained using the EU 40 hydraulic pressure machine when testing the fragments of each specimen that had remained after the three-point bending test, see Figure 3.13. The fragments were loaded in the pressure machine over an area of 40 mm × 40 mm and at a speed of 2400 ± 200 N/s until the maximum load-bearing capacity was reached. Each fragment was tested in the same perpendicular

direction as during the three-point bending test. The results of the tests performed are given in the following chapter. In addition to mechanical properties, changes in the density ρ were constantly studied because they are related to structural transformations and mineralogical changes during heating [29].

Fig. 3.13 Hydraulic pressure machine EU 40 with test details.

Chapter 4

Results and discussion

4.1 Evaluation of previous experiments

As mentioned in the previous chapter, part of the complex research was to present the impact of different doses of the presented Microporan 2 air-entraining agent on the mechanical properties of the aluminous cement-based paste and the influence of the amount of water in the mixture on the effects of this agent. As mentioned in previous subchapter 3.1.1, cement pastes were combined with an air-entraining additive dosage, up to 10 % by the weight of the cement dose. Micro-size air bubbles created by the air-entraining agent will remain as a part of the hardened composite. They also help to improve the workability and facilitate the final compaction of the fresh mixture [112].

The results of flexural and compressive strength, as shown in Figure 4.1 and Figure 4.2, are in line with the results of density. There is an obvious effect of the air-entraining dose in each mixture of MP specimens.

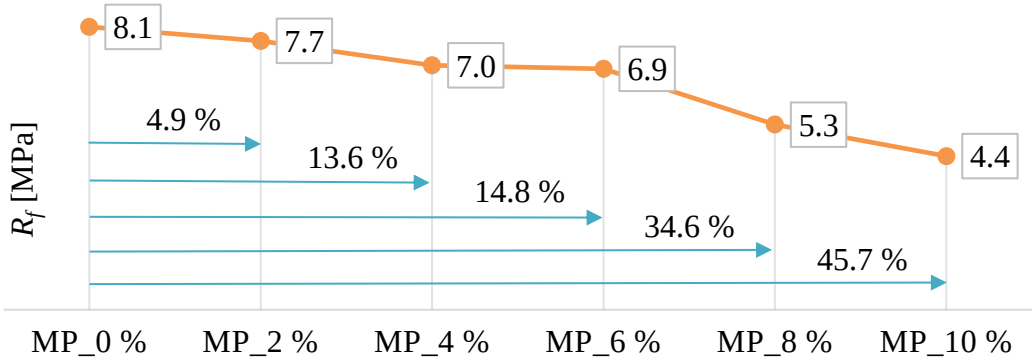

Fig. 4.1 Relative values of flexural strength, specimens dried at 105 °C.

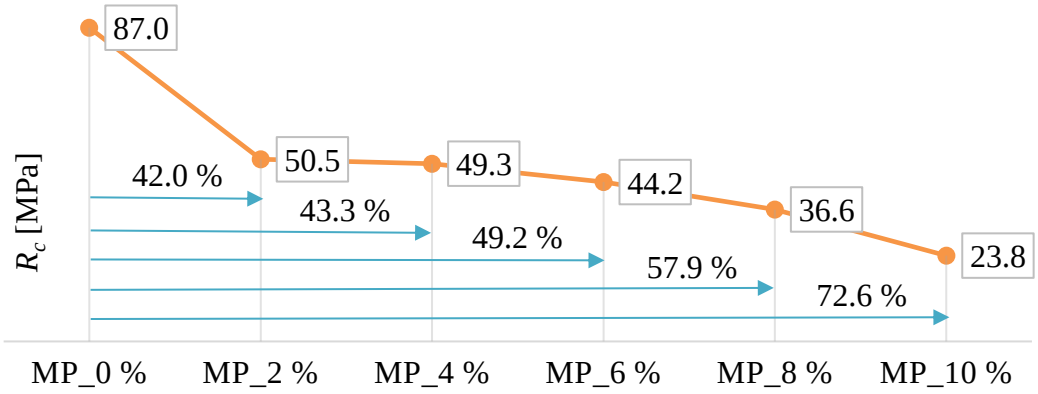

Fig. 4.2 Relative values of compressive strength, specimens dried at 105 °C.

Figure 4.3 shows the density values of the dried cement-based specimens. The values are affected by the dosage of the air-entraining additive. The presented MP specimens with an air-entraining additive over 8 % have shown values of density below 1800 kg/m^3, along with satisfactory strength results.

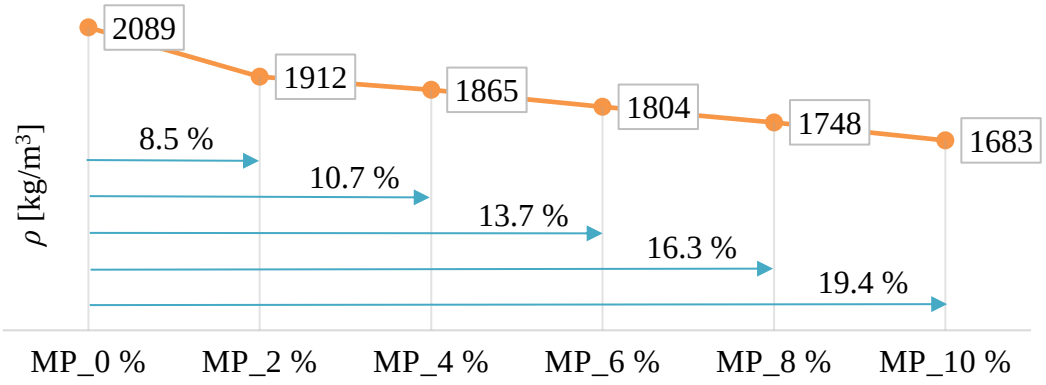

Fig. 4.3 Relative values of density, specimens dried at 105 °C.

Within the research, the influence of the water-cement ratio on a mixture containing an air-entraining additive was also investigated. The mixture with a water-cement ratio of 0.25 showed the most satisfying results of density and proved the assumption for a combination with chopped fibers, see Figure 4.4.

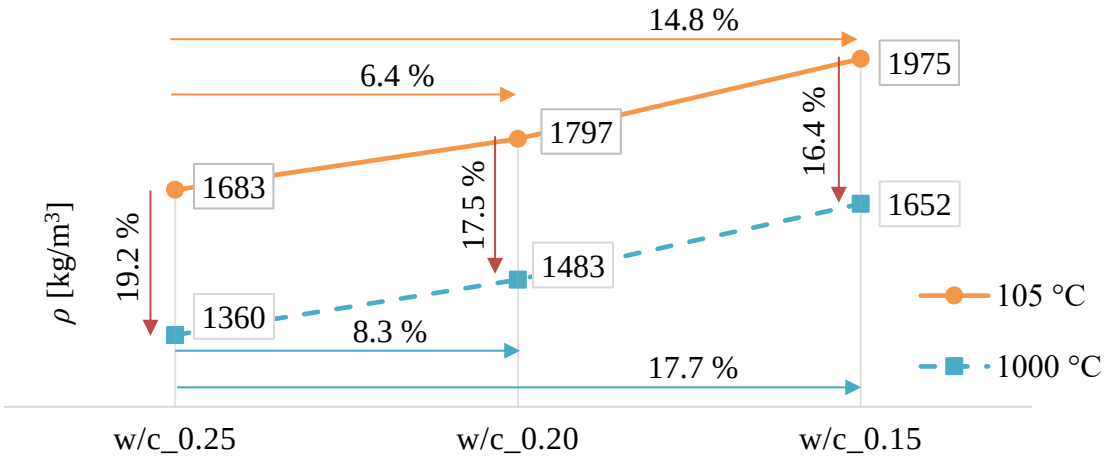

Fig. 4.4 Density development of the cement-based paste with a 10% dose of an air-entraining additive, in correlation with different water-cement ratios.

Another part of the comprehensive research was the investigation of reinforcing fibers and their structural effect in an aluminous cement paste. The final resistance of fiber-reinforced cement-based composites is affected by the used type of fibers. Three different types of fibers were tested: basalt, carbon, and aramid fibers. The primary characteristics

that are desirable for reinforcement are high modulus, high strength, high thermo-mechanical stability, low density, and low cost [78]. The production of carbon and aramid fibers is a relatively energy-intensive process, but the popularity of these fibers is growing because of their excellent properties and low weight.

The testing of these fibers was performed under similar conditions as described in the previous chapter and on the same prismatic specimens. Many scientists have investigated LWC containing 0.25–2.0 % of fibers by concrete volume [10, 16, 86, 127]. According to the behavior of fibers in the fresh mixture and their effects on hardened cement composites, it was decided to dose 1 % of fibers from the total volume of the mixture. All mixtures also included a dose of an air-entraining additive set at 10 % by the weight of cement. As confirmed by the results shown in Figure 4.5, the application of fiber reinforcement in the form of short fibers ensures an increased load capacity of the tested refractories. The series of values, identified as REF, represents fiber-free cement paste specimens.

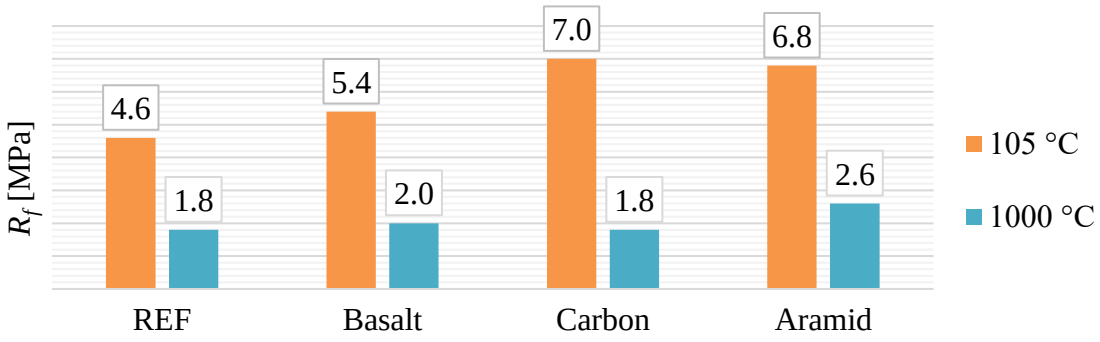

Fig. 4.5 Residual values of flexural strength.

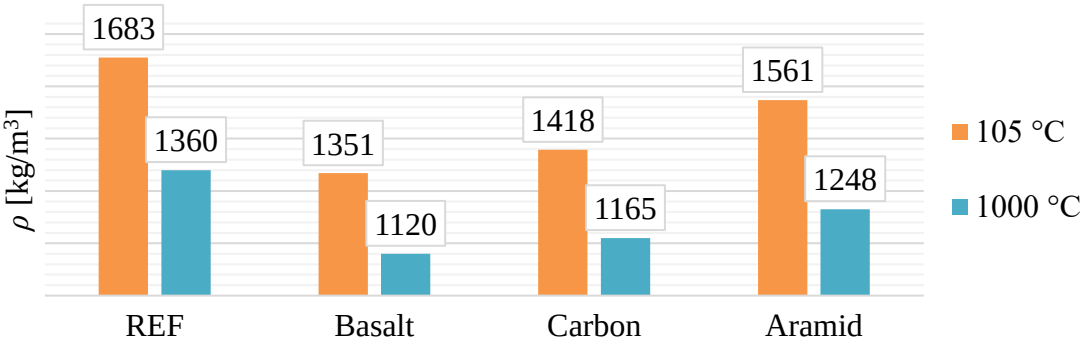

Fig. 4.6 Residual values of density.

In this fiber-reinforcement experiment, the highest values of flexural strength after exposure to high temperatures were reached by the composites containing aramid fibers. Nevertheless, considering the fiber production cost and the values of density shown in Figure 4.6, the specimens containing basalt fibers have obtained the most satisfactory results.

4.2 Physical changes caused by high temperatures

4.2.1 Color change

When it is necessary to evaluate the condition of concrete after exposure to a high temperature, the change in color is a physical property of concrete that can be used as an assessment method. Nowadays, some of the developed techniques make it possible to evaluate the color change of heated concrete [36].

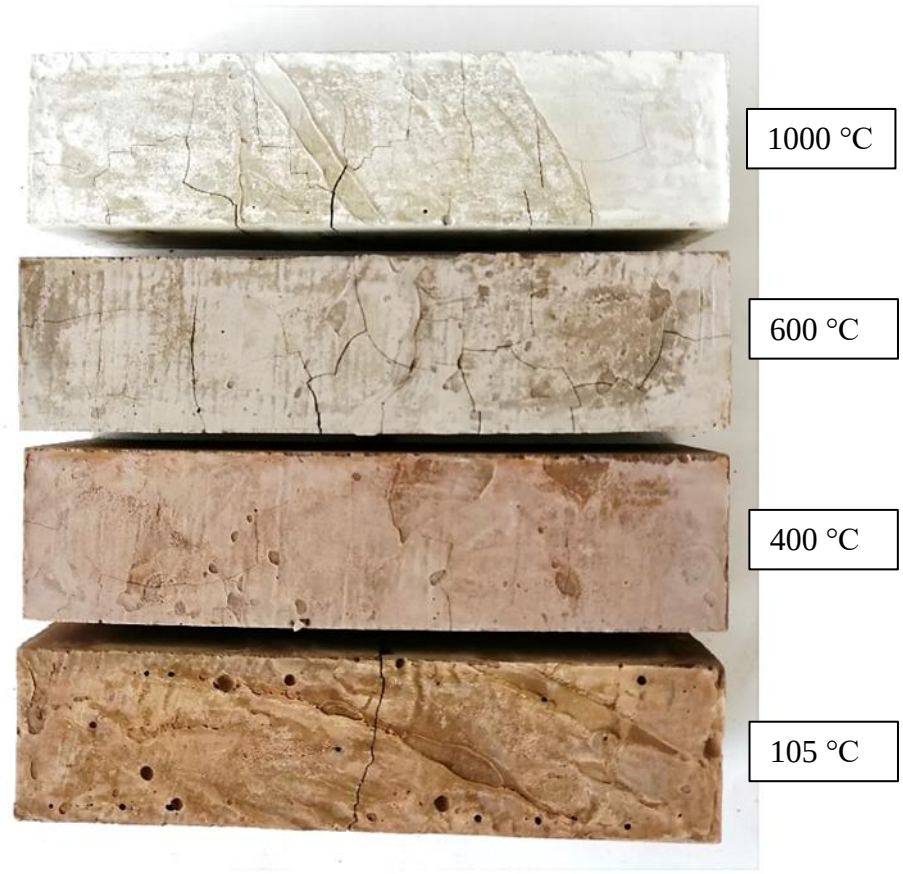

Fig. 4.7 Color change of an aluminous cement-based composite.

The color change of heated cement composite results principally from the gradual water removal and dehydration of the cement paste [36]. As shown in Figure 4.7, the color change is already visible between 105 °C and 400 °C. As the temperature increases, the color of the red-brown specimen, containing iron oxide (Fe_2O_3) pigments, turns to pale shades of white and grey. The most intense color change appears by reaching a temperature of 1000 °C.

4.2.2 Shrinkage

The key hydraulic minerals of aluminous cement are CAs (Calcium Aluminates). Due to conversion, at higher temperatures, the metastable hydrates CAH_{10} and C_2AH_8 transform into the C_3AH_6 phase, which is highly thermodynamically stable and the least soluble of all calcium aluminate hydrates. When CAH_{10} is converted to C_3AH_6, there is a 52.5 % reduction of the solid volume of hydrates, and when C_2AH_8 is converted to C_3AH_6, there is a 33.7 % reduction. According to the study [34], the tricalcium aluminate hexahydrate (C_3AH_6) loses most of the water in the temperature range of 200–300 °C (around 80 %). This fact also applies to crystalline gibbsite (AH_3).

This outcome of this process is a massive increase in porosity and shrinkage and a decrease in mechanical strength. Thermal shrinkage is defined as a contracting deformation of a hardened concrete mixture due to the loss of chemically bonded water. Shrinkage causes an increase in tensile stress, which can lead to cracking, internal and external deformation, as shown in Figure 4.8. To minimize the shrinkage, the concrete mixture's total water content must be kept as low as is practically possible for the intended application.

Fig. 4.8 Visible cracks on the specimen surface after heating to 400°C.

4.2.3 Density

The mass of composite specimens was measured and compared with the consequent weight loss. The results of density, depending on the temperatures to which the specimens were exposed, are plotted in Figure 4.9 and Figure 4.11, completing the overall overview of the selected mechanical properties. All results are average values obtained from six separate specimens. Changes in the density values are related to structural transformation during heating. A graphical overview of the percentage mass loss with an increase in temperature is shown in Figure 4.10.

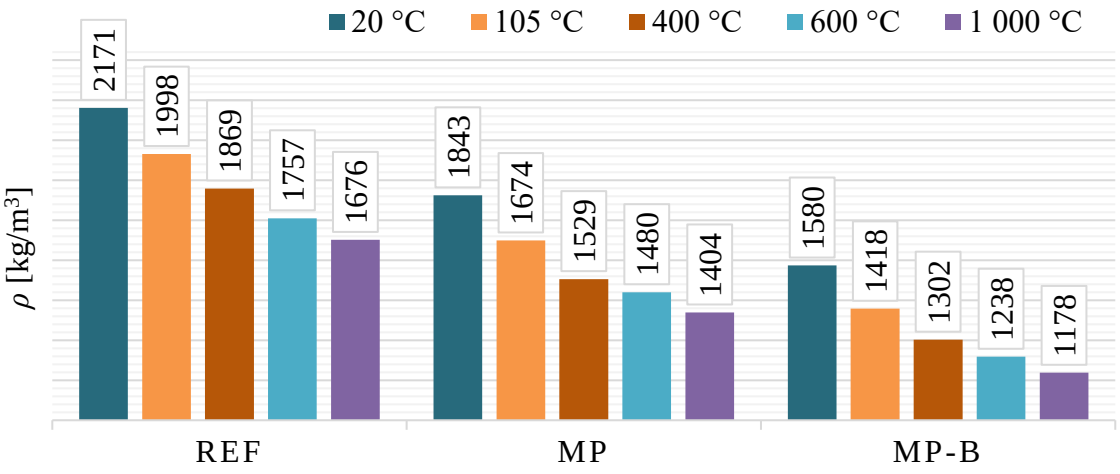

REF	represents fiber-free cement paste specimens.
MP	represents fiber-free cement paste specimens containing an air-entraining additive.
MP-B	represents fiber-reinforced cement paste specimens containing an air-entraining additive.

Fig. 4.9 Density values after exposure to elevated temperatures.

There is an obvious effect of the air-entraining dose in the MP and MP-B mixture. Apparently, in the case of the MP-B mixture, the combination of fibers and the air-entraining agent causes a considerable increase in the air content in the composites, which leads to a considerable reduction in density. Thanks to the air-entraining agent, micro-sized air bubbles are created during the plastic composite mixing and will remain as a part of the hardened mixture. This state can have a negative impact on the adhesion of fibers and the binding matrix. In fact, it can cause limitations in their application and

undesirable effects on the mechanical properties. On the other hand, fibers contribute to the limitation of volume changes during temperature loading and related crack formation [128].

The variation of mass loss versus exposure temperature can be divided into four phases. Between the ambient temperature and 105 °C, the variation of mass is rather strong. The loss of mass in this phase corresponds to the departure of free water contained in the capillary pores. When the temperature rises from 105 to 400 °C, another significant increase in the mass loss can be observed. The mass loss in this phase is due to the release of physically bound water and the onset of the release of chemically bound water. At this point, the total mass loss corresponds on average to 16.2 % of the initial mass. Between 400 and 600 °C, the mass loss rate comparatively slows down. Beyond 600 °C, the mass loss rate does not change appreciably. At 1000 °C, chemically bound water is no longer present, and the mass loss on average corresponds to 24 % of the initial mass.

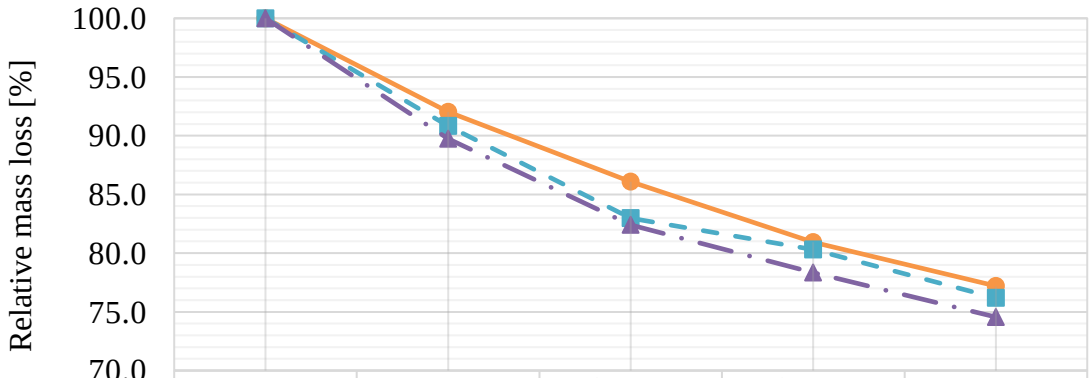

	20 °C	105 °C	400 °C	600 °C	1000 °C
REF	100.0	92.0	86.1	80.9	77.2
MP	100.0	90.8	83.0	80.3	76.2
MP-B	100.0	89.7	82.4	78.4	74.6

Fig. 4.10 Mass loss of specimens subjected to elevated temperatures.

For a complete summary, Figure 4.11 also shows the density values of the composites enriched with LWA Liaver, exposed to 1000 °C. Basalt fibers were present in the L1-B and L2-B mixtures. The values are affected by the LWA dosage. Naturally, when comparing the mixtures, the density values are lower for the specimens with LWA than for the specimens without it. The percentage decrease in density between the ambient temperature and 105 °C is higher for the specimens with LWA and fibers, caused by

increased amounts of free water. On the other hand, between 105 °C and 1000 °C, the difference in the percentage decrease in density is higher for the specimens without LWA due to the mineralogical transformation and chemical decomposition of larger amounts of hydrated products.

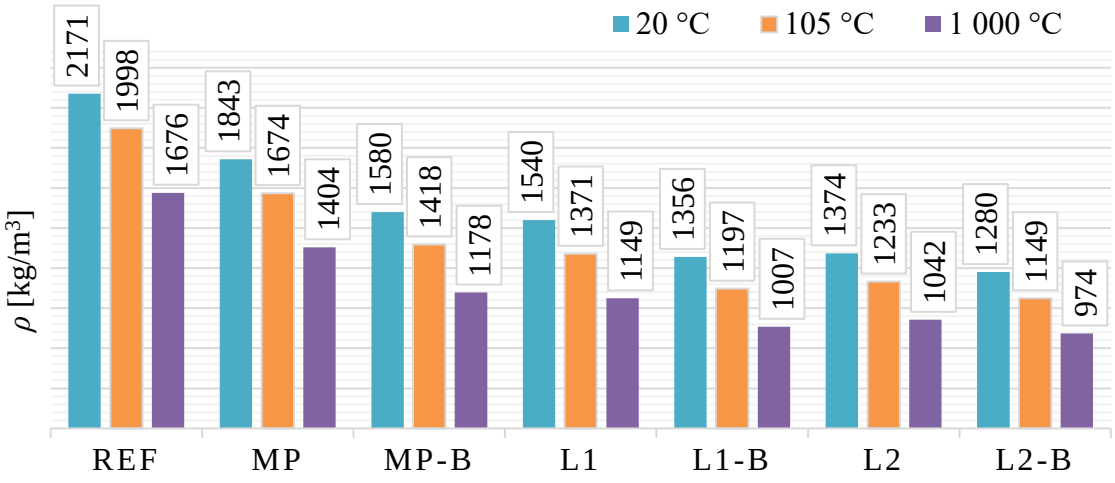

REF	represents fiber-free cement paste specimens.
MP	represents fiber-free cement paste specimens containing an air-entraining additive.
MP-B	represents fiber-reinforced cement paste specimens containing an air-entraining additive.
L1	represents fiber-free cement paste specimens containing an air-entraining additive and LWA.
L1-B	represents fiber-reinforced cement paste specimens containing an air-entraining additive and LWA.
L2	represents fiber-free cement paste specimens containing an air-entraining additive and double the amount of LWA.
L2-B	represents fiber-free cement paste specimens containing an air-entraining additive and double the amount of LWA.

Fig. 4.11 Residual density values after exposure to 1000 °C.

4.3 Residual mechanical properties

Residual mechanical properties determine the load-bearing capacity of a material after exposure to a high temperature and represent the necessary information to investigate the degree of the influence of the high temperature on the material. Material properties are closely related to the specific test method employed. For all measurement methods, the experiments were carried out on several specimens. The presented results are average

values without extreme deviations. In the graphs, the specimen closest to the average value of the given series is always used.

4.3.1 Flexural strength

The flexural strength R_f is the ability of a material to withstand the bending load, which is measured by a three-point or four-point bending test. The flexural strength of individual specimens was calculated based on the theory of plasticity with the help of the maximum reached force, from the equation:

$$R_f = max\,\sigma_f = \frac{max\,M}{W} \quad (1)$$

$$M = \frac{1}{4} F.l \quad (2)$$

$$W = \frac{1}{6} b.h^2 \quad (3)$$

where

R_f is flexural strength [MPa]

σ_f is flexural stress [MPa]

M is bending moment [N.mm]

W is the section modulus [mm^3]

F_f is maximum fracture load [N]

l is the length of the support span (= 100 mm) [mm]

b is specimen width (= 40 mm) [mm]

h is specimen height (= 40 mm) [mm]

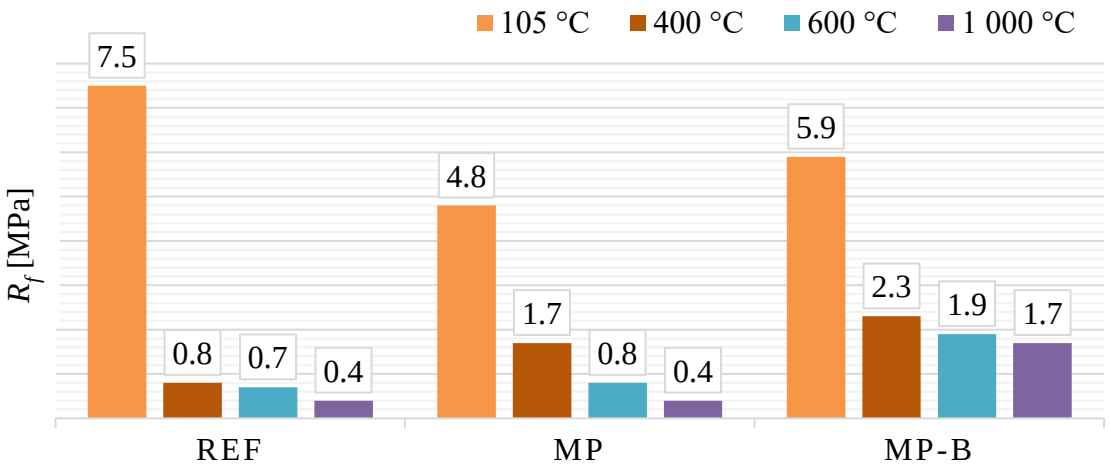

REF	represents fiber-free cement paste specimens.
MP	represents fiber-free cement paste specimens containing an air-entraining additive.
MP-B	represents fiber-reinforced cement paste specimens containing an air-entraining additive.

Fig. 4.12 Flexural strength after exposure to elevated temperatures.

Figure 4.12 presents the variations of residual flexural strength as a function of temperature. The lowest residual strengths are shown by the reference specimens, which lost almost more than 90 % of their original strength after exposure to a high temperature. As shown in Figure 4.13, the aerated MP samples show a lower percentage loss of strength after exposure to 400 °C, compared to the reference specimens. This is due to the easier leakage of physically bound water during heating, thus largely avoiding the internal stress inside the capillaries caused by the trapped steam. The application of basalt fibers is evident in the series of MP-B specimens. These fibers help to increase the flexural strength of the aerated composite and positively affect the residual flexural strength, even after exposure to 1000 °C.

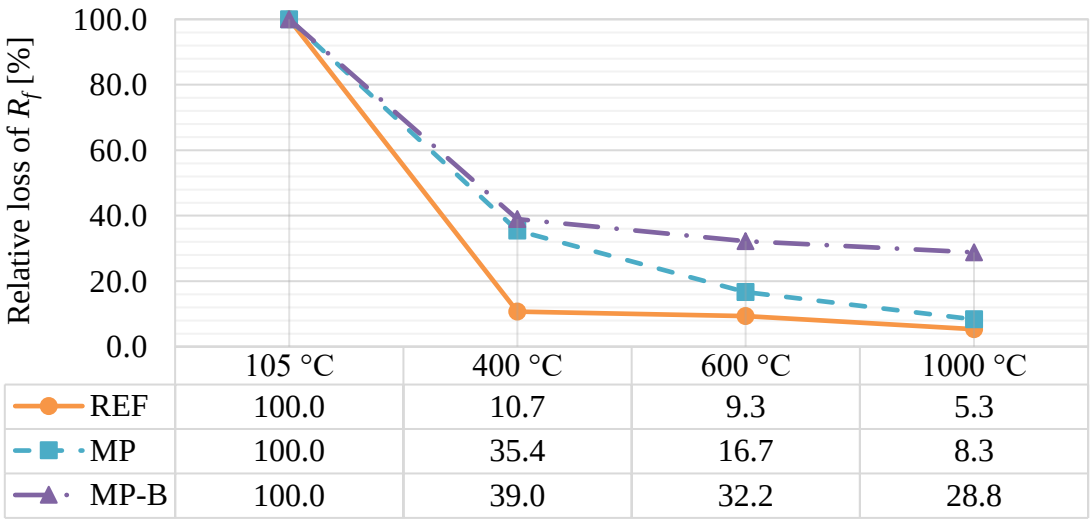

	105 °C	400 °C	600 °C	1000 °C
REF	100.0	10.7	9.3	5.3
MP	100.0	35.4	16.7	8.3
MP-B	100.0	39.0	32.2	28.8

Fig. 4.13 Loss of flexural strength as a function of elevated temperature.

Figure 4.14 compares the residual flexural strengths of all tested specimens after drying and exposure to 1000 °C. As mentioned, the reference specimens show the lowest residual strength. A noticeable reduction in strength occurs in the specimens containing LWA already after drying. However, after heating at 1000 °C, together with the fiber containing specimens, they retain the highest residual flexural strength values, especially the L2 and L2-B series.

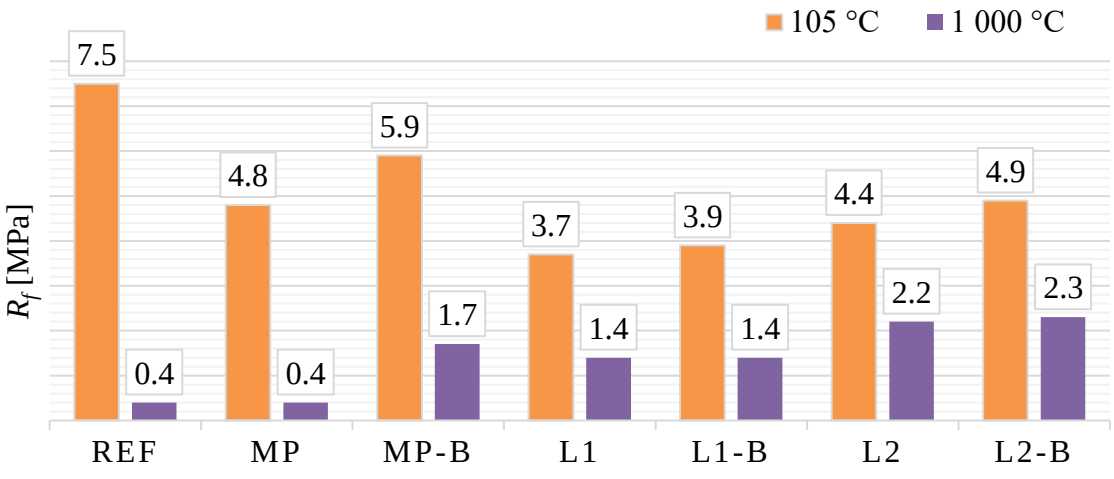

REF	represents fiber-free cement paste specimens.
MP	represents fiber-free cement paste specimens containing an air-entraining additive.
MP-B	represents fiber-reinforced cement paste specimens containing an air-entraining additive.

L1	represents fiber-free cement paste specimens containing an air-entraining additive and LWA.
L1-B	represents fiber-reinforced cement paste specimens containing an air-entraining additive and LWA.
L2	represents fiber-free cement paste specimens containing an air-entraining additive and double the amount of LWA.
L2-B	represents fiber-free cement paste specimens containing an air-entraining additive and double the amount of LWA.

Fig. 4.14 Residual flexural strength values after exposure to 1000 °C.

4.3.2 Fracture energy

Experimental records of the three-point bending test have been used to determine the fracture energy G_f, defined as the total energy dissipated over a unit crack area, based on the load-deflection curve according to RILEM [129]:

$$G_f = \frac{1}{b.h}\int_0^{\delta_{max}} F(\delta)d\delta \quad (4)$$

where

G_f is fracture energy [J/m^2]

F is loading force [N]

δ is deflection [mm]

b is specimen width (= 40 mm) [mm]

h is specimen height (= 40 mm) [mm]

The area under the load-deflection curve is used for the calculation of the work of fracture. As the complete fracture of the specimen was approached asymptotically in some cases during the three-point bending test, it was not possible to determine the endpoint of the test. Therefore, the test needs to be stopped at some point before the complete fracture, meaning that the measured work of fracture does not represent the complete fracture energy of the tested specimen. According to Lee [130], to overcome this state, a method has been proposed for estimating the complete fracture energy from the tested fracture energy using a far tail constant value.

From the results shown in Figure 4.15, it is evident that, due to the fibers, the fracture energy increases even after exposure to high temperatures. The MP series also records slightly higher fracture energies than the reference specimens after temperature loading.

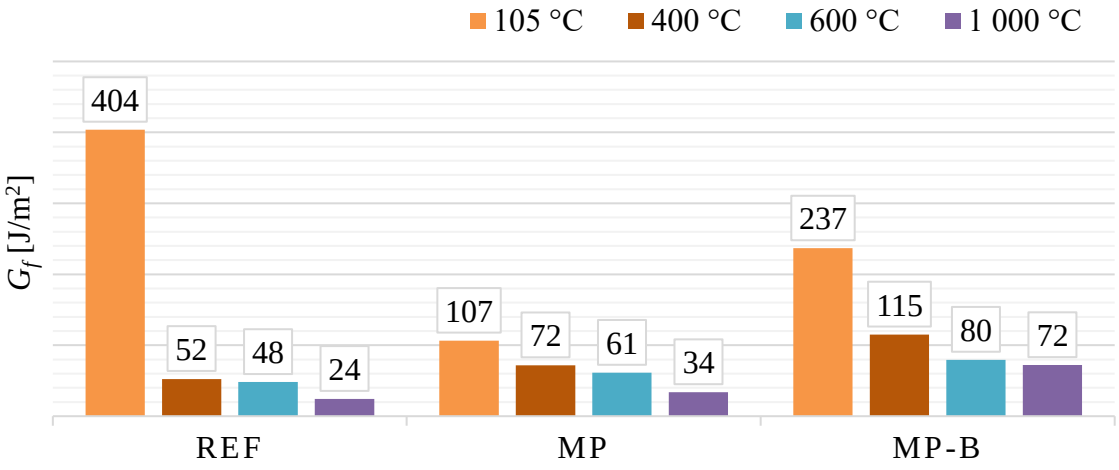

REF	represents fiber-free cement paste specimens.
MP	represents fiber-free cement paste specimens containing an air-entraining additive.
MP-B	represents fiber-reinforced cement paste specimens containing an air-entraining additive.

Fig. 4.15 Fracture energy values after exposure to elevated temperatures.

A cement-based composite (concrete), as a quasi-brittle material, usually exhibits a fracture process zone behind an existing notch or crack front. The experiments in this thesis were set up without a notch to monitor the entire destruction of the specimens, which were exposed to elevated temperatures. Due to the increased temperature, cracks begin to form on the surface, which is the most exposed area of the specimen. The chosen approach allows better comparisons between the specimens.

According to the load-deflection curves in Figure 4.16, it is clear that the specimens undergo a brittle fracture after drying. The residual resistance of the fibers to fracture is evident in the series of MP-B specimens, according to the development of the post-peak curve. In the following graphs, due to the formation of microcracks at elevated temperatures, some composites soften.

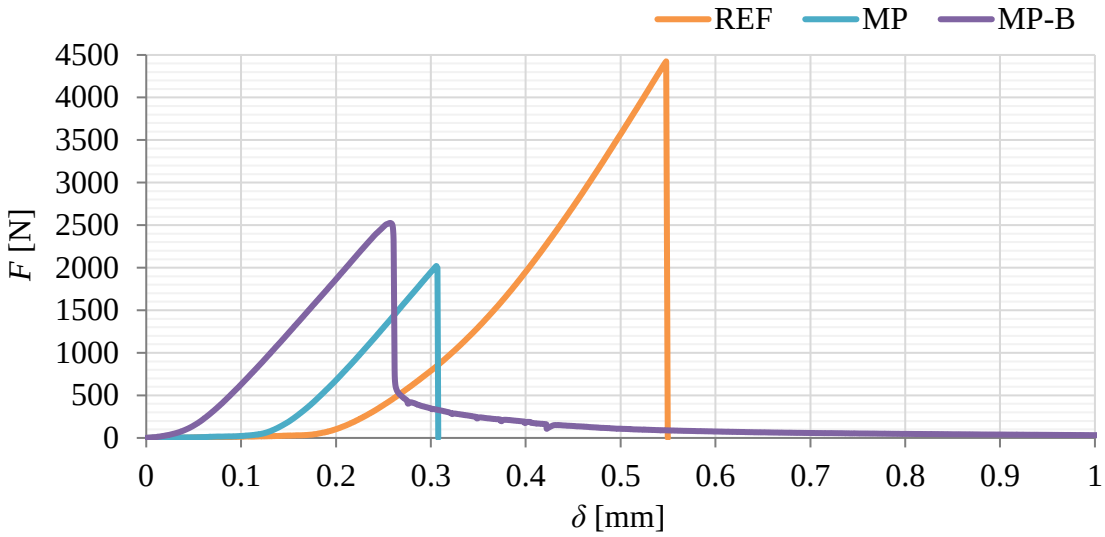

Fig. 4.16 Load-deflection curve for the evaluation of fracture energy after 105 °C.

As shown in Figure 4.17, after heating the specimens to 400 °C, the mentioned softening of the specimens has already occurred. The influence of temperatures of 600 °C and 1000 °C on the development of the load-deflection curve is shown in Figures 4.18 and 4.19. With an increasing temperature, the curves of the REF and MP series gradually decrease and show only a weak resistance to fracture, while the MP-B series maintains approximately the same curve shape at elevated temperatures, with a clear maximum peak load.

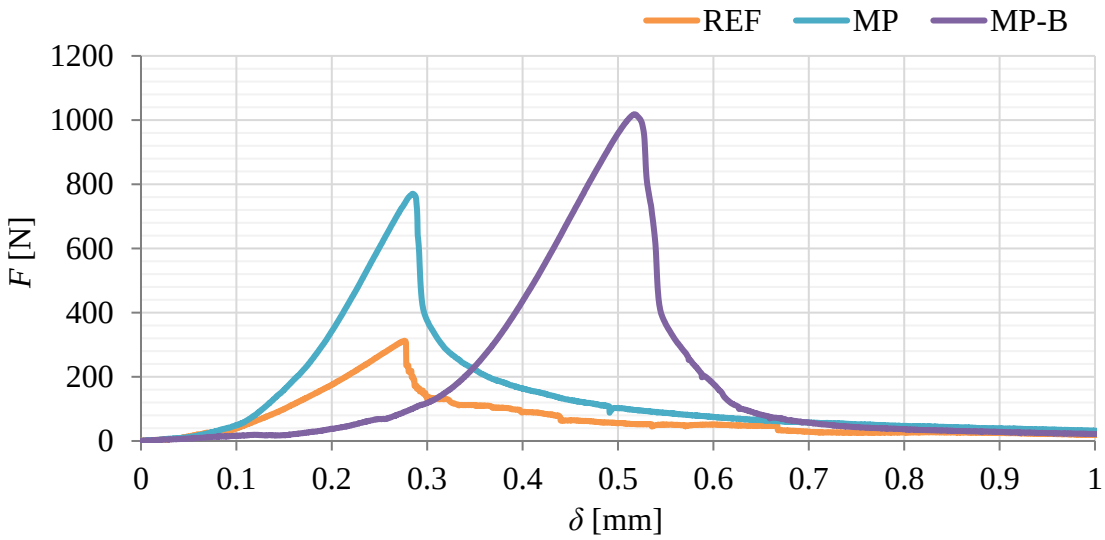

Fig. 4.17 Load-deflection curve for the evaluation of fracture energy after 400 °C.

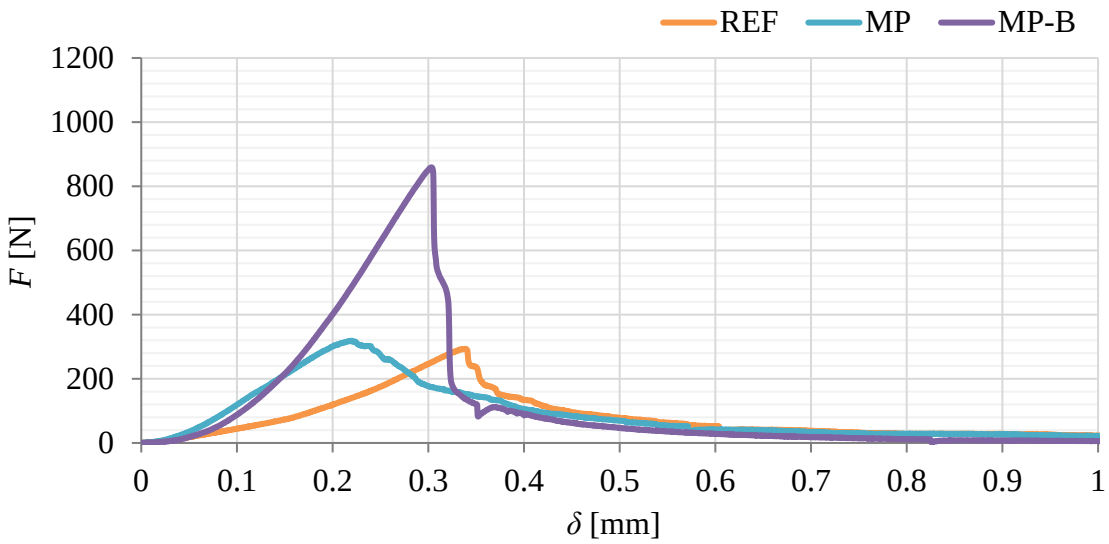

Fig. 4.18 Load-deflection curve for the evaluation of fracture energy after 600 °C.

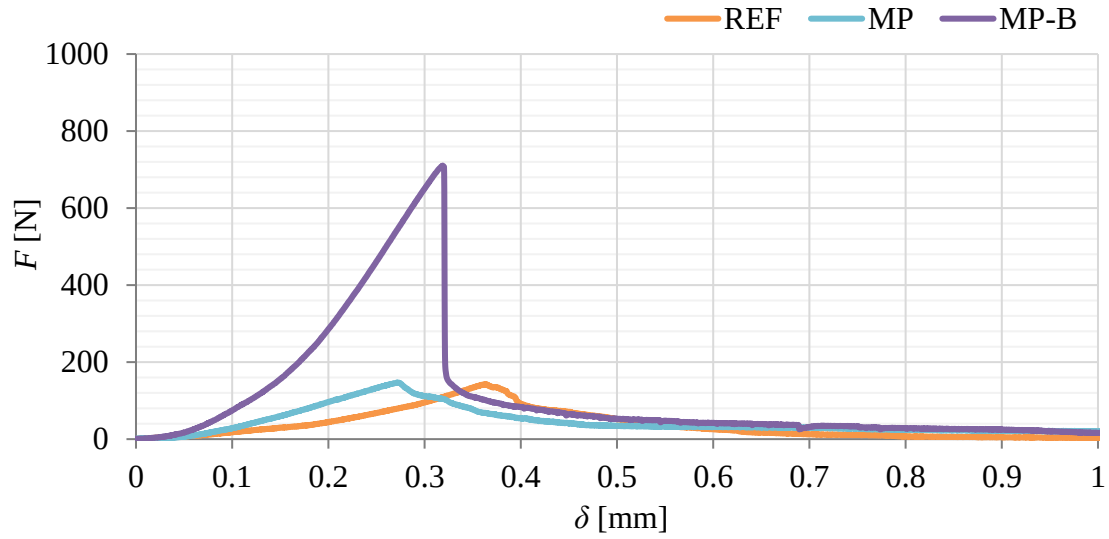

Fig. 4.19 Load-deflection curve for the evaluation of fracture energy after 1000 °C.

Figure 4.20 compares the fracture energy values of the tested specimens with and without LWA, dried at 105 °C and heated at 1000 °C. After drying, the highest result of fracture energy is declared by the reference specimens. However, the same series of specimens also shows the lowest result after high-temperature treatment. After heating at 1000 °C, the presence of fibers appears to be beneficial, even in combination with LWA. For example, the L2-B series presents excellent values after drying as well as after heating. At the same time, they have a much lower density than the reference specimens.

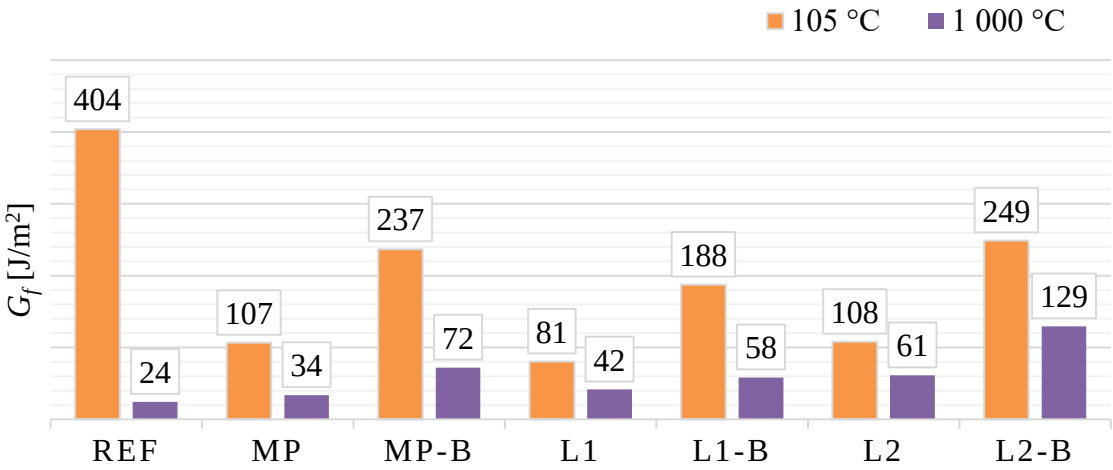

REF	represents fiber-free cement paste specimens.
MP	represents fiber-free cement paste specimens containing an air-entraining additive.
MP-B	represents fiber-reinforced cement paste specimens containing an air-entraining additive.
L1	represents fiber-free cement paste specimens containing an air-entraining additive and LWA.
L1-B	represents fiber-reinforced cement paste specimens containing an air-entraining additive and LWA.
L2	represents fiber-free cement paste specimens containing an air-entraining additive and double the amount of LWA.
L2-B	represents fiber-free cement paste specimens containing an air-entraining additive and double the amount of LWA.

Fig. 4.20 Residual fracture energy values after exposure to 1000 °C.

The following diagrams show the load-deflection curves of the specimens with the content of LWA, which are graphically compared with the curves of the specimens without LWA.

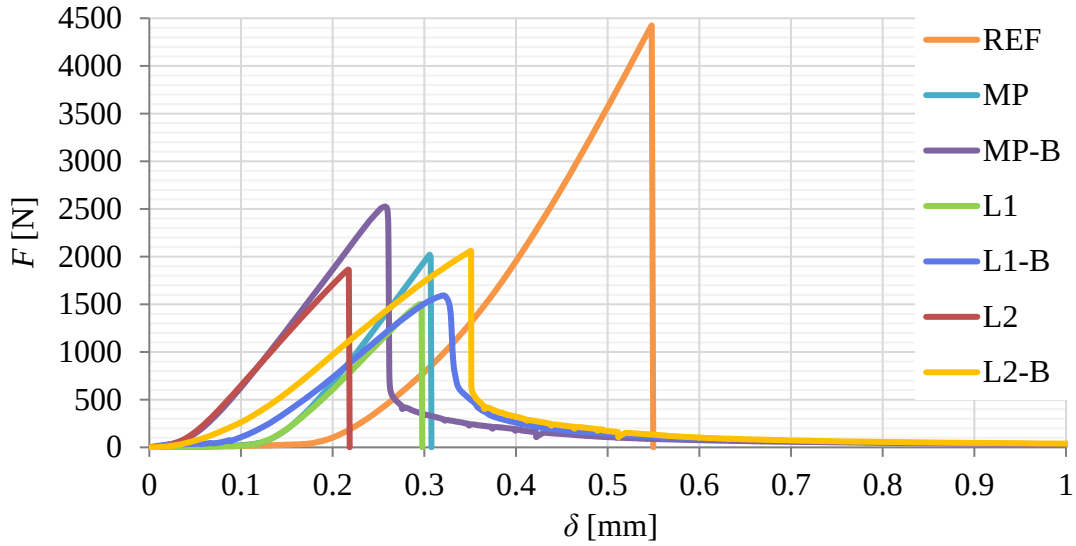

Fig. 4.21 Load-deflection curve of specimens subjected to 105 °C.

In Figures 4.21 and 4.22, it can be observed from all load-deflection curves of each specimen, that the curve is predominantly a straight line before it reaches the peak. As in the previous cases, for the specimens with LWA after drying, a brittle fracture occurs when the maximum load-bearing capacity is reached. Similarly, a brittle fracture occurs after exposure to a temperature of 1000 °C, as is the case with the MP-B series.

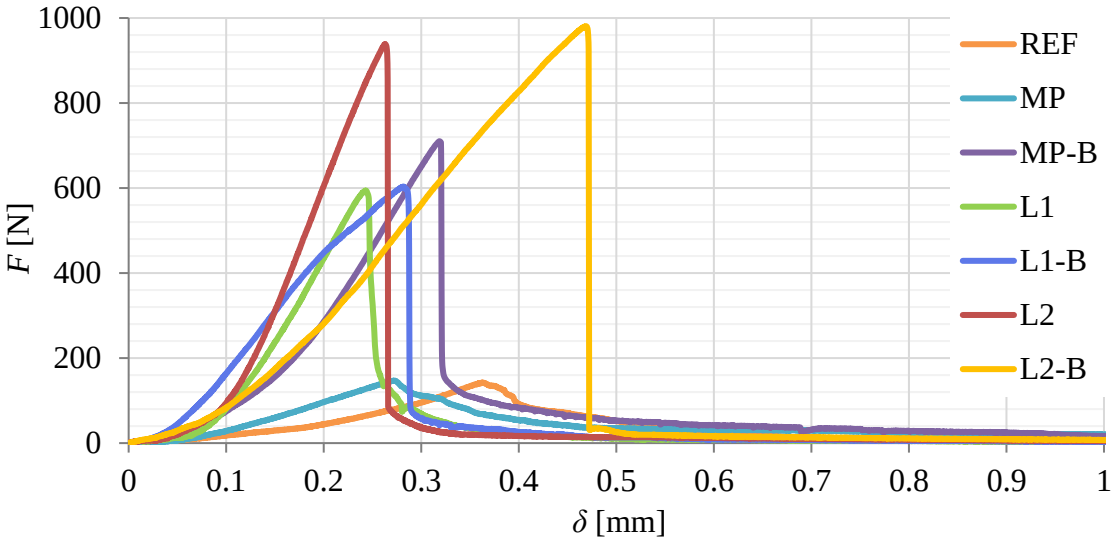

Fig. 4.22 Load-deflection curve of specimens subjected to 1000 °C.

4.3.3 Compressive strength

As only simple compression was applied, special emphasis was placed on centering the arrangement. The ultimate force was recorded as in the case of flexural strength. The compressive strength R_c tested on the fragments left after the three-point bending test was calculated from the equation:

$$R_c = max\ \sigma_c = \frac{F_c}{A} \tag{5}$$

where

R_c is compressive strength [MPa]

σ_f is compressive stress [MPa]

F_c is maximum failure load [N]

A is the load area (= 40 mm × 40 mm) [mm^2]

The residual compressive strength values of the specimens after drying at 150 °C and after heating to 400, 600, and 1000 °C are presented in Figure 4.24. When applying an air-entraining agent and basalt fibers, there is an obvious decrease in strength. The strength values correspond to the density values of individual specimens. It is obvious from the results that the largest decrease in strength occurs between 105 and 400 °C. In the case of the series of MP specimens, there was also a significant reduction in strength between 600 and 1000 °C. The largest losses between individual load cycles occur in the series of REF specimens, but they also retain the highest values of residual compressive strength.

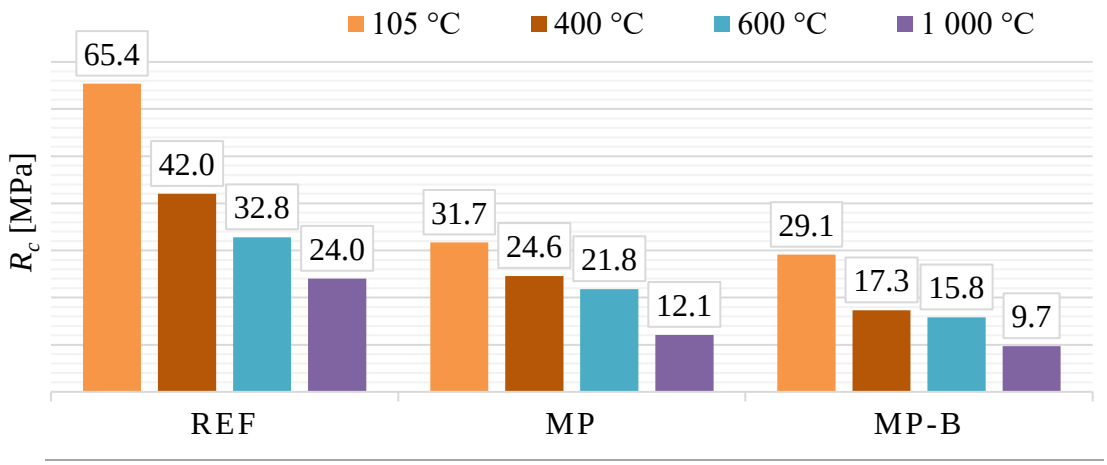

REF	represents fiber-free cement paste specimens.
MP	represents fiber-free cement paste specimens containing an air-entraining additive.
MP-B	represents fiber-reinforced cement paste specimens containing an air-entraining additive.

Fig. 4.23 Compressive strength after exposure to elevated temperatures.

Figure 4.24 shows the percentage compressive strength drop with temperature starting from 400 °C. Three temperature ranges are observed, 105 to 400 °C, 400 to 600 °C, and 600 to 1000 °C. The largest loss of strength occurs in the first temperature range (105 to 400 °C). In the second temperature range (400 to 600 °C), the compressive strength decreases with the increasing temperature. However, the rate of the strength loss comparatively slows down. Beyond 600 °C, during the third temperature range (600 to 1000 °C), the specimens lose the last remnants of chemically bound water and the decrease in strength continues, most notably in the MP series.

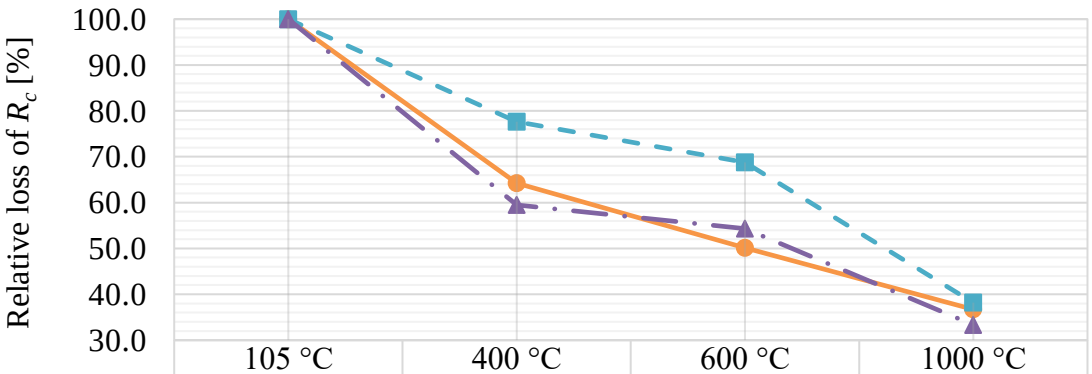

	105 °C	400 °C	600 °C	1000 °C
REF	100.0	64.2	50.2	36.7
MP	100.0	77.6	68.8	38.2
MP-B	100.0	59.5	54.3	33.3

Fig. 4.24 Loss of compressive strength as a function of elevated temperature.

To compare all mixtures, Figure 4.25 shows the residual compressive strength of all composites dried and exposed to 1000 °C. In the case of lightweight specimens, there was a significant reduction in strength after drying. For the series of specimens without LWA, the strength drops between 61.8 and 66.7 % after exposure to 1000 °C. On the other hand, in the case of the specimens with LWA, the values of residual compressive strength are more stable and do not show a significant difference in strength between 105 and 1000 °C.

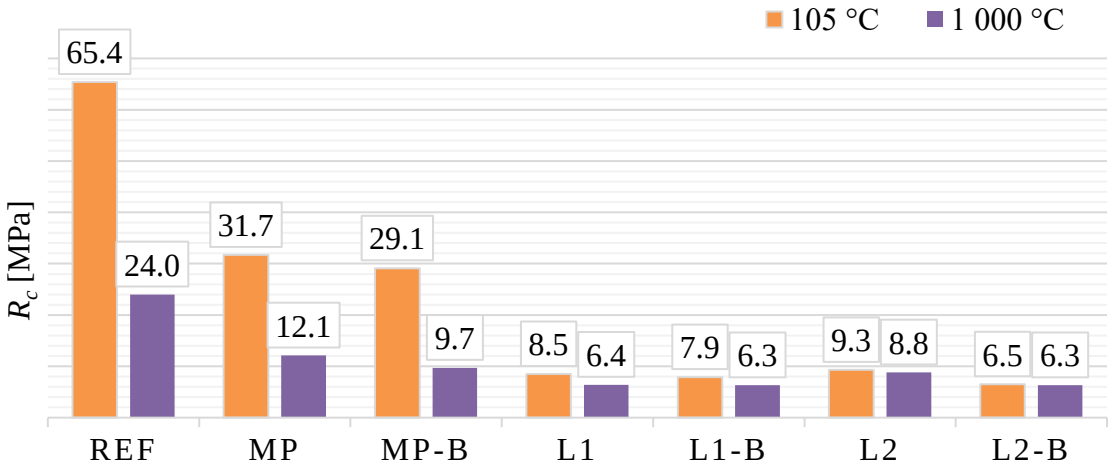

REF	represents fiber-free cement paste specimens.
MP	represents fiber-free cement paste specimens containing an air-entraining additive.
MP-B	represents fiber-reinforced cement paste specimens containing an air-entraining additive.
L1	represents fiber-free cement paste specimens containing an air-entraining additive and LWA.
L1-B	represents fiber-reinforced cement paste specimens containing an air-entraining additive and LWA.
L2	represents fiber-free cement paste specimens containing an air-entraining additive and double the amount of LWA.
L2-B	represents fiber-free cement paste specimens containing an air-entraining additive and double the amount of LWA.

Fig. 4.25 Residual compressive strength values after exposure to 1000 °C.

Chapter 5

Conclusion

5.1 Summary results of the experiments

The composites designed in this paper contained an air-entraining additive and chopped basalt fibers in combination with LWA Liaver to secure the necessary values of density and were, therefore, classified as lightweight composites. Short fibers have also been used to promote resistance to internal stresses caused by high-temperature loads and to achieve better residual properties. The list of test specimens is summarized in Table 5.1.

Table 5.1 Identification of test specimens.

REF	represents fiber-free cement paste specimens.
MP	represents fiber-free cement paste specimens containing an air-entraining additive.
MP-B	represents fiber-reinforced cement paste specimens containing an air-entraining additive.
L1	represents fiber-free cement paste specimens containing an air-entraining additive and LWA.
L1-B	represents fiber-reinforced cement paste specimens containing an air-entraining additive and LWA.
L2	represents fiber-free cement paste specimens containing an air-entraining additive and double the amount of LWA.
L2-B	represents fiber-free cement paste specimens containing an air-entraining additive and double the amount of LWA.

The impact of high temperatures on cement-based composites concerns both the physical and chemical changes taking place in the matrix and the phenomena involved in the mass movement (gases and liquids). The effects of various changes taking place in the heated composite are the alterations of its physical and mechanical properties.

The presented data have been selected from both the author's most recent research and published literature to provide a brief outline of the subject. The research has demonstrated that changes in the strength of composites as a function of temperature are related to the composite composition and thus the density of the specimens.

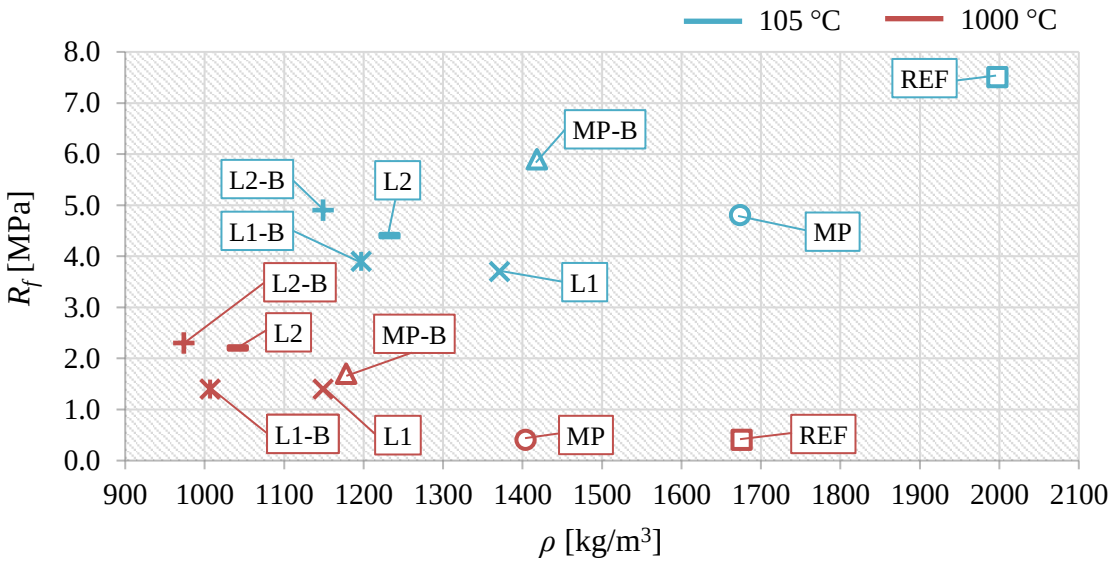

Fig. 5.1 Relation between flexural strength and density of specimens.

In Figure 5.1, the graphical representation of the reached results obtained after exposure to the highest experimental temperature of 1000 °C shows the increase in the residual flexural strength values associated with a dose of basalt fibers and a higher content of LWA, which also caused a composite's weight reduction, therefore, Liaver appears to be a satisfactory component in the refractory mixture.

In the case of reference specimens, the flexural strength decreases by almost 95 % after high-temperature loading, when the most significant loss of strength occurs at 400 °C according to the results presented in the previous chapter. The series of MP-B specimens shows a considerable decrease in density, which as well results in a general loss of strength. However, these specimens achieve higher residual strength than the reference specimens. After high-temperature loading, the strength is reduced by 71 %. In

terms of flexural strength, the specimens containing basalt fibers and LWA appear to be the most stable. Not only do they reach density values below 1200 kg/m^3, but in the L2-B series, after exposure to 1000 °C, almost 50 % of the original strength is maintained. Tanyildizi has achieved similar results in his study [131], in which a positive effect of carbon fibers on the mechanical properties of LWAC exposed up to 800 °C is presented.

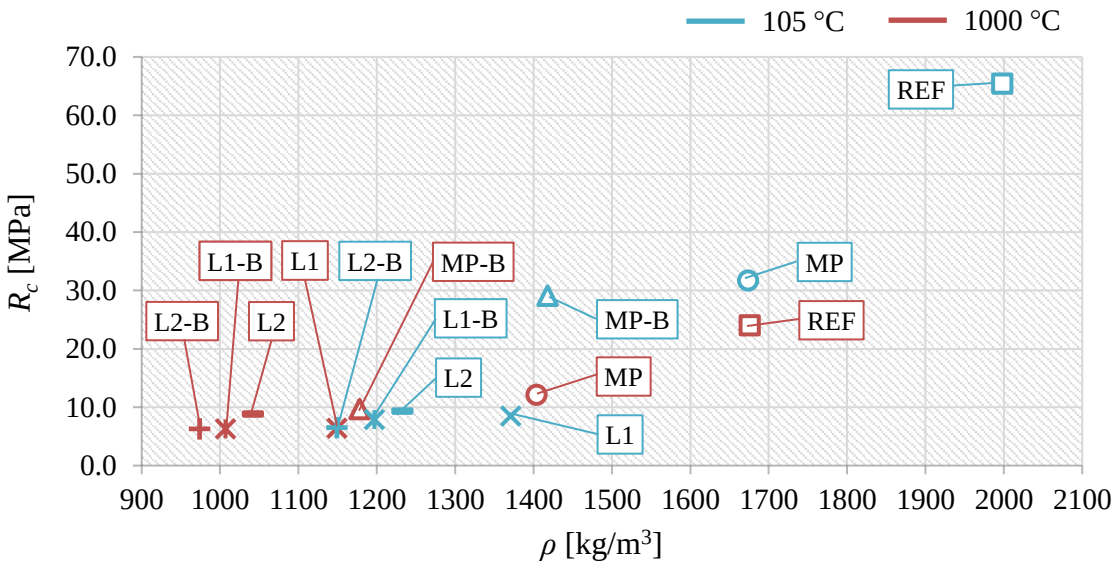

Fig. 5.2 Relation between compressive strength and density of specimens.

According to Naus [25], lightweight refractory concretes are classified by density (880 to 1680 kg/m^3) and service temperature (927 to 1760 °C). Their cold compressive strengths vary between 1.4 and 3.4 MPa, for materials with a density up to 800 kg/m^3 and between 6.9 and 17.2 MPa for materials with a density of 1200 to 1600 kg/m^3. As shown in Figure 5.2, the compressive strength of the tested REF, MP, and MP-B specimens naturally decreases with the increase in temperature. It was only the series of specimens containing LWA that showed the stability of compressive strength after exposure to 1000 °C. These specimens, together with the MP-B series, also comply with the above-mentioned classification of lightweight refractory concretes. Likewise, the stability and excellent high-temperature resistance of the cement-based composite containing LWA are also confirmed in the research by Yao et al. [102], which is based on a limited loss of mass and strength after exposure to high temperature.

5.2 Achieved goals

This subchapter recapitulates the achieved goals, which were the key factors in this work:

- Utilization of environmentally friendly components.

LWA made by recycling glass has proven to be a beneficial part of LWRCC. LWA plays an important role in today's move toward sustainable concrete. Even though most LWAs require energy to manufacture, when used and evaluated from the whole building's perspective, the overall carbon footprint of a structure is often lowered. According to Ries et al. [52] and Tenza-Abril et al. [103], the use of LWA provides strategies to enhance cement hydration, improve the energy performance of structures, reduce life-cycle costs, and reduce the environmental impacts of material transport and construction.

- Application of fibers.

Attention has been paid to the determination of the influence of basalt fibers. The motivation was to reach better residual properties of LWRCC with the help of fibers and, if possible, also contribute to the reduction of the environmental impact. The experimental results show that the fiber content in the specimens helps to partially transfer the internal stresses caused by high temperatures and generally increases the flexural strength. Thus, the positive effect of the fibers used in refractory composites is evident, even after loading with a temperature of 1000 °C, see Figure 5.3. Fibers allow better operational resistance than fiber-free cement-based composites due to the limited volume changes and increased tensile strength [132].

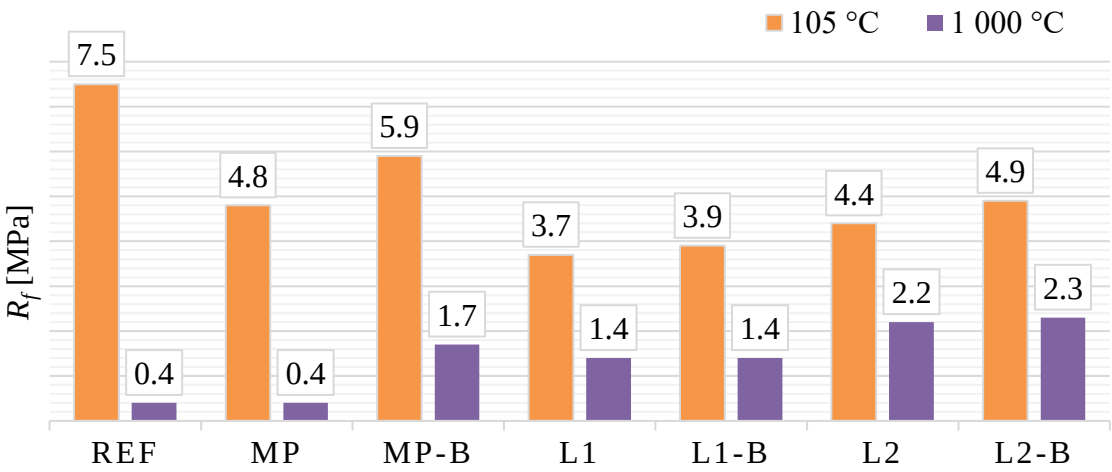

REF	represents fiber-free cement paste specimens.
MP	represents fiber-free cement paste specimens containing an air-entraining additive.
MP-B	represents fiber-reinforced cement paste specimens containing an air-entraining additive.
L1	represents fiber-free cement paste specimens containing an air-entraining additive and LWA.
L1-B	represents fiber-reinforced cement paste specimens containing an air-entraining additive and LWA.
L2	represents fiber-free cement paste specimens containing an air-entraining additive and double the amount of LWA.
L2-B	represents fiber-free cement paste specimens containing an air-entraining additive and double the amount of LWA.

Fig. 5.3 Residual flexural strength values after exposure to 1000 °C.

- Easy workability in arbitrary shapes.

The workability level of fresh mixtures was monitored using the flow table test. The fiber-free mixtures were particularly fluid and could be poured directly into molds without difficulty. The subsequent presence of an air-entraining agent and basalt fibers in the fresh cement mixture helped to increase the formation of small air bubbles. This made the mixture creamier. After adding LWA to the mixture, the presence of air increased. The mixture was consistent and stable, with satisfactory workability. There was an even distribution of fibers in the mixture, which was greatly aided by a larger dose of LWA.

- Achieving values of density less than 1800 kg/m^3.

A lightweight composite can increase the economic efficiency by reducing the weight of the structure. In general, the limit value for lightweight composites is set at 1800 kg/m^3.

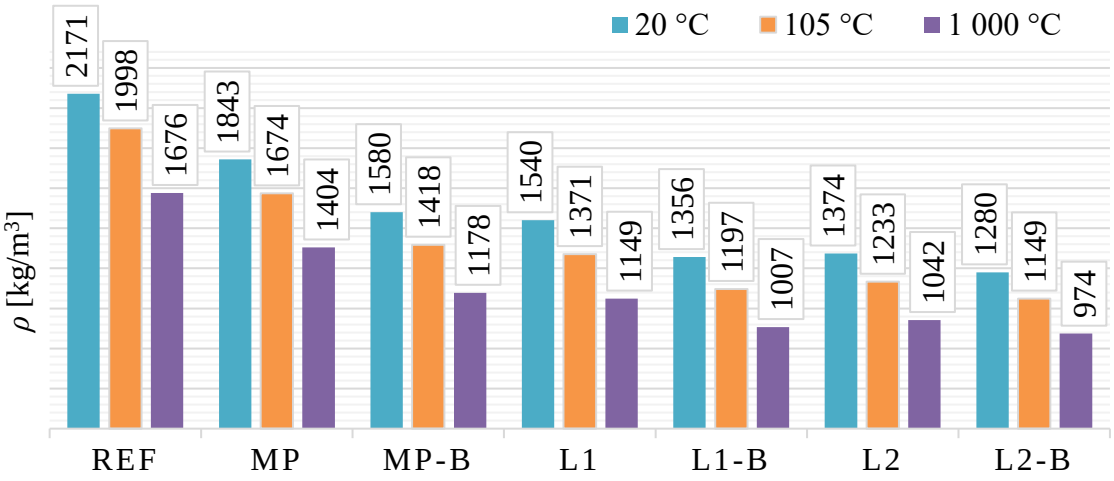

REF	represents fiber-free cement paste specimens.
MP	represents fiber-free cement paste specimens containing an air-entraining additive.
MP-B	represents fiber-reinforced cement paste specimens containing an air-entraining additive.
L1	represents fiber-free cement paste specimens containing an air-entraining additive and LWA.
L1-B	represents fiber-reinforced cement paste specimens containing an air-entraining additive and LWA.
L2	represents fiber-free cement paste specimens containing an air-entraining additive and double the amount of LWA.
L2-B	represents fiber-free cement paste specimens containing an air-entraining additive and double the amount of LWA.

Fig. 5.4 Residual density values after exposure to 1000 °C.

Looking at the density values of the tested specimens in Figure 5.4, it is obvious that the application of an air-entraining agent, basalt fibers, and LWA appears to be very effective in forming a lightweight cement-based composite. Such a refractory composite reaches density values below 1400 kg/m^3 at room temperature.

- Sufficient dimensional stability.

After high-temperature loading, the specimens did not show any significant dimensional changes that would not be related to the expected microstructural transformation of the hydrated products during their dehydration under elevated temperatures.

- Prevention of explosive spalling under temperature loads.

The mass and density of the composite specimens reduced significantly as the temperature increased, especially between 105 °C and 400 °C, see Table 5.2. According to Majorana [43], as the heating rate was set at 10 ° C/min, there was a significant risk of explosive spalling. However, no explosive spalling occurred during the temperature loads described in this experiment. Not even at constant temperatures of 400 °C, 600 °C, and 1000 °C for 3 hours. Water (free water and bound water) had suitable conditions for migration from the specimens at increasing temperatures.

Table 5.2 Mass loss of specimens subjected to elevated temperatures.

	Relative mass loss [%]				
	20 °C	105 °C	400 °C	600 °C	1000 °C
REF	0.0	8.0	13.9	19.1	22.8
MP	0.0	9.2	17.0	19.7	23.8
MP-B	0.0	10.3	17.6	21.7	25.4

- Satisfactory residual strength after exposure to temperatures up to 1000 °C.

As the summary results in the previous subchapter 5.1 present, the created composites containing basalt fibers and LWA show satisfactory residual strength required to be classified as LWRC. The components forming the experimental composites significantly contribute to keeping the stability of the mechanical properties after high-temperature loading. That is proven by the results of the residual strengths measured and compared with the reference specimens.

5.3 Proposals for future research

The final findings were summarized in the following recommendations:

- The following experiments should focus on optimizing the amount of LWA in the composition of refractory cement-based composites. The results prove that LWA in the cement composite contributes to the stability and resistance of refractory products under temperature loads up to 1000 °C. Future research should also include the analysis of the application of other LWAs made from secondary raw materials by high-temperature treatment and thus expand the field of their possible use.

- A lightweight composite can increase the economic efficiency by reducing the weight of the structure. This also leads to increased thermal insulation. In addition to the air-entraining additive, another way to achieve a lightweight cementitious matrix is to apply a foaming agent, mixed with water and air from a generator. The density of foam concrete usually varies from 400 to 1600 kg/m^3. Thanks to this method, a solid, stable, and fine structure of air pores is created, which can better withstand the changes associated with exposure to high temperatures.

- It is an increasingly common trend to improve the composition of cement-based composites with suitable fine pozzolanic components (e.g., metakaolin, metashale, brick waste ash), which also partially replace the amount of cement. This can lead to a reduction in the consumption of expensive CAC and thus has a positive effect on the economic and environmental aspects of refractory products.

- Since the tests in this thesis were performed at room temperature after exposure to high temperatures, the results do not indicate how the refractory composite will behave under actual loads at elevated temperatures. The following experiments should focus on the previously mentioned hot testing to obtain a more detailed analysis and provide a better understanding when creating a refractory barrier in an optional form.

- Furthermore, it is recommended to investigate the mechanical properties of the cement-based refractory composite after exposure to a temperature higher than 1000 °C, which may ultimately be beneficial and lead to an increase in strength due to re-sintering.

References

[1] KEPPERT, Martin, E. VEJMELKOVÁ, S. ŠVARCOVÁ, P. BEZDIČKA and R. ČERNÝ. Microstructural changes and residual properties of fiber reinforced cement composites exposed to elevated temperatures. *Cement, Wapno, Beton* [online]. 2012, **17/79**(2), 77–89 [accessed. 2021-01-02]. ISSN 14258129. Availableat: https://scholar.google.cz/scholar?cluster=2386330505637750092&hl=en&oi=scholarr

[2] ABYZOV, V. A. Lightweight refractory concrete based on aluminum-magnesium-phosphate binder. In: *Procedia Engineering* [online]. B.m.: Elsevier Ltd, 2016, p. 1440–1445. ISSN 18777058. Available at: doi:10.1016/j.proeng.2016.07.077

[3] SADIK, Chaouki, Iz Eddine EL AMRANI and Abderrahman ALBIZANE. Recent advances in silica-alumina refractory: A review. *Journal of Asian Ceramic Societies* [online]. 2014, **2**(2), 83–96. ISSN 21870764. Available at: doi:10.1016/j.jascer.2014.03.001

[4] KATSAVOU, I. D., M. K. KROKIDA and I. C. ZIOMAS. Effect of production conditions on structural properties of refractory materials. *Materials Research Innovations* [online]. 2011, **15**(1), 47–52 [accessed. 2021-01-04]. ISSN 14328917. Available at: doi:10.1179/143307511X12922272563824

[5] KATSAVOU, I. D., M. K. KROKIDA and I. C. ZIOMAS. Determination of mechanical properties and thermal treatment behavior of alumina-based refractories. *Ceramics International* [online]. 2012, **38**(7), 5747–5756. ISSN 02728842. Available at: doi:10.1016/j.ceramint.2012.04.021

[6] HOLČAPEK, Ondřej, Pavel REITERMAN and Petr KONVALINKA. Binder for refractory cement composites – Hydration, changing due to high temperatures and fracture energy. In: *Materials Science Forum* [online]. B.m.: Trans Tech Publications Ltd, 2015, p. 185–190 [accessed. 2021-01-02]. ISBN 9783038355090. Available at: doi:10.4028/www.scientific.net/MSF.824.185

[7] HAQUE, M. N., H. AL-KHAIAT and O. KAYALI. Strength and durability of lightweight concrete. *Cement and Concrete Composites* [online]. 2004, **26**(4), 307–314. ISSN 09589465. Available at: doi:10.1016/S0958-9465(02)00141-5

[8] CUI, H. Z., Tommy Yiu LO, Shazim Ali MEMON and Weiting XU. Effect of lightweight aggregates on the mechanical properties and brittleness of lightweight aggregate concrete. *Construction and Building Materials* [online]. 2012, **35**, 149–158 [accessed. 2021-01-03]. ISSN 09500618. Available at: doi: 10.1016/j. conbuildmat.2012.02.053

[9] OSMAN, Moustafa, H. MARZOUK and Sherief HELMY. Behavior of high-strength lightweight concrete slabs under punching loads. *ACI Structural Journal* [online]. 2000, **97**(3), 492–498 [accessed. 2021-01-03]. ISSN 08893241. Available at: doi:10.14359/4644

[10] KAYALI, O., M. N. HAQUE and B. ZHU. Some characteristics of high strength fiber reinforced lightweight aggregate concrete. *Cement and Concrete Composites* [online]. 2003, **25**(2), 207–213. ISSN 09589465. Available at: doi:10.1016/S0958-9465(02)00016-1

[11] LIBRE, Nicolas Ali, Mohammad SHEKARCHI, Mehrdad MAHOUTIAN and Parviz SOROUSHIAN. Mechanical properties of hybrid fiber reinforced lightweight aggregate concrete made with natural pumice. *Construction and Building Materials* [online]. 2011, **25**(5), 2458–2464. ISSN 09500618. Available at: doi:10.1016/j.conbuildmat.2010.11.058

[12] CHOI, Jisun, Goangseup ZI, Shinichi HINO, Kohei YAMAGUCHI and Soye KIM. Influence of fiber reinforcement on strength and toughness of all-lightweight concrete. *Construction and Building Materials* [online]. 2014, **69**, 381–389. ISSN 09500618. Available at: doi:10.1016/j.conbuildmat.2014.07.074

[13] KIM, Jihwan, Dong Joo KIM, Seuntg Hun PARK and Goangseup ZI. Investigating the flexural resistance of fiber reinforced cementitious composites under biaxial condition. *Composite Structures* [online]. 2015, **122**, 198–208. ISSN 02638223. Available at: doi:10.1016/j.compstruct.2014.11.055

[14] SIM, Jongsung, Cheolwoo PARK and Do Young MOON. Characteristics of basalt fiber as a strengthening material for concrete structures. *Composites Part B: Engineering* [online]. 2005, **36**(6–7), 504–512. ISSN 13598368. Available at: doi:10.1016/j.compositesb.2005.02.002

[15] MIRZA, Faiz A. and Parviz SOROUSHIAN. Effects of alkali-resistant glass fiber reinforcement on crack and temperature resistance of lightweight concrete. *Cement and Concrete Composites* [online]. 2002, **24**(2), 223–227 [accessed. 2021-01-03]. ISSN 09589465. Available at: doi:10.1016/S0958-9465(01)00038-5

[16] AYUB, Tehmina, Nasir SHAFIQ and M. Fadhil NURUDDIN. Effect of chopped basalt fibers on the mechanical properties and microstructure of high performance fiber reinforced concrete. *Advances in Materials Science and Engineering* [online]. 2014, **2014**. ISSN 16878442. Available at: doi:10.1155/2014/587686

[17] WANG, Xinzhong, Jun HE, Ayman S. MOSALLAM, Chuanxi LI and Haohui XIN. The effects of fiber length and volume on material properties and crack resistance of basalt fiber reinforced concrete (BFRC). *Advances in Materials Science and Engineering* [online]. 2019, **2019**. ISSN 16878442. Available at: doi:10.1155/2019/7520549

[18] BODNÁROVÁ, Lenka, Jiří ZACH, Jitka HROUDOVÁ and Jaroslav VÁLEK. Methods for determination of the quality of concretes with respect to their high temperature behaviour. In: *Procedia Engineering* [online]. 2013, p. 260–265. ISSN 18777058. Available at: doi:10.1016/j.proeng.2013.09.040

[19] JIAO, Yubo, Hanbing LIU, Xianqiang WANG, Yuwei ZHANG, Guobao LUO and Yafeng GONG. Temperature effect on mechanical properties and damage identification of concrete structure. *Advances in Materials Science and Engineering* [online]. 2014, **2014**. ISSN 16878442. Available at: doi:10.1155/2014/191360

[20] ŠPEDLOVÁ, Veronika and Dana KOŇÁKOVÁ. Behavior of cement composites loaded by high temperature. In: *Materials Science Forum* [online]. B.m.: Trans Tech Publications Ltd, 2015, p. 121–125 [accessed. 2021-01-03]. ISBN 9783038355090. Available at: doi:10.4028/www.scientific.net/MSF.824.121

[21] VEJMELKOVÁ, Eva, Petr KONVALINKA, Pavel PADEVĚT, Lubomír KOPECKÝ, Martin KEPPERT and Robert ČERNÝ. Mechanical, hygric, and thermal properties of cement-based composite with hybrid fiber reinforcement subjected to high temperatures. *International Journal of Thermophysics* [online]. 2009, **30**(4), 1310–1322 [accessed. 2021-01-04]. ISSN 0195928X. Available at: doi:10.1007/s10765-009-0609-z

[22] HOLČAPEK, Ondřej, Pavel REITERMAN and Petr KONVALINKA. Fracture characteristics of refractory composites containing metakaolin and ceramic fibers. *Advances in Mechanical Engineering* [online]. 2015, **7**(3), 1–13. ISSN 16878140. Available at: doi:10.1177/1687814015573619

[23] LI, Zongjin. *Advanced concrete technology* [online]. Hoboken, New Jersey: John Wiley & Sons, Inc., 2011 [accessed. 2021-01-06]. ISBN 978-0-470-90243-1. Available at: https://books.google.cz/books?hl=cs&lr=&id=1lthdPkTS9wC&oi=fnd&pg=PP7&dq=Advanced+concrete+technology&ots=4C_8OPgVYF&sig=1IxBSpX0J7k9_NaJKB544fScNYQ&redir_esc=y#v=onepage&q&f=false

[24] HARRISSON, Arthur Michael. Constitution and specification of Portland cement. In: *Lea's Chemistry of Cement and Concrete* [online]. B.m.: Elsevier, 2019, p. 87–155. ISBN 9780081007730. Available at: doi:10.1016/B978-0-08-100773-0.00004-6

[25] NAUS, Dan J. *The effect of elevated temperature on concrete materials and structures - A literature review.* [online]. 2005 [accessed. 2021-01-05]. Available at: doi:10.2172/974590

[26] QUIROGA, Pedro Nel and David W. FOWLER. *ICAR 104-1F, The effects of aggregate characteristics on the performance of portland cement concrete* [online]. 2003 [accessed. 2021-01-05]. Available at: https://repositories.lib.utexas.edu/handle/2152/35333

[27] BODNÁROVÁ, L., Jaroslav VÁLEK, Libor SITEK and Josef FOLDYNA. Effect of high temperatures on cement composite materials in concrete structures. *Acta Geodynamica et Geomaterialia* [online]. 2013, **10**(2), 173–180. ISSN 12149705. Available at: doi:10.13168/AGG.2013.0017

[28] KHOURY, Gabriel Alexander. Effect of fire on concrete and concrete structures. *Progress in Structural Engineering and Materials* [online]. 2000, **2**(4), 429–447 [accessed. 2021-01-02]. ISSN 1365-0556. Available at: doi:10.1002/pse.51

[29] BODNAROVA, Lenka, Tomas JAROLIM, Jaroslav VALEK, Jiri BROZOVSKY and Rudolf HELA. Selected properties of cementitous composites with Portland cements and blended Portland cements in extreme conditions. In: *Applied Mechanics and Materials* [online]. B.m.: Trans Tech Publications Ltd, 2014, p. 443–448 [accessed. 2021-01-04]. ISBN 9783038350071. Available at: doi:10.4028/www.scientific.net/AMM.507.443

[30] KODUR, Venkatesh. Properties of concrete at elevated temperatures. *ISRN Civil Engineering* [online]. 2014, **2014**. ISSN 20905114. Available at: doi:10.1155/2014/468510

[31] TOLENTINO, Evandro, Fernando S. LAMEIRAS, Abdias M. GOMES, Cláudio A. Rigo da SILVA and Wander L. VASCONCELOS. Structural evaluation and performance of Portland cement concretes after exposure to high temperatures. *Materials Research* [online]. 2002, **5**(1), 27–36. ISSN 1516-1439. Available at: doi:10.1590/s1516-14392002000100005

[32] XIE, Qifang, Lipeng ZHANG, Shenghua YIN, Baozhuang ZHANG and Yaopeng WU. Effects of high temperatures on the physical and mechanical properties of carbonated ordinary concrete. *Advances in Materials Science and Engineering* [online]. 2019, **2019**. ISSN 16878442. Available at: doi:10.1155/2019/5753232

[33] ESEN, Yuksel and Alper KURT. Effect of high temperature in concrete for different mineral additives and rates. *KSCE Journal of Civil Engineering* [online]. 2018, **22**(4), 1288–1294 [accessed. 2021-01-05]. ISSN 19763808. Available at: doi:10.1007/s12205-017-1224-3

[34] WANG, Jin. *Modeling of concrete dehydration and multiphase transfer in nuclear containment concrete wall during loss of cooling accident* [online]. B.m., 2016 [accessed. 2021-02-19]. Université Paul Sabatier - Toulouse III. Available at: https://tel.archives-ouvertes.fr/tel-01578096

[35] KORPA, A. and R. TRETTIN. The influence of different drying methods on cement paste microstructures as reflected by gas adsorption: Comparison between freeze-drying (F-drying), D-drying, P-drying and oven-drying methods. *Cement and Concrete Research* [online]. 2006, **36**(4), 634–649. ISSN 00088846. Available at: doi:10.1016/j.cemconres.2005.11.021

[36] HAGER, I. Behaviour of cement concrete at high temperature. *Bulletin of the Polish Academy of Sciences: Technical Sciences* [online]. 2013, **61**(1), 145–154. ISSN 02397528. Available at: doi:10.2478/bpasts-2013-0013

[37] PANCAR, Erhan Burak. Reducing high temperature effect on concrete by changing concrete mixture. *International Journal of Structural and Civil Engineering Research* [online]. 2017, **6**(4), 258–262. Available at: doi:10.18178/ijscer.6.4.258-262

[38] TUFAIL, Muhammad, Khan SHAHZADA, Bora GENCTURK and Jianqiang WEI. Effect of elevated temperature on mechanical properties of limestone, quartzite and granite concrete. *International Journal of Concrete Structures and Materials* [online]. 2017, **11**(1), 17–28 [accessed. 2021-01-05]. ISSN 22341315. Available at: doi:10.1007/s40069-016-0175-2

[39] CASTELLOTE, Marta, Cruz ALONSO, Carmen ANDRADE, Xavier TURRILLAS and Javier CAMPO. Composition and microstructural changes of cement pastes upon heating, as studied by neutron diffraction. *Cement and Concrete Research* [online]. 2004, **34**(9), 1633–1644. ISSN 00088846. Available at: doi:10.1016/S0008-8846(03)00229-1

[40] NIRY, R. R., A. L. BEAUCOUR, R. HEBERT, A. NOUMOWÉ, B. LEDÉSERT and R. BODET. Thermal stability of different siliceous and calcareous aggregates subjected to high temperature. In: P. PIMIENTA and F. MEFTAH, eds. *MATEC Web of Conferences* [online]. B.m.: EDP Sciences, 2013, p. 07001 [accessed. 2021-01-13]. ISBN 9782759810741. Available at: doi:10.1051/matecconf/20130607001

[41] SAVVA, A., P. MANITA and K. K. SIDERIS. Influence of elevated temperatures on the mechanical properties of blended cement concretes prepared with limestone and siliceous aggregates. *Cement and Concrete Composites* [online]. 2005, **27**(2), 239–248. ISSN 09589465. Available at: doi:10.1016/j.cemconcomp.2004.02.013

[42] HACHEMI, Samia and Abdelhafid OUNIS. The effects of high temperature on the mechanical and physical properties of ordinary, high strength and high performance concrete. In: *Proceedings of the 10th fib International PhD Symposium in Civil Engineering* [online]. 2014, p. 201–207 [accessed. 2021-01-05]. ISBN 9782980676215. Available at: https://www.researchgate.net/publication/273130528_The_effects_of_high_temperature_on_the_mechanical_and_physical_properties_of_ordinary_high_strength_and_high_performance_concrete

[43] MAJORANA, C. E., V. A. SALOMONI, G. MAZZUCCO and G. A. KHOURY. An approach for modelling concrete spalling in finite strains. *Mathematics and Computers in Simulation* [online]. 2010, **80**(8), 1694–1712. ISSN 03784754. Available at: doi:10.1016/j.matcom.2009.05.011

[44] ZHENG, W. Z., X. M. HOU, D. S. SHI and M. X. XU. Experimental study on concrete spalling in prestressed slabs subjected to fire. *Fire Safety Journal* [online]. 2010, **45**(5), 283–297. ISSN 03797112. Available at: doi:10.1016/j.firesaf.2010.06.001

[45] BAŽANT, Zdeněk P. Analysis of pore pressure, thermal stress and fracture in rapidly heated concrete,. *Nist* [online]. 1997, 155–164 [accessed. 2021-01-12]. Available at: https://www.nist.gov/publications/analysis-pore-pressure-thermal-stress-and-fracture-rapidly-heated-concrete

[46] FU, Yufang and Lianchong LI. Study on mechanism of thermal spalling in concrete exposed to elevated temperatures. *Materials and Structures/Materiaux et Constructions* [online]. 2011, **44**(1), 361–376 [accessed. 2021-01-15]. ISSN 13595997. Available at: doi:10.1617/s11527-010-9632-6

[47] KHOURY, Gabriel Alexander. Fire and Concrete. In: *Encontro Nacional Betão Estrutural* [online]. 2008, p. 21–34 [accessed. 2021-01-15]. Available at: http://www.hms.civil.uminho.pt/events/be2008/21.pdf

[48] OZAWA, Mitsuo, Shinya UCHIDA, Toshiro KAMADA and Hiroaki MORIMOTO. Study of mechanisms of explosive spalling in high-strength concrete at high temperatures using acoustic emission. *Construction and Building Materials* [online]. 2012, **37**, 621–628. ISSN 09500618. Available at: doi:10.1016/j.conbuildmat.2012.06.070

[49] CHOI, Won Chang and Hyun Do YUN. Effect of expansive admixtures on the shrinkage and mechanical properties of high-performance fiber-reinforced cement composites. *The Scientific World Journal* [online]. 2013, **2013**. ISSN 1537744X. Available at: doi:10.1155/2013/418734

[50] WATANABE, Kazuo, Mugume Rodgers BANGI and Takashi HORIGUCHI. The effect of testing conditions (hot and residual) on fracture toughness of fiber reinforced high-strength concrete subjected to high temperatures. *Cement and Concrete Research* [online]. 2013, **51**, 6–13. ISSN 00088846. Available at: doi:10.1016/j.cemconres.2013.04.003

[51] MOHAMMADHOSSEINI, Hossein, Nor Hasanah Abdul Shukor LIM, Abdul Rahman Mohd SAM and Mostafa SAMADI. Effects of elevated temperatures on residual properties of concrete reinforced with waste polypropylene carpet fibres. *Arabian Journal for Science and Engineering* [online]. 2018, **43**(4), 1673–1686 [accessed. 2021-01-04]. ISSN 21914281. Available at: doi:10.1007/s13369-017-2681-1

[52] RIES, J. P., J. SPECK and K. S. HARMON. Lightweight Aggregate Optimizes the Sustainability of Concrete. In: *Concrete Sustainability Conference* [online]. 2010, p. 15 [accessed. 2021-01-29]. Available at: https://silo.tips/download/ph-704-fax-704

[53] HE, Ke Cheng, Rong Xin GUO, Qian Min MA, Feng YAN, Zhi Wei LIN and Yan Lin SUN. Experimental Research on High Temperature Resistance of Modified Lightweight Concrete after Exposure to Elevated Temperatures. *Advances in Materials Science and Engineering* [online]. 2016, **2016**. ISSN 16878442. Available at: doi:10.1155/2016/5972570

[54] HOLČAPEK, Ondřej, Jaroslava KOŤÁTKOVÁ, Petr KONVALINKA and Pavel REITERMAN. Response of refractory cement based composite to gradual temperature loading. *Periodica Polytechnica Civil Engineering* [online]. 2018, **62**(3). ISSN 15873773. Available at: doi:10.3311/PPci.11080

[55] FU, Tengfei, Matthew P ADAMS and Jason H IDEKER. A Preliminary Study on A Calcium Aluminate Cement Concrete Maturity Theory in Predicting Conversion. *14th International Congress on the Chemistry of Cement* [online]. 2016. Available at: doi:10.13140/RG.2.1.2606.5369

[56] SCHEINHERROVÁ, Lenka and Anton TRNÍK. Hydration of calcium aluminate cement determined by thermal analysis. In: *AIP Conference Proceedings* [online]. B.m.: American Institute of Physics Inc., 2017, p. 040034 [accessed. 2021-01-04]. ISBN 9780735415461. Available at: doi:10.1063/1.4994514

[57] SCRIVENER, Karen L. and Alain CAPMAS. Calcium aluminate cements. In: *Lea's Chemistry of Cement and Concrete* [online]. B.m.: Elsevier Ltd., 2003, p. 713–782. ISBN 9780750662567. Available at: doi:10.1016/B978-075066256-7/50025-4

[58] REITERMAN, Pavel, Ondřej HOLČAPEK, Marcel JOGL and Petr KONVALINKA. Physical and mechanical properties of composites made with aluminous cement and basalt fibers developed for high temperature application. *Advances in Materials Science and Engineering* [online]. 2015, **2015**. ISSN 16878442. Available at: doi:10.1155/2015/703029

[59] ANTONOVIČ, Valentin, Jadvyga KERIENE, Renata BORIS and Marius ALEKNEVIČIUS. The effect of temperature on the formation of the hydrated calcium aluminate cement structure. In: *Procedia Engineering* [online]. B.m.: Elsevier Ltd, 2013, p. 99–106. ISSN 18777058. Available at: doi:10.1016/j.proeng.2013.04.015

[60] *Kerneos Inc.* [online]. [accessed. 2021-01-19]. Available at: http://www.kerneos inc.com/refractory.php

[61] SCHWARZ, H.-G. Aluminum Production and Energy. In: *Encyclopedia of Energy* [online]. B.m.: Elsevier, 2004, p. 81–95. Available at: doi:10.1016/b0-12-176480-x/00372-7

[62] KIRCA, Önder. *Temperature effect on calcium aluminate cement based composite binders* [online]. B.m., 2006 [accessed. 2021-03-03]. Middle East Technical University. Available at: https://open.metu.edu.tr/handle/11511/16464

[63] OLIVEIRA, I. R., F. S. ORTEGA and V. C. PANDOLFELLI. Hydration of CAC cement in a castable refractory matrix containing processing additives. *Ceramics International* [online]. 2009, **35**(4), 1545–1552. ISSN 02728842. Available at: doi:10.1016/j.ceramint.2008.08.014

[64] KOŇÁKOVÁ, Dana. *Thermal Resistance of Calcium Aluminate Cement Based Composites* [online]. B.m., 2018. Czech Technical University in Prague. Available at: https://dspace.cvut.cz/handle/10467/79216

[65] BORIS, R., V. ANTONOVICH, R. STONIS, A. VOLOCHKO and I. BELOV. Effect of holding temperature on properties of different types of heat-resistant concrete. *Refractories and Industrial Ceramics* [online]. 2014, **54**(5), 397–400 [accessed. 2021-01-02]. ISSN 10834877. Available at: doi:10.1007/s11148-014-9619-x

[66] LITWINEK, Ewa and Dominika MADEJ. Structure, microstructure and thermal stability characterizations of C3AH6 synthesized from different precursors through hydration. *Journal of Thermal Analysis and Calorimetry* [online]. 2020, **139**(3), 1693–1706 [accessed. 2021-01-22]. ISSN 15882926. Available at: doi:10.1007/s10973-019-08656-0

[67] NILFOROUSHAN, Mohammad Reza and Nasrien TALEBIAN. The hydration products of a refractory calcium aluminate cement at intermediate temperatures. *Iranian Journal of Chemistry and Chemical Engineering* [online]. 2007, **26**(3), 19–24 [accessed. 2021-01-04]. ISSN 10219986. Available at: http://www.ijcce.ac.ir/article_7626.html

[68] HEIKAL, Mohamed, Mohamed Mahmoud RADWAN and Mohamed Saad MORSY. Influence of curing temperature on the physicomechanical, characteristics of calcium aluminate cement with air-cooled slag or water-cooled slag. *Ceramics - Silikaty* [online]. 2004, **48**(4), 185–196 [accessed. 2021-01-25]. ISSN 08625468. Available at: https://www.ceramics-silikaty.cz/2004/2004_04_185.htm

[69] SCRIVENER, Karen L., Jean Louis CABIRON and Roger LETOURNEUX. High-performance concretes from calcium aluminate cements. *Cement and Concrete Research* [online]. 1999, **29**(8), 1215–1223. ISSN 00088846. Available at: doi:10.1016/S0008-8846(99)00103-9

[70] TOPÇU, Ilker Bekir and Tayfun UYGUNOĞLU. Effect of aggregate type on properties of hardened self-consolidating lightweight concrete (SCLC). *Construction and Building Materials* [online]. 2010, **24**(7), 1286–1295. ISSN 09500618. Available at: doi:10.1016/j.conbuildmat.2009.12.007

[71] ADHIKARY, Suman Kumar and Zymantas RUDZIONIS. Influence of expanded glass aggregate size, aerogel and binding materials volume on the properties of lightweight concrete. In: *Materials Today: Proceedings* [online]. B.m.: Elsevier Ltd, 2020, p. 712–718. ISSN 22147853. Available at: doi:10.1016/j.matpr. 2020.03.323

[72] ALONSO, M. C., V. FLOR-LAGUNA and M. SANCHEZ. Microstructural response of polypropylene fibres at high temperature to protect concrete from spalling. In: *MATEC Web of Conferences* [online]. B.m.: EDP Sciences, 2013. ISBN 9782759810741. Available at: doi:10.1051/matecconf/20130602001

[73] VEJMELKOVÁ, Eva and Robert ČERNÝ. Thermal properties of PVA-fiber reinforced cement composites at high temperatures. In: *Applied Mechanics and Materials* [online]. B.m.: Trans Tech Publications Ltd, 2013, p. 45–49 [accessed. 2021-01-04]. ISBN 9783037858080. Available at: doi:10.4028/ www.scientific.net/AMM.377.45

[74] HOLČAPEK, Ondřej, Jaroslava KOT'ÁTKOVÁ and Pavel REITERMAN. Development of Composite for Thermal Barriers Reinforced by Ceramic Fibers. *Advances in Civil Engineering* [online]. 2018, **2018**, 1–10. ISSN 1687-8086. Available at: doi:10.1155/2018/3251523

[75] BANGI, Mugume Rodgers and Takashi HORIGUCHI. Pore pressure development in hybrid fibre-reinforced high strength concrete at elevated temperatures. *Cement and Concrete Research* [online]. 2011, **41**(11), 1150–1156. ISSN 00088846. Available at: doi:10.1016/j.cemconres.2011.07.001

[76] XIAO, Jianzhuang and H. FALKNER. On residual strength of high-performance concrete with and without polypropylene fibres at elevated temperatures. *Fire Safety Journal* [online]. 2006, **41**(2), 115–121. ISSN 03797112. Available at: doi:10.1016/j.firesaf.2005.11.004

[77] AKBAR, Arslan and K. M. LIEW. Influence of elevated temperature on the microstructure and mechanical performance of cement composites reinforced with recycled carbon fibers. *Composites Part B: Engineering* [online]. 2020, **198**, 108245. ISSN 13598368. Available at: doi:10.1016/j.compositesb.2020.108245

[78] SCHEINHERROVÁ, Lenka, Jan FOŘT, Zbyšek PAVLÍK and Robert CERNÝ. Simultaneous thermal analysis and thermodilatometry of hybrid fiber reinforced UHPC. In: *AIP Conference Proceedings* [online]. B.m.: American Institute of Physics Inc., 2017, p. 040033 [accessed. 2021-01-04]. ISBN 9780735415461. Available at: doi:10.1063/1.4994513

[79] LIN, Ro Ting, Lung Chang CHIEN, Masamine JIMBA, Sugio FURUYA and Ken TAKAHASHI. Implementation of national policies for a total asbestos ban: a global comparison. *The Lancet Planetary Health* [online]. 2019, **3**(8), e341–e348. ISSN 25425196. Available at: doi:10.1016/S2542-5196(19)30109-3

[80] KNOWLES, Scott Gabriel. Asbestos and fire: Technological trade-offs and the body at risk (review). *Technology and Culture* [online]. 2007, **48**(1), 175–177 [accessed. 2021-01-04]. ISSN 1097-3729. Available at: doi:10.1353/tech.2007.0025

[81] *White asbestos to be banned in all EU countries* [online]. B.m.: Elsevier BV. 1999. Available at: doi:10.1016/s1350-4789(99)90354-9

[82] TAKAHASHI, Ken and Philip J. LANDRIGAN. *The Global Health Dimensions of Asbestos and Asbestos-Related Diseases* [online]. B.m.: Elsevier USA. 1. January 2016. ISSN 22149996. Available at: doi:10.1016/j.aogh.2016.01.019

[83] LEDDA, Caterina, Cristoforo POMARA, Massimo BRACCI, Dario MANGANO, Vincenzo RICCERI, Andrea MUSUMECI, Margherita FERRANTE, Giuseppe MUSUMECI, Carla LORETO, Concettina FENGA, Lory SANTARELLI and Venerando RAPISARDA. Natural carcinogenic fiber and pleural plaques assessment in a general population: A cross-sectional study. *Environmental Research* [online]. 2016, **150**, 23–29. ISSN 10960953. Available at: doi:10.1016/j.envres.2016.05.024

[84] KIM, Su Young, Young Chan KIM, Yongku KIM and Won Hwa HONG. Predicting the mortality from asbestos-related diseases based on the amount of asbestos used and the effects of slate buildings in Korea. *Science of the Total Environment* [online]. 2016, **542**, 1–11. ISSN 18791026. Available at: doi:10.1016/j.scitotenv.2015.10.115

[85] ROCCARO, Paolo and Federico G.A. VAGLIASINDI. Indoor release of asbestiform fibers from naturally contaminated water and related health risk. *Chemosphere* [online]. 2018, **202**, 76–84. ISSN 18791298. Available at: doi:10.1016/j.chemosphere.2018.03.040

[86] LACOURT, Aude, Mickael RINALDO, Céline GRAMOND, Stéphane DUCAMP, Annabelle Gilg SOIT ILG, Marcel GOLDBERG, Jean Claude PAIRON and Patrick BROCHARD. Co-exposure to refractory ceramic fibres and asbestos and risk of pleural mesothelioma. *European Respiratory Journal* [online]. 2014, **44**(3), 725–733 [accessed. 2021-01-04]. ISSN 13993003. Available at: doi:10.1183/09031936.00079814

[87] ZHANG, Yao, J. Woody JU, Qing CHEN, Zhiguo YAN, Hehua ZHU and Zhengwu JIANG. Characterizing and analyzing the residual interfacial behavior of steel fibers embedded into cement-based matrices after exposure to high temperatures. *Composites Part B: Engineering* [online]. 2020, **191**, 107933. ISSN 13598368. Available at: doi:10.1016/j.compositesb.2020.107933

[88] ABID, Muhammad, Xiaomeng HOU, Wenzhong ZHENG, Raja Rizwan HUSSAIN, Shaojun CAO and Zhihao LV. Creep behavior of steel fiber reinforced reactive powder concrete at high temperature. *Construction and Building Materials* [online]. 2019, **205**, 321–331. ISSN 09500618. Available at: doi:10.1016/j.conbuildmat.2019.02.019

[89] BAREIRO, Walter Gabriel, Flávio DE ANDRADE SILVA and Elisa Dominguez SOTELINO. Thermo-mechanical behavior of stainless steel fiber reinforced refractory concrete: Experimental and numerical analysis. *Construction and Building Materials* [online]. 2020, **240**, 117881. ISSN 09500618. Available at: doi:10.1016/j.conbuildmat.2019.117881

[90] HOLČAPEK, Ondřej, Pavel REITERMAN and Petr KONVALINKA. Applicability of carbon fibres in refractory cement composites. *Acta Polytechnica* [online]. 2018, **58**(6), 346–354 [accessed. 2021-01-04]. ISSN 18052363. Available at: doi:10.14311/AP.2018.58.0346

[91] ASHKEZARI, Ghasem Dehghani and Mehrdad RAZMARA. Thermal and mechanical evaluation of ultra-high performance fiber-reinforced concrete and conventional concrete subjected to high temperatures. *Journal of Building Engineering* [online]. 2020, **32**, 101621. ISSN 23527102. Available at: doi:10.1016/j.jobe.2020.101621

[92] RUANO, Gonzalo, Facundo ISLA, Bibiana LUCCIONI, Raúl ZERBINO and Graciela GIACCIO. Steel fibers pull-out after exposure to high temperatures and its contribution to the residual mechanical behavior of high strength concrete. *Construction and Building Materials* [online]. 2018, **163**, 571–585. ISSN 09500618. Available at: doi:10.1016/j.conbuildmat.2017.12.129

[93] ANDIÇ-ÇAKIR, Özge and Selim HIZAL. Influence of elevated temperatures on the mechanical properties and microstructure of self consolidating lightweight aggregate concrete. *Construction and Building Materials* [online]. 2012, **34**, 575–583. ISSN 09500618. Available at: doi:10.1016/j.conbuildmat.2012.02.088

[94] YUN, Tae Sup, Yeon Jong JEONG, Tong Seok HAN and Kwang Soo YOUM. Evaluation of thermal conductivity for thermally insulated concretes. *Energy and Buildings* [online]. 2013, **61**, 125–132. ISSN 03787788. Available at: doi:10.1016/j.enbuild.2013.01.043

[95] KOKSAL, Fuat, Osman GENCEL and Mehmet KAYA. Combined effect of silica fume and expanded vermiculite on properties of lightweight mortars at ambient and elevated temperatures. *Construction and Building Materials* [online]. 2015, **88**, 175–187. ISSN 09500618. Available at: doi:10.1016/j.conbuildmat.2015.04.021

[96] HASSANPOUR, Mahmoud, Payam SHAFIGH and Hilmi Bin MAHMUD. Lightweight aggregate concrete fiber reinforcement - A review. *Construction and Building Materials* [online]. 2012, **37**, 452–461. ISSN 09500618. Available at: doi:10.1016/j.conbuildmat.2012.07.071

[97] SCHUMACHER, Katrin, Nils SASSMANNSHAUSEN, Christian PRITZEL and Reinhard TRETTIN. Lightweight aggregate concrete with an open structure and a porous matrix with an improved ratio of compressive strength to dry density. *Construction and Building Materials* [online]. 2020, **264**, 120167. ISSN 09500618. Available at: doi:10.1016/j.conbuildmat.2020.120167

[98] THIENEL, Karl Christian, Timo HALLER and Nancy BEUNTNER. Lightweight concrete-from basics to innovations. *Materials* [online]. 2020, **13**(5), 1120 [accessed. 2021-01-31]. ISSN 19961944. Available at: doi:10.3390/ma13051120

[99] MA, Qianmin, Rongxin GUO, Zhiman ZHAO, Zhiwei LIN and Kecheng HE. Mechanical properties of concrete at high temperature-A review. *Construction and Building Materials* [online]. 2015, **93**, 371–383. ISSN 09500618. Available at: doi:10.1016/j.conbuildmat.2015.05.131

[100] TANYILDIZI, Harun and Ahmet COSKUN. Performance of lightweight concrete with silica fume after high temperature. *Construction and Building Materials* [online]. 2008, **22**(10), 2124–2129. ISSN 09500618. Available at: doi:10.1016/j.conbuildmat.2007.07.017

[101] SANCAK, Emre, Y. DURSUN SARI and Osman SIMSEK. Effects of elevated temperature on compressive strength and weight loss of the light-weight concrete with silica fume and superplasticizer. *Cement and Concrete Composites* [online]. 2008, **30**(8), 715–721. ISSN 09589465. Available at: doi:10.1016/j.cemconcomp.2008.01.004

[102] YAO, Weijing, Jianyong PANG and Yushan LIU. Performance degradation and microscopic analysis of lightweight aggregate concrete after exposure to high temperature. *Materials* [online]. 2020, **13**(7), 1566 [accessed. 2021-01-31]. ISSN 19961944. Available at: doi:10.3390/ma13071566

[103] TENZA-ABRIL, A. J., D. BENAVENTE, C. PLA, F. BAEZA-BROTONS, J. VALDES-ABELLAN and A. M. SOLAK. Statistical and experimental study for determining the influence of the segregation phenomenon on physical and mechanical properties of lightweight concrete. *Construction and Building Materials* [online]. 2020, **238**, 117642. ISSN 09500618. Available at: doi:10.1016/j.conbuildmat.2019.117642

[104] SHEN, Lin, Hamed BAHRAMI JOVEIN, Zhihui SUN, Qian WANG and Wenmei LI. Testing dynamic segregation of self-consolidating concrete. *Construction and Building Materials* [online]. 2015, **75**, 465–471. ISSN 09500618. Available at: doi:10.1016/j.conbuildmat.2014.11.010

[105] PANESAR, D. K. and B. SHINDMAN. The effect of segregation on transport and durability properties of self consolidating concrete. *Cement and Concrete Research* [online]. 2012, **42**(2), 252–264. ISSN 00088846. Available at: doi:10.1016/j.cemconres.2011.09.011

[106] CHOI, Yun Wang, Yong Jic KIM, Hwa Cheol SHIN and Han Young MOON. An experimental research on the fluidity and mechanical properties of high-strength lightweight self-compacting concrete. *Cement and Concrete Research* [online]. 2006, **36**(9), 1595–1602. ISSN 00088846. Available at: doi:10.1016/j.cemconres.2004.11.003

[107] HOLČAPEK, Ondřej. Resistance of refractory cement composite to cyclic temperature loading. In: *Key Engineering Materials* [online]. B.m.: Trans Tech Publications Ltd, 2016, p. 23–28 [accessed. 2021-01-05]. ISBN 9783038355793. Available at: doi:10.4028/www.scientific.net/KEM.677.23

[108] HOLČAPEK, Ondřej, Pavel REITERMAN and Marcel JOGL. Refractory cement composite reinforced by various types of fibers. In: *Materials Science Forum* [online]. B.m.: Trans Tech Publications Ltd, 2015, p. 173–177 [accessed. 2021-01-04]. ISBN 9783038355090. Available at: doi:10.4028/www.scientific.net/MSF.824.173

[109] JOGL, M. and P. REITERMAN. Experimental assessment of the effect of plasticizing and air-entraining additives on mechanical properties of refractory cement composite. In: *4th Brazilian Conference on Composite Materials* [online]. 2018, p. 66–72 [accessed. 2021-01-04]. ISBN 978-85-85083-00-7. Available at: doi:10.21452/bccm4.2018.02.03

[110] JOGL, Marcel, Pavel REITERMAN, Ondřej HOLČAPEK and Jaroslava KOŤÁTKOVÁ. Proposal of fire resistant composites with application of lightweight aggregate Liaver. In: *Advanced Materials Research* [online]. B.m.: Trans Tech Publications Ltd, 2014, p. 43–47 [accessed. 2021-01-02]. ISBN 9783038353171. Available at: doi:10.4028/www.scientific.net/AMR.1054.43

[111] KOŇÁKOVÁ, Dana, Eva VEJMELKOVÁ, Veronika ŠPEDLOVÁ, Kirill POLOZHIY and Robert ČERNÝ. Cement composites for high temperature applications. In: *Advanced Materials Research* [online]. B.m.: Trans Tech Publications Ltd, 2014, p. 154–158 [accessed. 2021-01-03]. ISBN 9783038351726. Available at: doi:10.4028/www.scientific.net/AMR.982.154

[112] JOGL, Marcel and Pavel REITERMAN. Utility of air-entraining additive in the development of lightweight alumina-based refractories. In: *Materials Science Forum* [online]. B.m.: Trans Tech Publications Ltd, 2020, p. 147–152 [accessed. 2021-04-26]. ISBN 9783035716207. Available at: doi:10.4028/www.scientific.net/MSF.975.147

[113] *MICROPORAN 2* [online]. [accessed. 2021-03-14]. Available at: https://prisadydobetonu.stachema.cz/produkty/provzdusnujici-prisady:c3/microporan-2:p267.htm

[114] LI, Zongjin, Xiangming ZHOU and Bin SHEN. Fiber-cement extrudates with perlite subjected to high temperatures. *Journal of Materials in Civil Engineering* [online]. 2004, **16**(3), 221–229 [accessed. 2021-01-04]. ISSN 0899-1561. Available at: doi:10.1061/(asce)0899-1561(2004)16:3(221)

[115] LAIBLOVÁ, Lenka, Tomáš VLACH, Alexandru CHIRA, Magdaléna NOVOTNÁ, Ctislav FIALA, Michal ŽENÍŠEK and Petr HÁJEK. Technical textiles as an innovative material for reinforcing of elements from high performance concretes (HPC). In: *Advanced Materials Research* [online]. B.m.: Trans Tech Publications Ltd, 2014, p. 110–115. ISBN 9783038353171. Available at: doi:10.4028/www.scientific.net/AMR.1054.110

[116] JIANG, Chaohua, Ke FAN, Fei WU and Da CHEN. Experimental study on the mechanical properties and microstructure of chopped basalt fibre reinforced concrete. *Materials and Design* [online]. 2014, **58**, 187–193. ISSN 18734197. Available at: doi:10.1016/j.matdes.2014.01.056

[117] COLOMBO, C., L. VERGANI and M. BURMAN. Static and fatigue characterisation of new basalt fibre reinforced composites. *Composite Structures* [online]. 2012, **94**(3), 1165–1174. ISSN 02638223. Available at: doi:10.1016/j.compstruct.2011.10.007

[118] LI, Zongwen, Jianxun MA, Hongmin MA and Xin XU. Properties and applications of basalt fiber and its composites. In: *IOP Conference Series: Earth and Environmental Science* [online]. B.m.: Institute of Physics Publishing, 2018, p. 012052 [accessed. 2021-01-05]. ISSN 17551315. Available at: doi:10.1088/1755-1315/186/2/012052

[119] DHARMENDRA SONDARVA and DR. ANKUR C. BHOGAYATA. Usage of Chopped Basalt Fibers in Concrete Composites: A Review. *International Journal of Engineering Research and* [online]. 2017, **V6**(09) [accessed. 2021-03-16]. Available at: doi:10.17577/ijertv6is090164

[120] JOGL, Marcel, Pavel REITERMAN, Ondřej HOLČAPEK, Jaroslava KOŤÁTKOVÁ and Petr KONVALINKA. Residual properties of fiber-reinforced refractory composites with a fireclay filler. *Acta Polytechnica* [online]. 2016, **56**(1), 27–32 [accessed. 2021-01-04]. ISSN 18052363. Available at: doi:10.14311/APP.2016.56.0027

[121] NETINGER, Ivanka, Ivana KESEGIC and Ivica GULJAS. The effect of high temperatures on the mechanical properties of concrete made with different types of aggregates. *Fire Safety Journal* [online]. 2011, **46**(7), 425–430. ISSN 03797112. Available at: doi:10.1016/j.firesaf.2011.07.002

[122] BERNHARDT, Markus, Hilde TELLESBØ, Harald JUSTNES and Kjell WIIK. Mechanical properties of lightweight aggregates. *Journal of the European Ceramic Society* [online]. 2013, **33**(13–14), 2731–2743. ISSN 09552219. Available at: doi:10.1016/j.jeurceramsoc.2013.05.013

[123] EN 196-1. *Methods of testing cement - Part 1: Determination of strength* [online]. 2005 [accessed. 2021-04-27]. Available at: https://standards.iteh.ai/catalog/standards/cen/37b8816e-4085-4dcc-a642-a383d9bddd6c/en-196-1-2016

[124] EN 1015-3. *Methods of test for mortar for masonry - Part 3: Determination of consistence of fresh mortar (by flow table)* [online]. 1999 [accessed. 2021-01-07]. Available at: https://standards.globalspec.com/std/733841/EN 1015-3

[125] TAYLOR, Peter C. *Curing concrete* [online]. B.m.: CRC Press, 2013 [accessed. 2021-03-18]. ISBN 9780203866139. Available at: doi:10.1201/b15519

[126] CARDOSO, Fábio A., Murilo D.M. INNOCENTINI, Mario M. AKIYOSHI and Victor C. PANDOLFELLI. Effect of curing time on the properties of CAC bonded refractory castables. *Journal of the European Ceramic Society* [online]. 2004, **24**(7), 2073–2078. ISSN 09552219. Available at: doi:10.1016/S0955-2219(03)00371-6

[127] GAO, Jianming, Wei SUN and Keiji MORINO. Mechanical properties of steel fiber-reinforced, high-strength, lightweight concrete. *Cement and Concrete Composites* [online]. 1997, **19**(4), 307–313. ISSN 09589465. Available at: doi:10.1016/S0958-9465(97)00023-1

[128] KOŇÁKOVÁ, Dana, Veronika ŠPEDLOVÁ, Monika ČÁCHOVÁ, Eva VEJMELKOVÁ and Robert ČERNÝ. Influence of basalt fibres and aggregates on the thermal expansion of cement-based composites. In: *Advanced Materials Research* [online]. B.m.: Trans Tech Publications Ltd, 2014, p. 17–21 [accessed. 2021-01-02]. ISBN 9783038353171. Available at: doi:10.4028/www.scientific.net/AMR.1054.17

[129] RILEM TCS. Determination of the fracture energy of mortar and concrete by means of three-point bend tests on notched beams. *Materials and Structures* [online]. 1985, **18**(6), 484 [accessed. 2021-01-04]. ISSN 00255432. Available at: doi:10.1007/BF02498757

[130] LEE, Jaeha and Maria M. LOPEZ. An Experimental Study on Fracture Energy of Plain Concrete. *International Journal of Concrete Structures and Materials* [online]. 2014, **8**(2), 129–139 [accessed. 2021-04-30]. ISSN 22341315. Available at: doi:10.1007/s40069-014-0068-1

[131] TANYILDIZI, Harun. Prediction of the strength properties of carbon fiber-reinforced lightweight concrete exposed to the high temperature using artificial neural network and support vector machine. *Advances in Civil Engineering* [online]. 2018, **2018** [accessed. 2021-06-24]. ISSN 16878094. Available at: doi:10.1155/2018/5140610

[132] BANTHIA, N. Durability enhancements in concrete with fiber reinforcement. In: *Int. Conf: Sustainable construction materials and technologie*. 2007, p. 209–219.